AD-A062 480 J B F SCIENTIFIC CORP WILMINGTON MA F/G 13/3
LABORATORY INVESTIGATION OF THE DYNAMICS OF MUD FLOWS GENERATED--ETC(U)
AUG 78 G HENRY, R W NEAL, S H GREENE DACW39-76-C-0173
UNCLASSIFIED WES-TR-D-78-46 NL

1 OF 2
AD
A062480

Report on

LEVEL

DREDGED MATERIAL RESEARCH PROGRAM

TECHNICAL REPORT D-78-46

LABORATORY INVESTIGATION OF THE DYNAMICS OF MUD FLOWS GENERATED BY OPEN-WATER PIPELINE DISPOSAL OPERATIONS

by

George [illegible], Robert V. [illegible], Stephen H. [illegible]

JBF Scientific Corporation
2 [illegible]
Wilmington, Mass. 01887

[illegible]

WES

TR-D-78-46

163p.

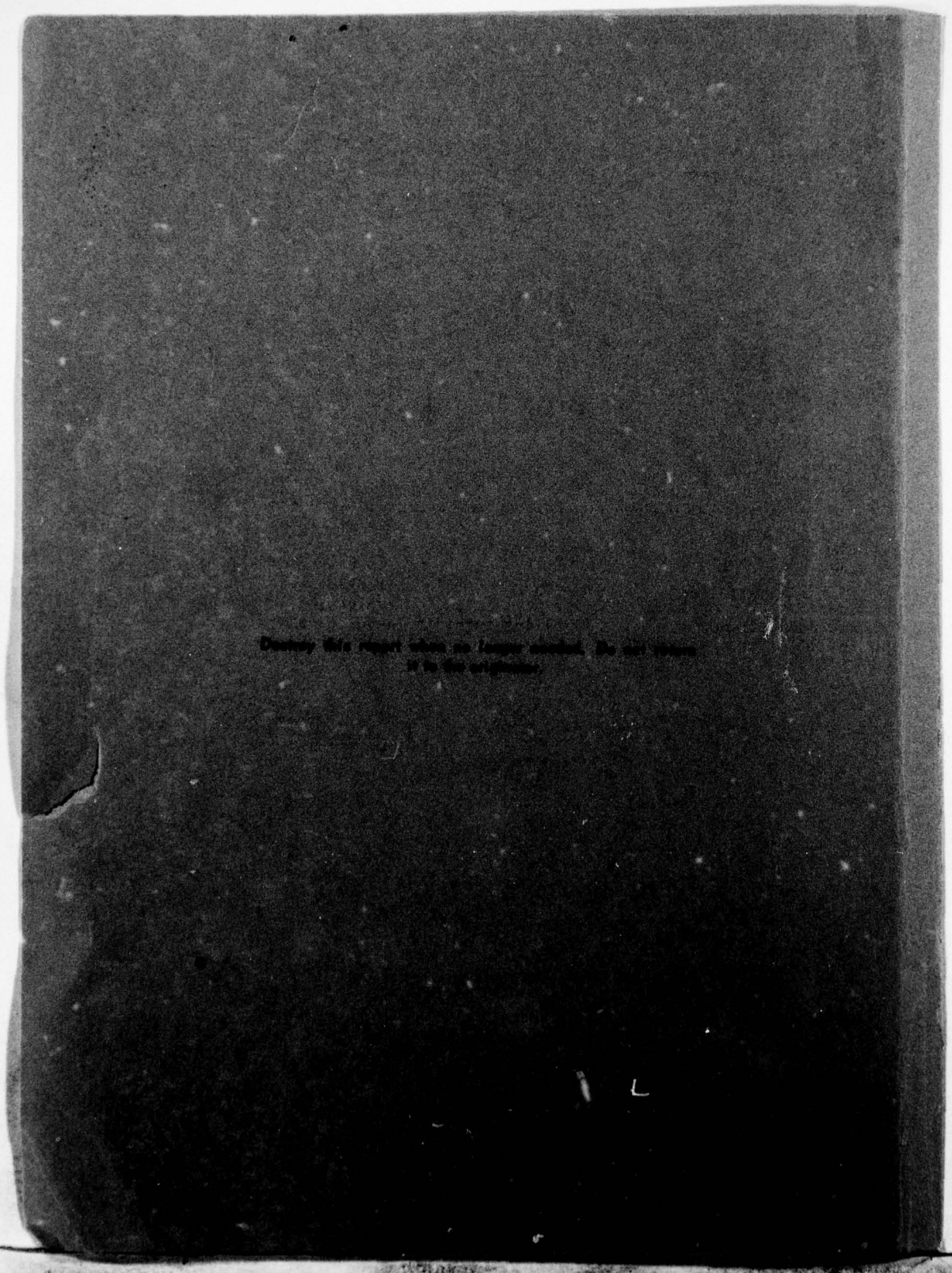

DEPARTMENT OF THE ARMY
WATERWAYS EXPERIMENT STATION, CORPS OF ENGINEERS
P. O. BOX 631
VICKSBURG, MISSISSIPPI 39180

IN REPLY REFER TO: WESEV

30 September 1978

SUBJECT: Transmittal of Technical Report D-78-46

TO: All Report Recipients

1. The technical report transmitted herewith represents the results of one research effort (Work Unit 6C09) initiated as part of Task 6C entitled "Turbidity Prediction and Control" of the Corps of Engineers' Dredged Material Research Program (DMRP). Task 6C, included as part of the Disposal Operations Project of the DMRP, was concerned with investigating the problem of turbidity and developing methods to predict the nature, extent, and duration of turbidity generated by dredging and disposal operations. Equal emphasis was also placed on evaluating both chemical and physical methods for controlling turbidity generation around dredging and disposal operations.

2. Although there are still many questions about the direct and indirect effects of different levels of suspended solids on various aquatic organisms, it may be necessary, under certain circumstances, to be able to predict the dispersive nature of the dredged material resuspended by a particular dredging or disposal operation as a means of evaluating the necessity for different control measures. Field studies of the short-term fate of dredged material slurry at open-water pipeline disposal sites indicate that the vast majority of any discharged fine-grained slurry descends rapidly to the bottom of the disposal site and forms a fluid mud layer. Although field measurements have provided a general indication of the physical nature and dispersive characteristics of this fluid mud dredged material, a laboratory investigation of the dynamics of fluid mud flows was undertaken to complement the field measurements and expand the understanding of fluid mud accumulation and movement. The primary objective of this study was to define the dynamics of the mud system through laboratory flume tests and to quantify the primary variables that control the behavior of the fluid mud including sediment composition, slurry solids concentration, bottom flow rates, currents, and surface waves. With a better understanding of the fluid mud system and the effect of different environmental variables on its dispersal, it is possible to better predict the dispersal patterns of fine-grained dredged material slurry disposed at open-water pipeline disposal sites.

WESEV 30 September 1978
SUBJECT: Transmittal of Technical Report D-78-46

3. This study addresses the generation of fluid mud flows around open-water pipeline disposal operations and represents one of a series of reports concerned with the dispersion of dredged material and the control of water column turbidity. Other studies within Task 6C provide information on silt curtains, submerged pipeline discharge, and the formation and dispersal of fluid mud dredged material around actual open-water pipeline disposal operations. All research results generated by Task 6C are synthesized in Technical Report DS-78-13 entitled "Prediction and Control of Dredged Material Dispersion Around Dredging and Open-Water Pipeline Disposal Operations."

JOHN L. CANNON
Colonel, Corps of Engineers
Commander and Director

Unclassified

SECURITY CLASSIFICATION OF THIS PAGE (When Data Entered)

REPORT DOCUMENTATION PAGE		READ INSTRUCTIONS BEFORE COMPLETING FORM
1. REPORT NUMBER Technical Report D-78-46	2. GOVT ACCESSION NO.	3. RECIPIENT'S CATALOG NUMBER
4. TITLE (and Subtitle) LABORATORY INVESTIGATION OF THE DYNAMICS OF MUD FLOWS GENERATED BY OPEN-WATER PIPELINE DISPOSAL OPERATIONS		5. TYPE OF REPORT & PERIOD COVERED Final report 6. PERFORMING ORG. REPORT NUMBER
7. AUTHOR(s) George Henry Robert W. Neal Stephen H. Greene		8. CONTRACT OR GRANT NUMBER(s) Contract No. DACW39-76-C-0173
9. PERFORMING ORGANIZATION NAME AND ADDRESS JBF Scientific Corporation 2 Jewel Drive Wilmington, Mass. 01887		10. PROGRAM ELEMENT, PROJECT, TASK AREA & WORK UNIT NUMBERS DMRP Work Unit No. 6C09
11. CONTROLLING OFFICE NAME AND ADDRESS Office, Chief of Engineers, U. S. Army Washington, D. C. 20314		12. REPORT DATE August 1978 13. NUMBER OF PAGES 155
14. MONITORING AGENCY NAME & ADDRESS(if different from Controlling Office) Environmental Laboratory U. S. Army Engineer Waterways Experiment Station P. O. Box 631, Vicksburg, Miss. 39180		15. SECURITY CLASS. (of this report) Unclassified 15a. DECLASSIFICATION/DOWNGRADING SCHEDULE

16. DISTRIBUTION STATEMENT (of this Report)

Approved for public release; distribution unlimited.

17. DISTRIBUTION STATEMENT (of the abstract entered in Block 20, if different from Report)

18. SUPPLEMENTARY NOTES

19. KEY WORDS (Continue on reverse side if necessary and identify by block number)

Dredged material	Open-water disposal
Dredged material disposal	Pipelines
Dredging	Slurries
Mud	Solids flow
Mud flows	

20. ABSTRACT (Continue on reverse side if necessary and identify by block number)

This was a laboratory study of the fluid mud system originating at the discharge point of open-water pipeline disposal operations. The objective was to define the dynamics of the mud system and to quantify the primary variables that control its behavior. These variables included salt content of the sediment, slurry solids concentration, bottom slope, slurry flow rate, water current, and surface waves. The fluid mud system was characterized by head wave velocity, cloud height, fluid mud layer thickness, concentration profiles,

(Continued)

DD FORM 1 JAN 73 1473 EDITION OF 1 NOV 65 IS OBSOLETE

Unclassified

SECURITY CLASSIFICATION OF THIS PAGE (When Data Entered)

20. ABSTRACT (Continued).

CONT'

and bottom sediment deposition. Settling played an important role in the mud system dynamics. When settling was present, the head wave and mud flow slowed down and eventually stopped. In its absence, the mud system sustained its motion. Slurry flow rate and solids concentration influenced the mud system in accordance with the constant densimetric Froude number relationship. The fresh and saltwater systems did not reveal evidence of flocculation. Bottom slope indicated the strongest control over the dynamics of the mud system. A minimum downslope angle of 0.75 deg (slope 1:76) was required for the flow to sustain itself. Water current generated more turbidity in the water column; these suspended solids were transported in the direction of the current. Surface waves set up orbital motion throughout the water column but did not hamper the net forward motion of the mud system. When the bottom orbital velocity exceeded 0.06 fps, suspended sediment at the water column/mudflow interface was transported upward in the water column.

Appendix A presents the head wave velocity as a function of downrange distance from the origin. Appendix B presents the sediment deposit profiles, and Appendix C presents the sediment concentration profiles.

THE CONTENTS OF THIS REPORT ARE NOT TO BE USED FOR ADVERTISING, PUBLICATION, OR PROMOTIONAL PURPOSES. CITATION OF TRADE NAMES DOES NOT CONSTITUTE AN OFFICIAL ENDORSEMENT OR APPROVAL OF THE USE OF SUCH COMMERCIAL PRODUCTS.

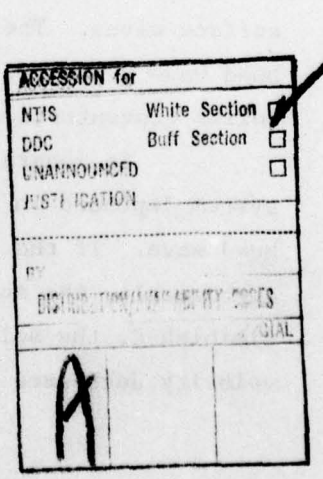

SUMMARY

Open-water pipeline discharge is a commonly used technique for the disposal of dredged channel material in adjacent shoal areas. In recent years its use has been curtailed because of the potential threat of environmental damage. During open-water disposal operations a small percentage of the dredged material becomes suspended in the water column. The large remaining fraction of material settles to the bottom where it forms a layer of fluid mud that may flow away from the discharge point and spreads over the bottom as a dense, thick blanket.

This study focused on the fluid mud system for the purpose of improving the basic understanding of its dynamics and quantifying the effect of major system variables on its behavior. The study was based on a laboratory test program in which two-dimensional mud flows were generated in a test tank where their behavior was observed as a function of system variables. The test facility included a 32-ft-long test tank (8 ft wide by 30 in. deep) equipped with several observation windows on each side, a freshwater supply, a saltwater mixing facility, a mud supply system, a water recirculation loop, and a wave generator. The test matrix of 25 tests was organized so that each variable was evaluated with respect to a reference test condition. Independent variables included salt and freshwater sediment, slurry solids concentration, bottom slope, slurry flow rate, water current velocity, and surface waves. The fluid mud system was characterized by measuring head wave velocity, cloud height, fluid mud layer thickness, suspended solids concentration profiles, and bottom sediment deposition.

In general the behavior of the two-dimensional fluid mud system depended on maintaining the solids concentration in the moving head wave. If the settling rate of the material in the flow was appreciable, the supply of sediment to the head wave continuously diminished, the solids concentration decreased, and the head wave velocity decreased until it finally stopped. When settling was

negligible (on downslopes greater than 0.75 degrees), the head wave solids concentration was maintained and the motion of the fluid mud system was self sustaining. The control applied by slurry flow rate followed the constant densimetric Froude number relationship for the head wave. As the slurry flow rate increased the fluid mud system thickened and the head wave travelled faster.

The behavior of the fresh and saltwater sediment systems was paradoxical in that the settling rate in fresh water exceeded that in salt water. The effects of flocculation in salt water were not apparent possibly because the sediment grain size was too large to promote significant flocculation and the test time was too short to allow its effects to be seen, or the freshwater sediment could have been flocculated by associated organics.

The head wave velocity of the fluid mud system was greatly enhanced by the presence of downslope. The concentration profiles and head wave velocities indicated that beyond a threshold slope the solids concentrations of the fluid mud layer became stable in time and identical in space so that the system sustained itself. The critical downslope was found to be at least 0.75 deg or 1:76. At this condition the gravity force component along the sloped bottom just balanced the friction forces acting on the mud layer and reduced the net settling of the suspended solids to zero.

Head wave velocity depended on slurry density as given by the constant densimetric Froude number relationship (i.e. $U \simeq \Delta\rho$). The slurry density influence was masked by the settling process so that it was only evident in the starting region of horizontal tests and at the terminal condition of downslope tests at or beyond the critical slope.

A 6-fpm current velocity doubled the thickness of the turbidity layer regardless of its flow direction (parallel or counter flow). Counter flow is also parallel but in the opposite direction. The counter current transported the turbid layer downstream and tended to

thin down the fluid mud layer. The parallel current transported the turbid layer in the direction of the mud flow with no apparent thinning of the mud layer.

Free surface waves generated orbital motion throughout the water column. As the mud flowed down the test tank it took on the oscillatory motion of the water column near the bottom; however, the orbital motion imposed on the mud flow did not interfere with its net forward motion. Above a threshold orbital velocity of 0.06 fps, the wave motion promoted turbidity generation and both fluid mud and turbidity layers thickened significantly.

PREFACE

This report presents the results of a laboratory study of the behavior of mud flows that may be generated by open-water pipeline disposal operations. The study was conducted by the JBF Scientific Corporation, Wilmington, Mass., under Contract No. DACW39-76-C-0173, dated 30 September 1976, under Dredged Material Research Program (DMRP) Task 6C, "Turbidity Prediction and Control," Work Unit 6C09, "Laboratory Investigation of the Dynamics of Mud Flows Generated by Open-Water Pipeline Disposal Operations." The DMRP was sponsored by the Office, Chief of Engineers, U.S. Army, and was administered by the Environmental Laboratory (EL), U.S. Army Engineer Waterways Experiment Station (WES).

The study was conducted by Messrs. George Henry, Robert W. Neal, and Stephen H. Greene, of JBF Scientific Corporation. The contract was monitored by Dr. William Barnard, Disposal Operations Project, EL, under the general supervision of Mr. Charles C. Calhoun, Jr., Project Manager, and Dr. John Harrison, Chief, EL.

Director of WES during the conduct of this study and the preparation of this report was COL John L. Cannon, CE. Technical Director was Mr. F.R. Brown.

CONTENTS

LIST OF TABLES

LIST OF FIGURES

LIST OF FIGURES

CONVERSION FACTORS, U.S. CUSTOMARY TO METRIC (SI)
UNITS OF MEASUREMENT

U.S. customary units of measurement used in this report can be converted to metric (SI) units as follows:

Multiply	By	To Obtain
inches	0.0254	metres
feet	0.3048	metres
fathoms	1.8288	metres
miles (U.S. statute)	1.609344	kilometres
miles (U.S. nautical)	1.852	kilometres
feet per second	0.3048	metres per second
feet per minute	0.3048	metres per minute
knots (international)	1.852	kilometres per hour
square feet	0.09290304	square metres
gallons (U.S. liquid)	3.785412	cubic decimetres
gallons (U.S. liquid) per minute	3.785412	cubic decimetres per minute

LABORATORY INVESTIGATION OF THE DYNAMICS OF MUD FLOWS GENERATED BY OPEN-WATER PIPELINE DISPOSAL OPERATIONS

CHAPTER I: INTRODUCTION

Background

1. In U.S. Army Corps of Engineers dredging operations, open-water discharge is a commonly used technique for the disposal of dredged channel material in adjacent shoal areas. At the discharge point the interaction between the flow of dredged slurry and the water column forces a small percentage of fine-grained material to be dispersed in a turbidity cloud or plume, while the remainder of the dredged material descends to the bottom where it forms a layer of relatively dense fluid mud. The turbidity generated during open-water disposal operations has been a concern because of the presence of suspended solids in the water column and the potential release of pollutants. The fluid mud system that is created on the bottom flows away from the discharge location and covers the bottom with a dense layer of material with extremely low dissolved oxygen levels and high levels of suspended solids. Mud flows observed by May,[1] Nichols et. al.,[2] and Johanson[3] have all demonstrated thicknesses of up to 2 ft,* dissolved oxygen contents of nearly zero, and solids concentration of 10 to 170 g/ℓ.

2. The pumping rates for hydraulic pipeline dredges can develop large-scale mud systems of high energy that are capable of travelling thousands of feet before their energy is finally dissipated. These flows are surprisingly dynamic in the manner in which they move over the bottom, and they reflect many of the characteristics of natural submarine mud flows.

3. In view of the highly dispersive nature of these mud systems, it becomes essential to predict their spreading characteristics so that the dredged material stays within the bounds of the designated disposal

---

* A table of factors for converting U. S. customary units of measurement to metric (SI) units can be found on page 10.

area and the impact of turbidity generation on the environment and community can be minimized. In any approach to the problem of prediction, the first step must be that of determining the dynamic properties of a fluid mud system whose source is continuous, and its behavioral response to changes in dredging operational procedures and environmental parameters. A program of this nature would be difficult to implement in the field because of the lack of control over current, waves, and slurry density. It is better suited to the laboratory where parameters can be controlled and effects uncoupled.

Purpose

4. The objective of this program was to improve the basic understanding of the dynamics of fluid mud dispersion by assessing the effect of certain system parameters on the dispersion process. The laboratory program was performed in order to quantify the influence of sediment composition, bottom slope, discharge velocity, slurry flow rate, salinity, current, and waves, thereby providing data that would aid in the evaluation and interpretation of field measurements of fluid mud behavior.

Scope

5. The objective of the project was accomplished by means of a laboratory test program with the capability of generating reproducible mud flows, varying environmental conditions, and measuring the resulting behavior of the system. The test matrix was arranged so that the control of each variable was established with respect to a reference baseline test condition. The independent variables included salt content of the sediment, three slurry suspension concentrations, five bottom slopes including upslope and downslope directions, three slurry flow rates, three current conditions including flow direction, and four surface wave conditions. Measurements were recorded for head wave velocity,

cloud height, fluid mud layer thickness, suspended solids concentration, and bottom sediment deposition. A total of twenty-five tests were conducted to fulfill the program requirements.

CHAPTER II: NATURE OF MUD FLOWS

6. A mud flow is a layer of fluid mud[2] that travels along the bottom of a body of water under the influence of gravity forces. It flows in the downslope direction away from the point of deposition on the bottom. The fluid mud is a mixture of sediment and water that is denser than the surrounding water column. The fact that a sediment-laden mass of water behaves as a homogeneously denser fluid was proposed by Forel in 1887 (in Dunbar and Rogers[4]) as the reason why denser turbid river waters flowed under the clear water of the lakes into which they discharged. In 1973 Kuenan[5] demonstrated in the laboratory that a sediment layer under a less dense water layer flows downslope under the forces of gravity. The sediment slurry is miscible with water in the sense that it can entrain water and be diluted if some degree of turbulence or agitation is provided to keep the solid sediment grains suspended. In the absence of turbulence the suspended sediment tends to settle to the bottom leaving the water column clear.

7. Natural sediment flows can be steady or they can be catastrophic. An example of the former is the flow of the Colorado River into Lake Mead. The sediment-laden river water discharges steadily into the upper end of the lake where it forms a continuous flow over the bottom under the clear, less dense lake water along the old river bed all the way to Hoover Dam, 120 miles downstream. When the Colorado River is in flood, the sediment flow moves at approximately 1.0 fps at the upper end of Lake Mead, but slows to 0.25 fps as it approaches Hoover Dam.[6] The classic example of a catastrophic mud flow or turbidity current originated during the Grand Banks earthquake of November 18, 1929.[7] The quake apparently caused the downslope movement of enormous masses of loose sediment. These masses entrained water and became dilute and fluid as they travelled downslope. Many submerged cables crossing the area, were severed by the leading edge of the turbidity current. From the recorded

break times and the cable locations investigators were able to trace the movement and establish the velocity of the turbidity current as it flowed down the slope from the continental shelf at 200 fathoms out onto the abyssal plane at 2800 fathoms. During the descent the moving sediment layer traversed a distance of more than 400 nautical miles in 13 hours. The leading edge travelled at 55 knots on the continental slope, but slowed down to 12 knots as it reached the ocean floor. It undoubtedly travelled many miles further before it finally came to rest. The widely different behavior of the Colorado River sediment flow and the Grand Banks turbidity current can probably be attributed to the higher energy developed by the enormous mass of material involved in the latter as well as the greater initial slopes.

8. The mud flows generated by an open-water pipeline disposal operation can be characterized by several distinct features. The pipeline discharge configuration may impart a directional property to the mud flow. If the discharge pipe is aimed vertically downward, the mud spreads in a radially symmetrical pattern from the point where it impacts the bottom. If the pipe is initially horizontal and either submerged or out of water, the mud flows along the bottom in a highly directional pattern that is centered on the azimuth angle of the pipe. Beyond the immediate region of the impact point the sediment layer comes under the influence of bottom slope and tends to flow in the direction of steepest downslopes of the bottom surface. The leading edge of the mud flow may form a distinct head wave immediately behind which follows a mud flow of relatively uniform thickness. The spreading and flowing phenomenon is somewhat analagous to that of light oil pouring onto a flat plate. As the oil puddles at the point of impact, the thickness of the puddle generates a hydrostatic pressure that cannot be sustained by the edges of the puddle. Consequently, the boundaries of the puddle move radially outward thereby reducing the hydrostatic pressure. If the plate is set at a slight angle, the oil will flow down the plate due to gravity forces acting on the oil layer.

The behavior of the mud layer on the bottom is similar except that the equivalent gravity force is reduced by the buoyant force acting on the mud layer.

9. The characteristics of the mud flow are controlled by the internal flows that exist within the head wave and the uniform layer that follows behind it. Previous mud flow studies conducted at JBF by Neal and Henry[8] demonstrated the nature of two-dimensional sediment flow within the head wave. As the head wave moves forward, sediment that is supplied to it sustains its motion. This sediment flows along the bottom at a forward velocity exceeding that of the head wave. When the sediment flow reaches the head wave, it rotates upward and over (Figure 1) as if in reaction to the wall of water ahead of the wave. As the sediment mixture rotates at the leading edge of the head wave, it opens to form a miriad of approximately vertical folds between which water enters the head wave envelope and becomes entrained. By the time the sediment reaches the top of the head wave its velocity is close to zero. An overview of the head wave shows it laying down an apparently stationary cloud behind it as it advances.

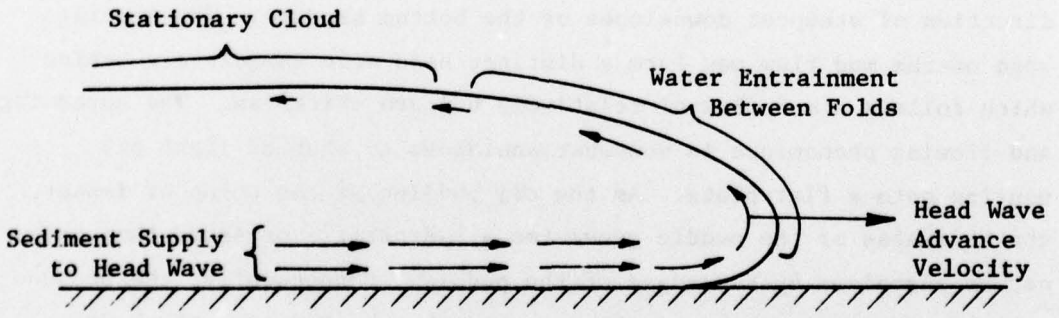

Figure 1. Sediment flow through the head wave

10. Underneath the stationary cloud and obscured by it is the active fluid mud flow that transports sediment to the head wave and away from the source of mud supply. From the schematic of the head wave, Figure 1, the main flow of fluid mud to the head wave is along the bottom so that velocity and concentration maximums occur within this fluid mud layer. In connection with modelling studies on sediment density currents, Tesaker[9] measured profiles in nearly uniform currents in both the laboratory and the field that demonstrate these characteristics. For illustration one set of Tesaker's profiles is reproduced in Figure 2 for a laboratory flow on a 1:10 slope.

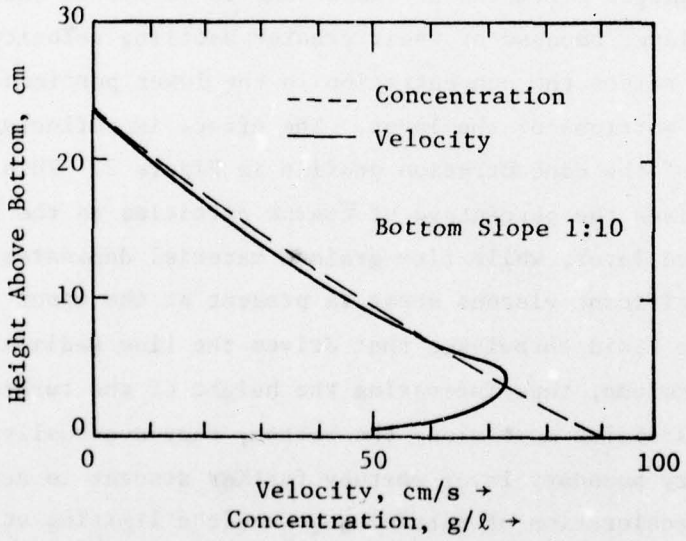

Figure 2. Profiles through a uniform mud flow (from Tesaker[9])

The motion of the mud layer over the bottom generates shear that results in the development of a velocity boundary layer at the lower interface as shown in Figure 2. A similar viscous shearing action occurs between the moving mud layer and water column above it. This is indicated in Figure 2 by the gradual diminution of velocity through the upper strata of the mud layer. The combination of viscous effects at both interfaces creates a maximum in the velocity profile at an intermediate height above the bottom.

11. In addition to viscous effects, the settling characteristics of the sediment play an important role in the behavior of the mud layer. The sediment is characterized by a grain-size distribution which in dredging operations may encompass sand (>0.62 mm), silt (0.0039 mm to 0.062 mm), and clay (<0.0039 mm) sizes. As the mud layer flows along the bottom the larger particles or flocs tend to settle to the lower portion of the layer because of their greater settling velocity. This settling action raises the concentration in the lower portions and lowers it in the upper portions of the layer. The effect is reflected in the negative slope of the concentration profile in Figure 2. This settling process also raises the percentage of coarse particles in the lower levels of the mud layer, while fine-grained material dominates the upper levels. If significant viscous shear is present at the upper interface, it will generate fluid turbulence that drives the fine sediment higher into the water column, thus increasing the height of the turbidity cloud. As the coarse particles move along the bottom, they eventually fall into the velocity boundary layer whereby further descent is accomplished by horizontal deceleration of particles. Once the limiting velocity for transport is reached, the particles settle out onto the bed. Partheniades and Mehta[10] established that a constant interaction takes place between the processes of deposition and bed erosion so that, while particles settle out from the fluid mud layer, other part[illegible]y simultaneously undergo erosion and become resuspended within [illegible]flow. When deposition and resuspension rates are equal, a sta[illegible] equilibrium exists and

the mud layer flows uniformly. If the deposition process dominates, the concentration of sediment in the mud layer diminishes as the material is deposited on the bed. If resuspension dominates, the sediment bottom is eroded while a solid bottom promotes uniform mud flow. Steeper bottom slopes raise the shear stress on the bed, thereby inhibiting the deposition process and enhancing rates of sediment resuspension.

12. With the fine-grained estuarine sediments encountered in maintenance dredging operations, settling characteristics are largely determined by the process of flocculation. Discrete particles are attached to one another to form larger flocs which in turn may stick to other flocs to form flocs of varying sizes. By virtue of its increased size, the floc has a greater fall velocity and settles faster than the individual particles. In estuarine environments flocculation of fine-grained material with particle diameters less than 0.030 mm is enhanced by the salinity of the water.[11] At suspension concentrations less than 0.3 g/ℓ, flocculation may not be appreciable because the particles are too widely spaced and contacts are too infrequent. In the range 0.3 to 10 g/ℓ, flocs form but in limited number and size because of the relative scarcity of sediment grains.[12] The flocs behave as individual particles in that they settle onto the bed and by resuspension take part in the continuous interchange of bed and suspended materials. Turbidity clouds generally fall in this concentration range up to 10 g/ℓ and hence are typified by the properties of these low concentration regimes. Above a solids concentration of 10 to 15 g/ℓ, flocs form a matrix of "fluff".[11,12] The settling of the flocced sediment proceeds only as fast as the interstitial water between the flocs can migrate upward through the matrix.[12] Because the structure of the matrix inhibits the settling action,[12] the process is referred to as "hindered settling". Since hindered settling occurs between suspension concentration of 10 to 200 g/ℓ ,[12] the "hindered settling" regime represents the properties and behavior of fluid mud. Beyond a concentration of 200 g/ℓ the floc matrix starts compressing under its own weight followed by a gradual breakdown of the floc matrix/structure.[13]

Throughout this transition phase, as interstitial water is released, bulk density of the sediment increases and the sediment gradually develops rigidity that prevents it from flowing as in the "hindered settling" phase.

13. Inasmuch as this laboratory study deals with the behavior of dynamic mud systems, primary concern is with the settling regimes up to and including "hindered settling" since this encompasses "fluid mud". Suspension concentrations of the pipeline slurry are maintained close to the upper limit for this regime (200 g/ℓ) while the maximum solids concentrations in the fluid mud layer are lower than the pipeline values by a factor of approximately two. In the subsequent sections of this report mud flow or mud system refers to the total mud layer comprised of the upper turbidity layer and the lower fluid mud layer. The turbidity layer or cloud is the upper layer of the mud flow extending from the clear water boundary (0.0 g/ℓ) down to the 10-g/ℓ isopleth. In this layer there is a constant interchange between material in suspension and in the upper levels of the fluid mud layer. The fluid mud layer is the denser bottom layer of the mud system extending from the 10-g/ℓ isopleth to the bottom. It reflects the properties of the "hindered settling" regime.

CHAPTER III: EXPERIMENTAL FACILITIES AND PROCEDURES

14. The test facilities that were utilized in this program included a large laboratory test tank and several support systems required to simulate the operating conditions and variables prescribed in the study. The support system included a freshwater supply, a saltwater mixing facility, a mud supply system, a recirculating current loop in the tank, and a wave generator. Hardware was built for water sampling stations and bottom sediment traps. Test procedures were developed for the operation of these support facilities, and laboratory procedures were designed for the evaluation of samples and sediment properties. The above facilities and procedures are described in detail in this Chapter.

Experimental Facilities

Test Tank

15. The test tank was specially designed for mud flow studies. It was constructed of wood and measured 32 ft long x 8 ft wide x 30 in. deep. Three Plexiglas viewing windows, each 4 ft long x 30 in. high, were installed in each side of the tank for visual access. Sump troughs were located at each end of the tank across its full width to facilitate filling, emptying, and cleaning procedures. External cross-over plumbing permitted filling and/or emptying from either or both ends and during emptying afforded good control over turbulence that tended to disturb the bottom sediment before the traps were removed. A portable wooden partition was installed lengthwise down the center of the tank to form two 4-ft-wide test sections. Previous studies showed that the 4-ft width had little or no effect on the flow properties of a unidirectional fluid mud system as compared to an 8-ft width. Use of the partition reduced the water usage from 3500 gals/test to 1750 gals/test and reduced the per test expense of filling, emptying, and cleaning the tank by the same factor. The two sides of the tank were isolated from each other by means of a pneumatic seal around the edges

of the partition and plate seals in the troughs. For the sloped bottom tests a false bottom was installed on each side of the tank. On one side the bottom was sloped at 1 degree and the other at 2 degrees so that all of the sloped tests (upslope and downslope) could be run with the two bottoms. Figures 3 and 4 show top and side views of the test tank.

Water Supply

16. The test plan required salt water of 10 ppt salinity for all tests except the one that utilized freshwater sediment in fresh water. The salt water was manufactured in the laboratory by dissolving enough granular salt in the tank of fresh water to raise its salinity to 10 ppt. Town water was used for the freshwater source although it contained such high levels of suspended solids that underwater visibility was too poor for photographic purposes. Water clarity was greatly improved by filtering during the filling cycle using a Purex filter, Model 2048 (Figure 5). This was a diatomaceous earth filter (48 sq ft) which in series with the town supply delivered clear water at the rate of 100 gpm. The granular salt was first dissolved in 300 gals of water in a brine tank that was equipped with an electric stirrer (Figure 6). The brine solution was then pumped through the Purex filter to remove undissolved solids, then directly into the clean empty test tank. Freshwater was then valved through the filter to the test tank until the water depth reached 24 in. Underwater visibility exceeded tank length (31 ft), and salinity was uniform throughout the water column.

Mud Supply

17. A complete processing procedure was developed for the preparation, mixing, and delivery of the mud slurry to the test tank. The consolidated in situ mud was initially weighed and a sample taken in the center of the mud mass. In situ solids ratio and moisture content were determined from the sample and along with the mud weight enabled the determination of the amount of water to be added to obtain the prescribed solids ratio for each test. The mud and water were combined

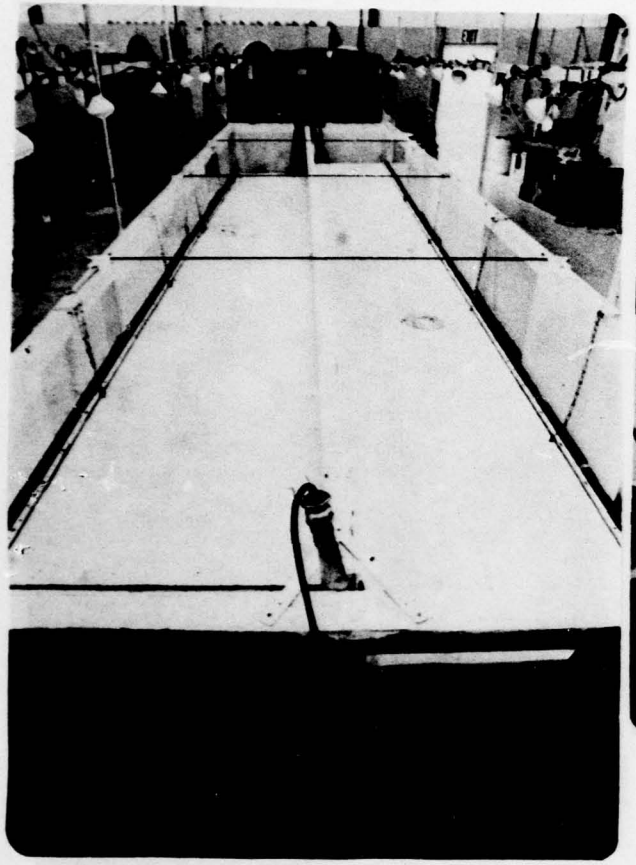

Figure 3. Test tank

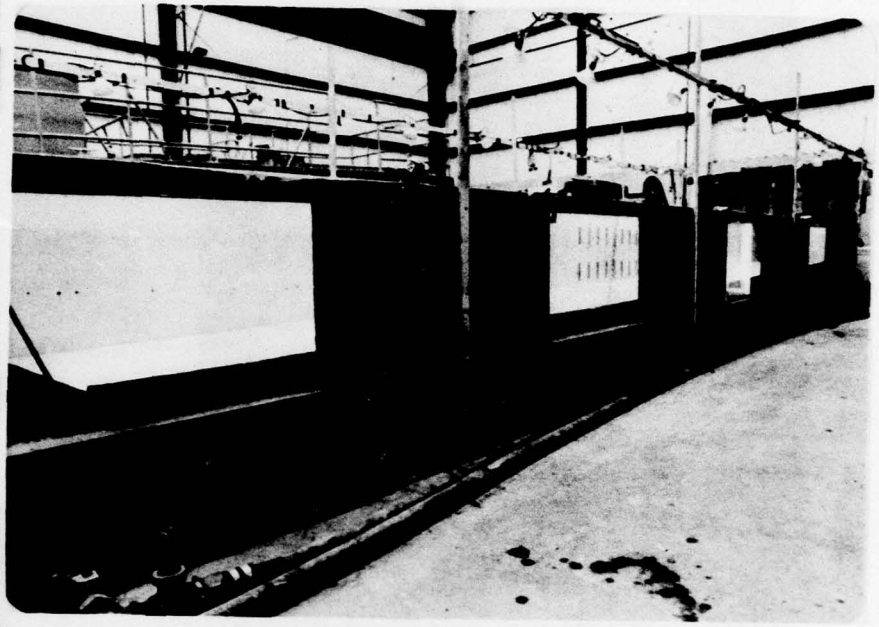

Figure 4. Test tank with sloped bottom

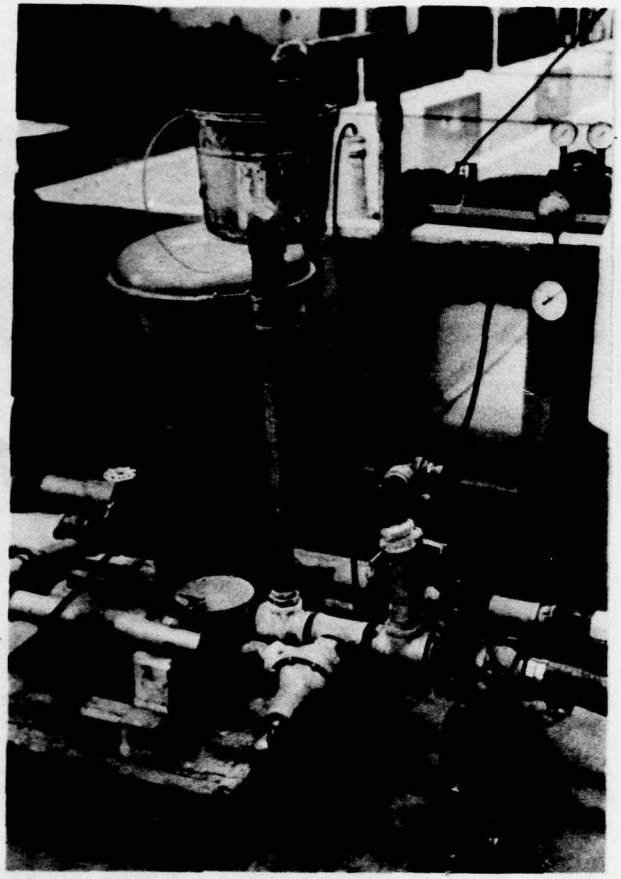

Figure 5. Filter for freshwater supply

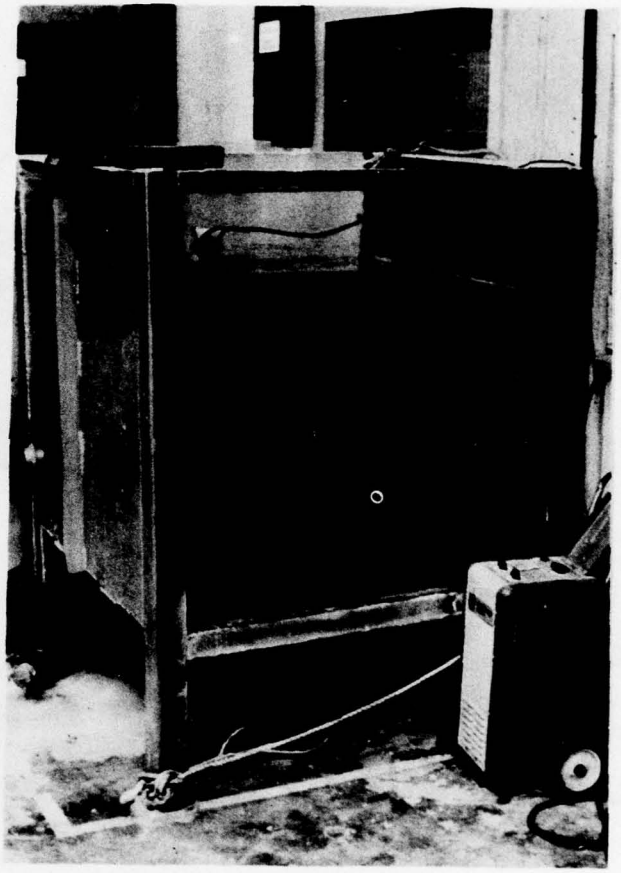

Figure 6. Brine tank

and stirred until the mixture was homogeneous. The slurry was passed through a mesh screen to remove large debris and was then stored in a 400-gal reservoir tank. The tank was located outside the laboratory because of the odor given off by the mud, and it was protected from the weather by a temporary enclosure that was maintained at shop air temperature. Approximately 350 gals of slurry was prepared at each mixing, and this quantity was enough for at least four tests. The last step in the slurry preparation was to add sufficient salt to the contents of the tank to raise the salinity of the slurry to 10 ppt, equal to that of the tank water. In shakedown tests it was found that lower salinity slurry generated turbidity "fingers" that rose out of the turbidity layer of the mud flow. The condition disappeared when the slurry salinity was raised to or above the water salinity.

18. For a period of at least an hour before each test, the mud slurry was stirred and recirculated continuously in order to keep the solids suspended. The plumbing schematic for the system is shown in Figure 7. The reservoir tank is shown in Figure 8; the transfer pump and control plumbing are pictured in Figure 9. In the recirculation mode valves A and B were open, valves C and D were closed. During a test, valves A, C, and D were open and the slurry flow rate to the tank was controlled by valve B. At maximum delivery valve B was closed and the flow rate at the tank was 33 gpm. Immediately before each test, valve B was adjusted and the flow rate was calibrated by timing the volume of slurry discharged into a calibration barrel at the test tank end of the system (valve B). The sampling valve was used to take slurry samples before and after each test as a monitor on solids content. After each test the contents of the delivery hose were drained back into the reservoir tank.

Sediment Properties

19. Each of the two sediment types was analyzed for grain-size distribution and total organic carbon. The Boston Harbor (saltwater) sample was a composite of samples taken from each of thirty-one 55-gal

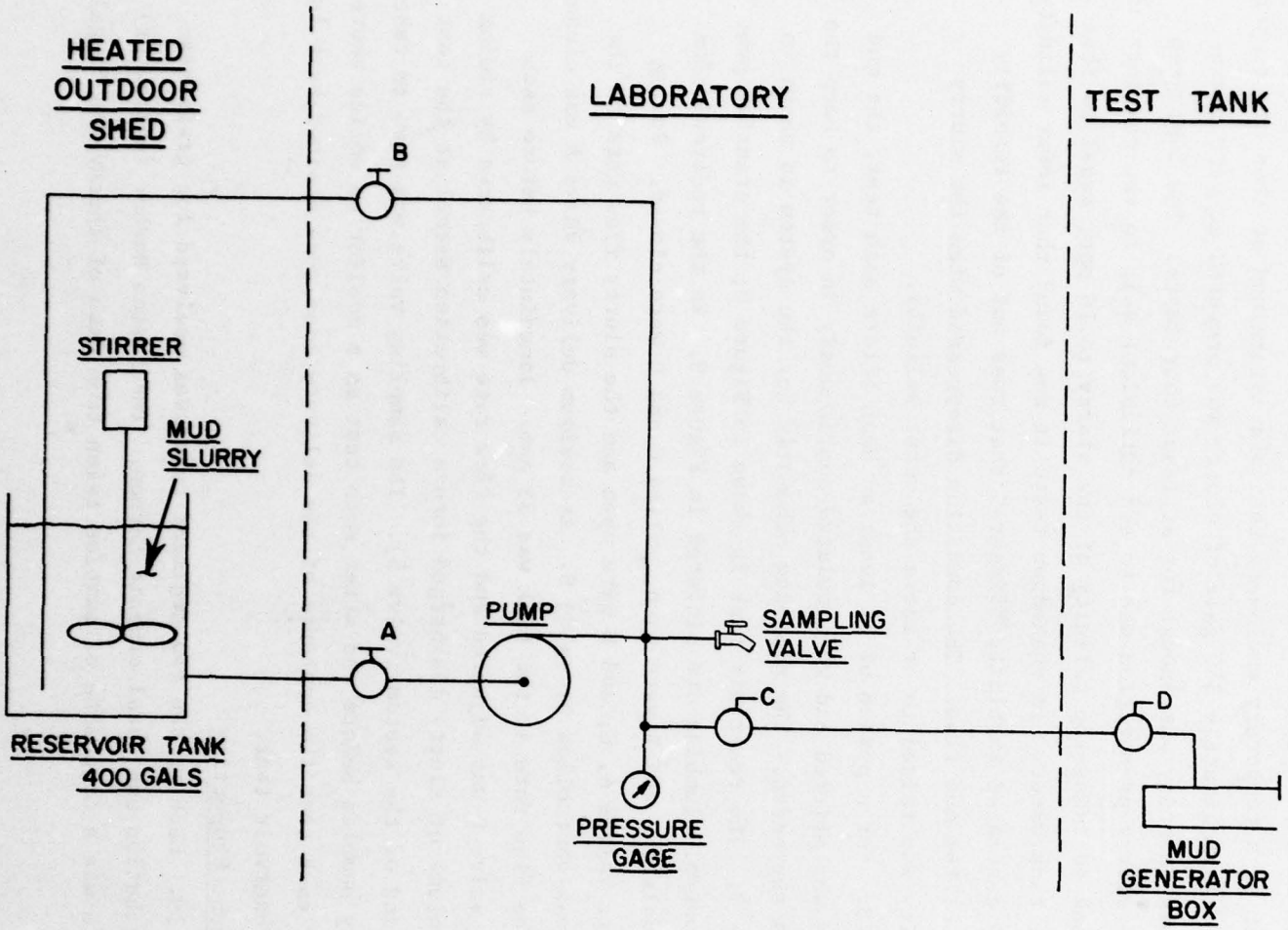

Figure 7. Plumbing schematic, mud supply system

Figure 8. Slurry reservoir tank

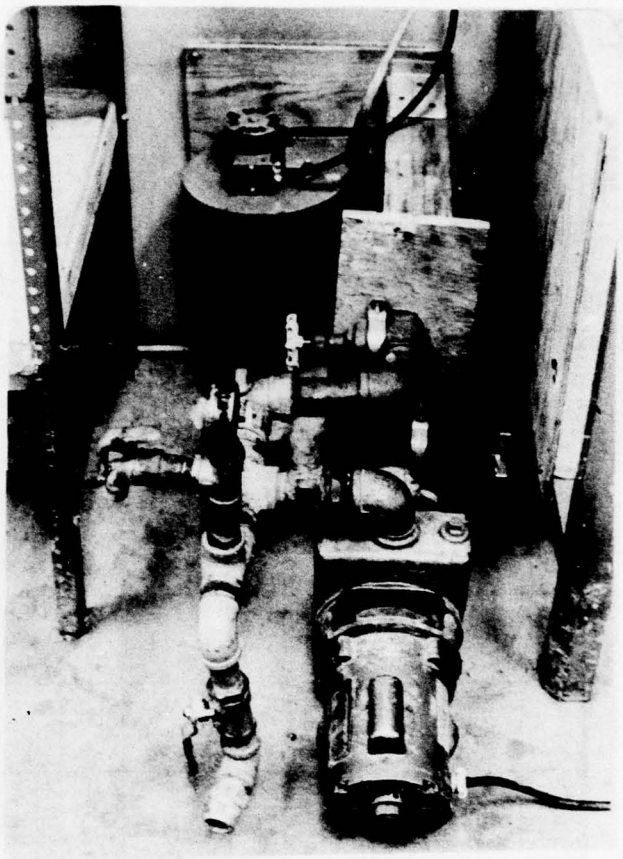

Figure 9. Slurry transfer pump and flow controls

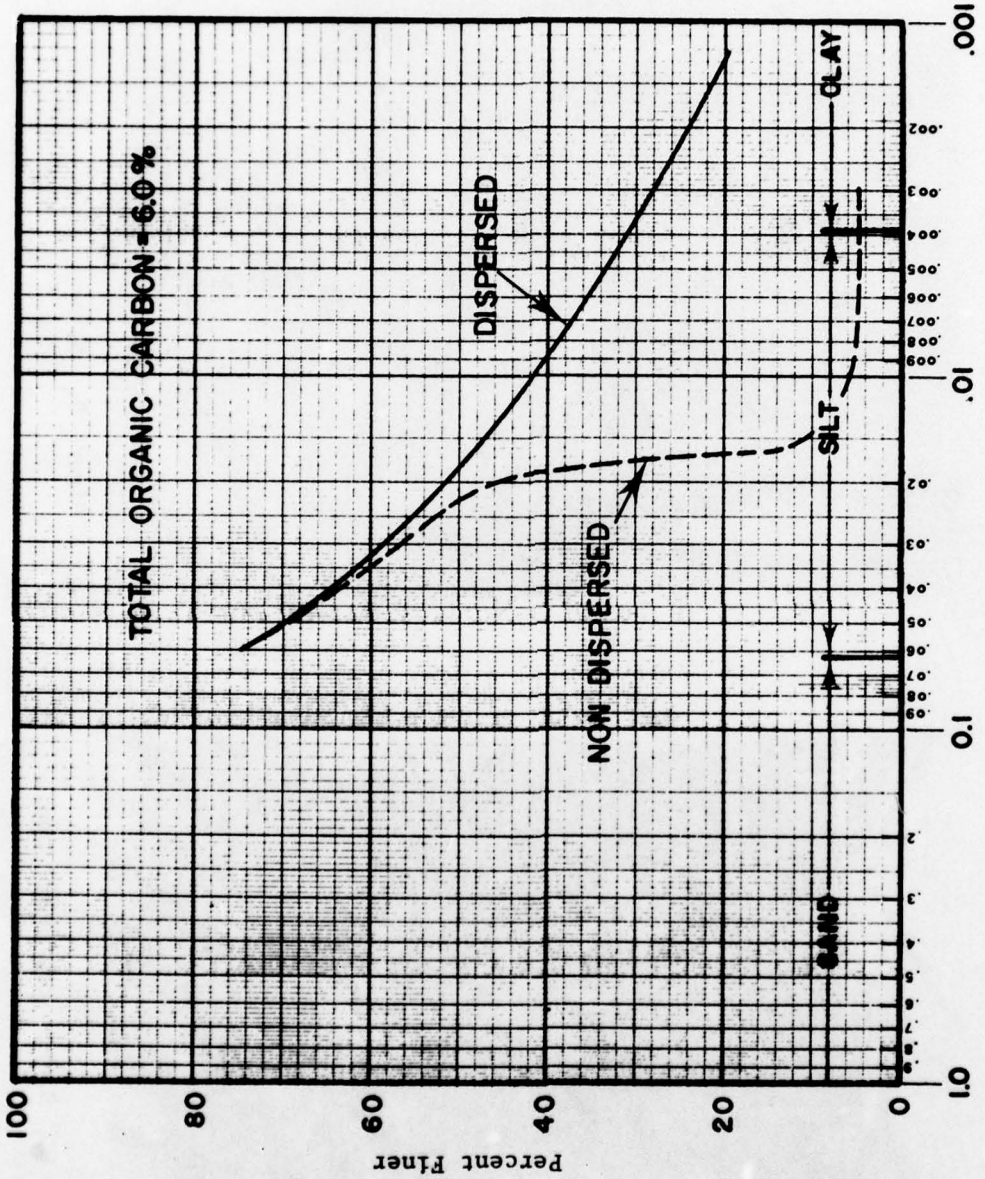

Figure 10. Grain-size distribution for saltwater (Boston Harbor) sediment

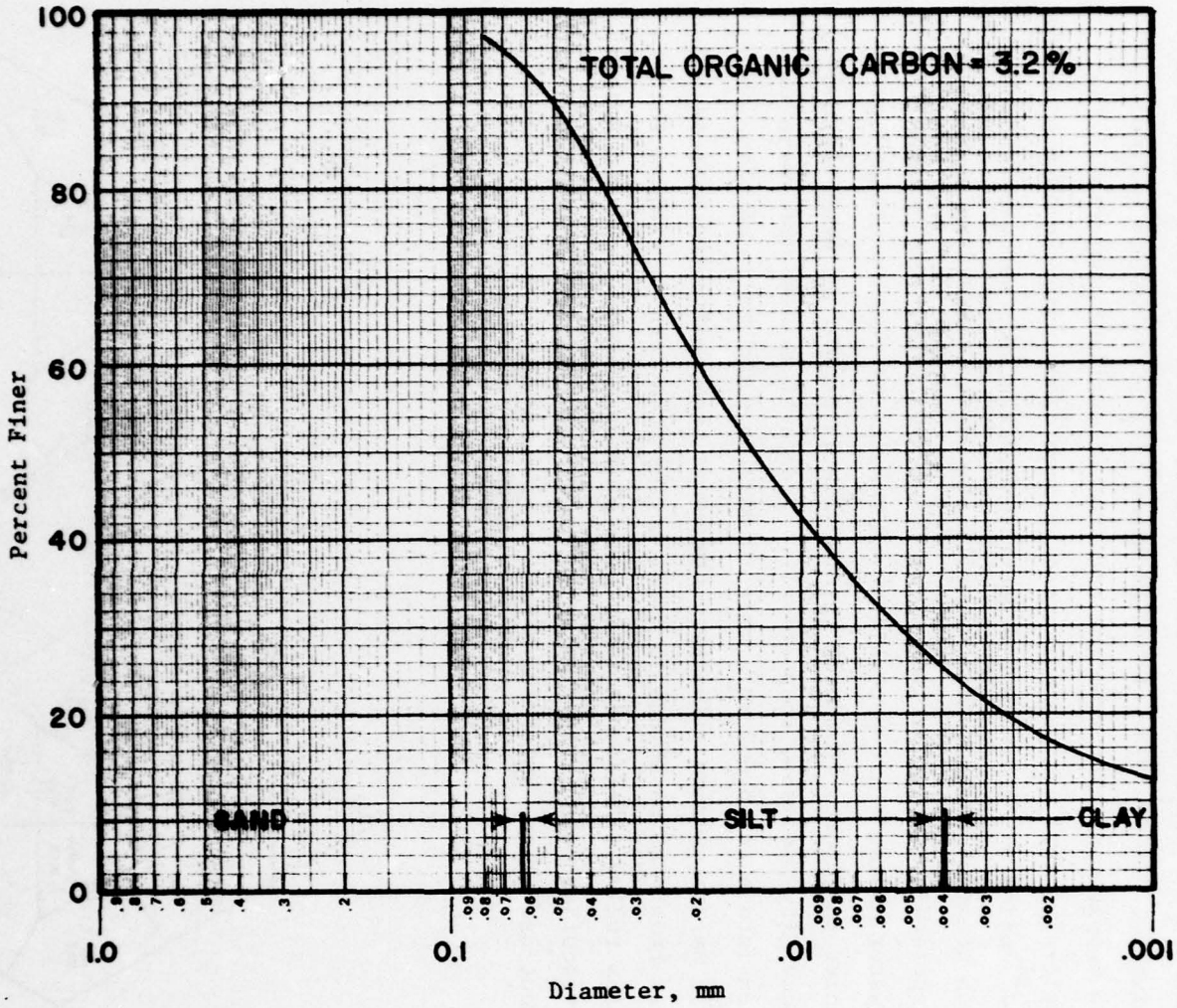

Figure 11. Grain-size distribution for freshwater (Michigan City) sediment

drums. The 31 samples were of equal volume and were taken at the center of each drum. They were combined in a single container and stirred until the mixture was homogeneous. The composite sample was then taken from the mixture. In the case of the Michigan City (freshwater) sediment a single sample was taken from the one drum of available material. The particle-size analysis was performed in accordance with the ASTM standard method[14] using a 151 H ASTM hydrometer. A dispersed test was conducted on each sediment using sodium metasilicate as the dispersing agent. A nondispersed test was carried out on the Boston Harbor sediment in a salt-water medium of 10 ppt salinity. Results of these analyses are presented in Figures 10 and 11 for the Boston Harbor sediment and the Michigan City sediment, respectively. The particle diameter range is divided into sand (0.062 mm), silt (0.0039 to 0.062 mm), and clay (0.0039 mm) categories. The percentages of sand, silt, and clay as derived from Figures 10 and 11 were plotted on a ternary diagram that contains twelve (12) distinct textural classes (Figure 12). The Boston Harbor sediment was classified as a "silty mud" and the Michigan City sediment as "clayey silt."

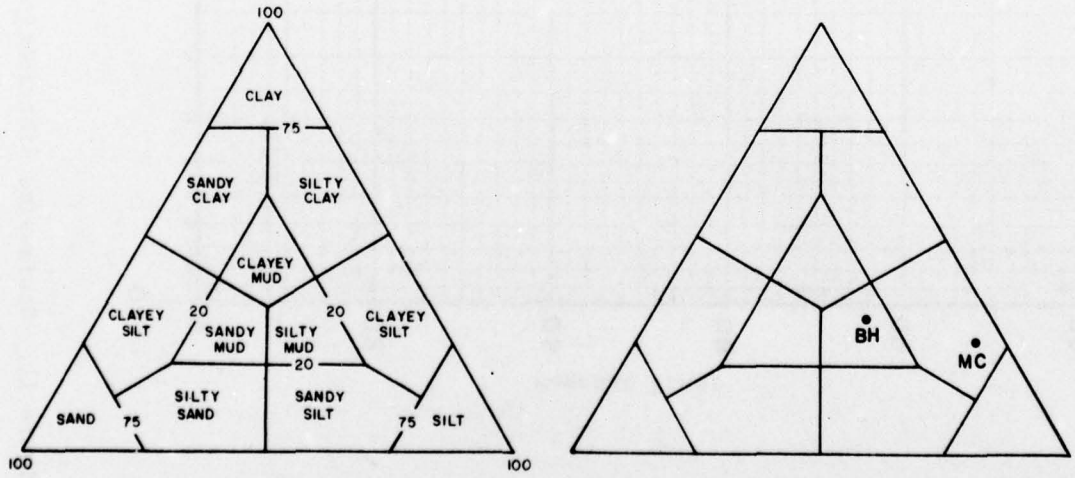

Figure 12. Textural classification of test sediments (after Shepard[15])

Total organic carbon content (TOC) is noted in Figures 10 and 11 for each sediment. TOC was determined by the combustion-infrared method as outlined in Standard Methods.[16]

Mud Flow Generator

20. The mud flow generator was the last component on the end of the mud delivery system (Figure 7); its function was to transform the pipeline slurry flow into a mud flow that propagated along the bottom of the test tank. From previous research on submerged discharge designs for open-water disposal operations,[8] it was known that the characteristics of the resulting mud flow reflected the design of the discharge system. Thus, a near horizontal pipe discharge, submerged just above the bottom, produces a high-velocity, thick head wave that exhibits some wall effects and generates excessive water column turbidity in the region around the impact point. The sediment concentration also suffers an order of magnitude dilution due to water entrainment as the sediment flows through the free jet, impinges on the bottom, and stabilizes in the direction of mud flow. A vertical discharge pipe, submerged but above bottom, produces an axially symmetric mud flow that is slow moving, thin, and turbidity free. It displays minor wall effects and a back flow that rebounds off the end wall and travels back to and through the discharge area. A vertically oriented conical shroud with circumferential bottom opening produces an axisymmetric mud flow with medium head wave velocity and thickness equivalent to the height of the bottom opening.

21. In accordance with previous experience the design requirements for the mud flow generator were specified as follows:

a. Slurry density will be maintained and controlled prior to discharge from the mud flow generator to ensure that the concentration of the discharged fluid mud layer will be known. Specifically, the slurry will be contained within the mud flow generator to prevent contact with the water column with attendant mixing and entrainment.

b. The fluid mud flow will be two dimensional at the discharge of the generator (i.e., it will be uniform across the width of the test channel) in order to eliminate wave reflections off the sides of the test tank.

c. The fluid mud system will be directed down the tank in one direction thereby eliminating back flows and end wall reflections.

d. The design will incorporate an adjustable discharge slot to control the thickness of the fluid mud system.

The specifications required that the two-dimensional fluid mud system be formed inside the mud flow generator so that upon discharge it would be of the proper physical size and configuration and its average density closely related to that of pipeline slurry. The best of several designs that were built and tested in the tank was the final design shown in Figures 13 and 14. It consisted of a flat box 36 in. long x 18 in. wide x 4 in. high that was closed except for the discharge slot along the bottom edge of the 36-in. side. The slurry was pumped vertically downward into the box through four 0.5-in. pipes that were equally spaced along the back edge of the box. The forward edge was adjustable so that the slot opening could be varied, and it was fitted with a curved cylindrical nozzle piece that smoothed the discharge flow. The flow path of the slurry through the box can be seen from the section view shown in Figure 14. The slurry flowed down through the four 0.5-in. pipes and into the box whereupon it impinged on the bottom, turned toward the open slot, and flowed out through the cylindrical nozzle along the bottom of the tank. Several shakedown tests were conducted in the test tank from which the baseline or reference operating conditions were established at a 2-in. slot height, a 22-gpm slurry flow rate, and a 15-pcs (percent solids) ratio. This combination produced a fluid mud flow of significant height (2 to 3 in.) and head wave speed that allowed a test period of approximately 3 minutes. The slurry flow rate was comfortably within the capability of the mud delivery system and the mud inventory.

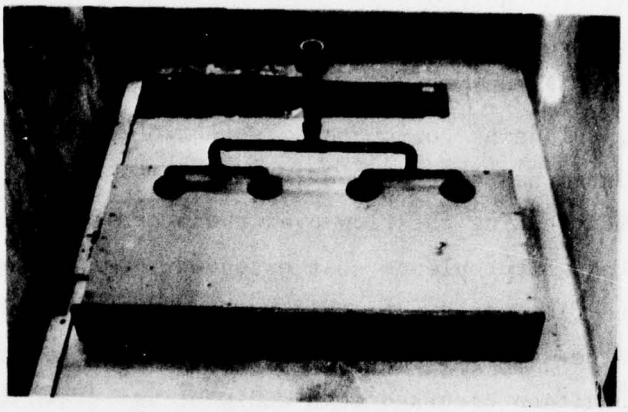

Figure 13. Mud flow generator box

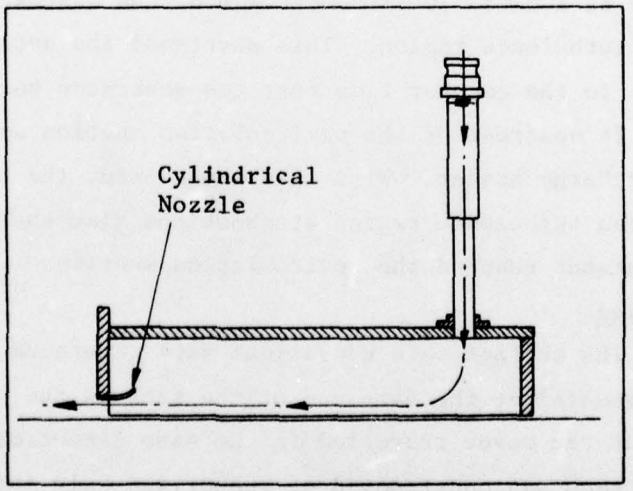

Figure 14. Section of mud flow generator box

Water Current Generator

22. Water current was generated in the test tank by recirculating water from one end to the other. A portable 375-gpm diesel pump drew the water from the downstream end of the tank and discharged it at the upstream end through a perforated header box that distributed the flow evenly over the cross-sectional flow area of the tank. At full power the recirculating system produced a maximum water current of 6 fpm over the 4-ft-wide x 2-ft-deep test channel. The current was measured by timing the travel velocity of a drogue.

23. In planning the current tests two limitations of the recirculating system had to be borne in mind. The discharge header box, although distributing the flow over the cross-sectional area, created a region of high turbulence that extended approximately 8 ft downstream. When the mud flow moved into this region it was immediately resuspended throughout the water column and visibility fell to zero. The other limiting condition occurred when sediment was drawn into the suction of the recirculation system. In a matter of seconds the sediment passed through the pump loop, out the discharge header, and into the turbulence region where it was dispersed throughout the water column and obscured the test area. In the parallel flow test the mud generator box had to be located 10 ft downstream of the discharge header box to avoid the turbulence region. This shortened the available test length to 16 ft. In the counter flow test the generator box had to be positioned 12 ft upstream of the recirculation suction and 16 ft downstream of the discharge header. With this arrangement the head wave reached the upstream turbulence region at about the time the turbidity in the counter current reached the recirculation suction.

Wave Machine

24. The surface wave conditions were generated by a wave machine that was mounted at the same end of the tank as the mud flow generator box so that the waves travelled in the same direction as the mud flow. A sloped beach was constructed of rubberized hair and mounted at the downstream end of the tank to eliminate reflections. The wave machine

consisted of a 42-in.-wide vertical paddle that was submerged 12 in. and hinged along its bottom edge. The paddle was driven by a rotating crank assembly that was powered by an air-driven reduction gear and an adjustable belt and pulley drive. The period of the wave was set by the rpm of the crank which could be controlled by adjusting both air pressure to the air motor and the reduction through the pulley drive. Wave amplitude was controlled by adjusting the length of the crank arm. A wave gauge was painted on the partition wall to indicate wave height. The wave machine is pictured in Figure 15.

Tank Markers

25. A series of vertical yardsticks was employed to indicate downrange distance and the heights of the head wave and the turbidity cloud. The yardsticks were positioned at 4-ft intervals along the center of each test tank starting at the origin (0 ft). They were located at ranges of 0, 4, 8, 12, 16, 20, and 24 ft, and stripes were painted on the bottom at 1-ft intervals for purposes of interpolation. The yardsticks were made from sheet metal and were thin so that when placed edge-to-the-flow they did not disturb the flowing mud nor did the mud move them. The scale on the yardsticks was color-coded to aid in reading heights. The range of each marker was marked clearly on the yardsticks so that it appeared in the photographic data.

Water Sampling System

26. The water sampling system was organized around the use of a sampler assembly that took four samples simultaneously at a fixed location. The assembly mounted four 50-cc syringes that were outfitted with 0.25-in. suction tubes. These were shaped and cut to lengths such that the samples were drawn horizontally at tube centerline heights of 3/16, 1/2, 3/4, 1-1/2 in. above the bottom of the tank. The syringe assembly is shown in Figure 16. The assembly was mounted on a vertical rod such that, when the end of the rod rested on the bottom, the tube ends were at their proper heights above the bottom. The lengths of the tubes were set so that the syringes were well above the turbidity cloud and did not interfere with the motion of the mud system. The plunger

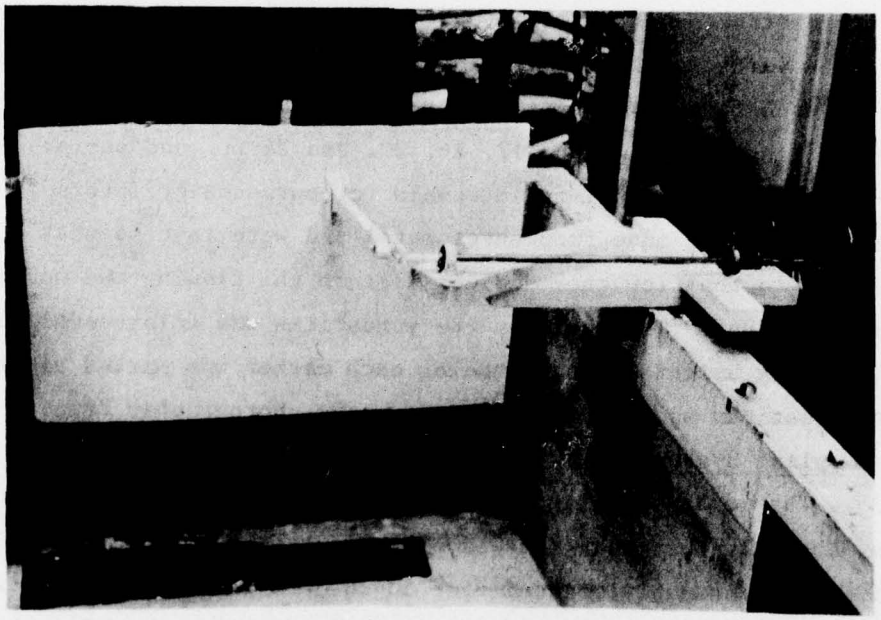

Figure 15. Wave machine

Figure 16. Syringe assembly

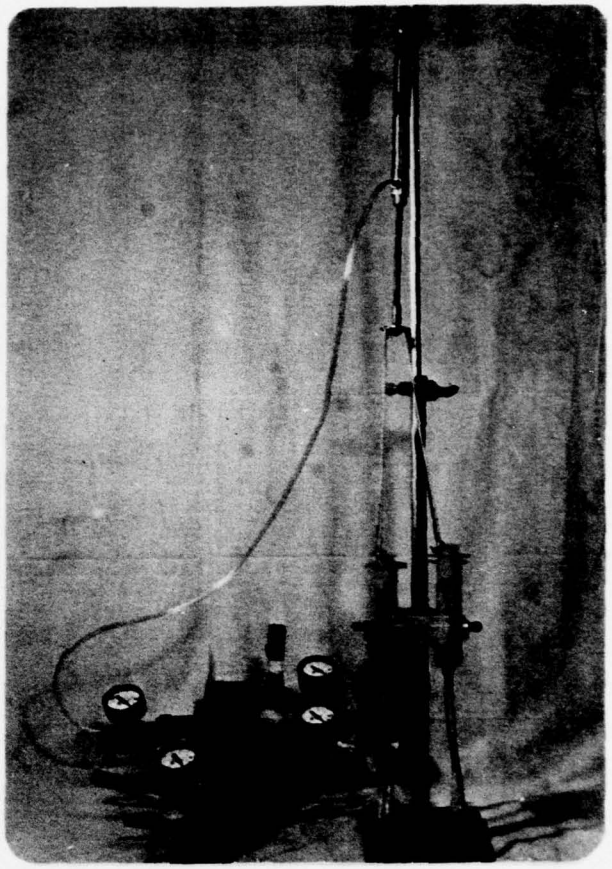

Figure 17. Water sampler assembly

of each of the four syringes was connected to a single pneumatic cylinder that simultaneously actuated all four plungers of the sampler assembly as shown in Figure 17.

27. A total of six water sampler assemblies, distributed at three locations along the tank, were actuated at three times during the test according to the progress of the head wave. These locations and the timing sequence are outlined in detail in Appendix C. The air lines to each sampler assembly were connected to a common manifold that incorporated shutoff valves and pressure gauges (Figure 17). At each sampling time the appropriate sampler assemblies were actuated by opening a single valve that pressurized their cylinders simultaneously.

Bottom Sediment Samples

28. As an outgrowth of earlier testing, bottom samples of settled sediment were obtained with a thin-walled sediment trap that sat on the bottom of the tank. The trap had the shape of a shallow channel and was formed by bending up opposite sides of a piece of sheet brass. The sides were aligned parallel to the flow direction to cause least disturbance to the motion of the mud system. Traps were located at every distance marker (4-ft intervals) over the 24-ft test length.

Photographic Equipment

29. Each test was visually recorded using both still and motion photography. The still photography was conducted with two 35-mm Nikon cameras, one hand-held and the other motor-driven and actuated automatically by an electronic timing control. The hand-held camera was used to follow the head wave as it moved down the tank, while the automatic camera was set up to monitor the discharge of the mud flow generator. The motorized camera and the electronic camera timing control are shown in Figures 18 and 19, respectively. Motion photography was obtained with a Nikon 8X Super 8 camera and was used exclusively for side coverage of the fluid mud system, particularly the head wave. Since the film was used as a timing device, each roll was time-calibrated by photographing a stopwatch, and once started the

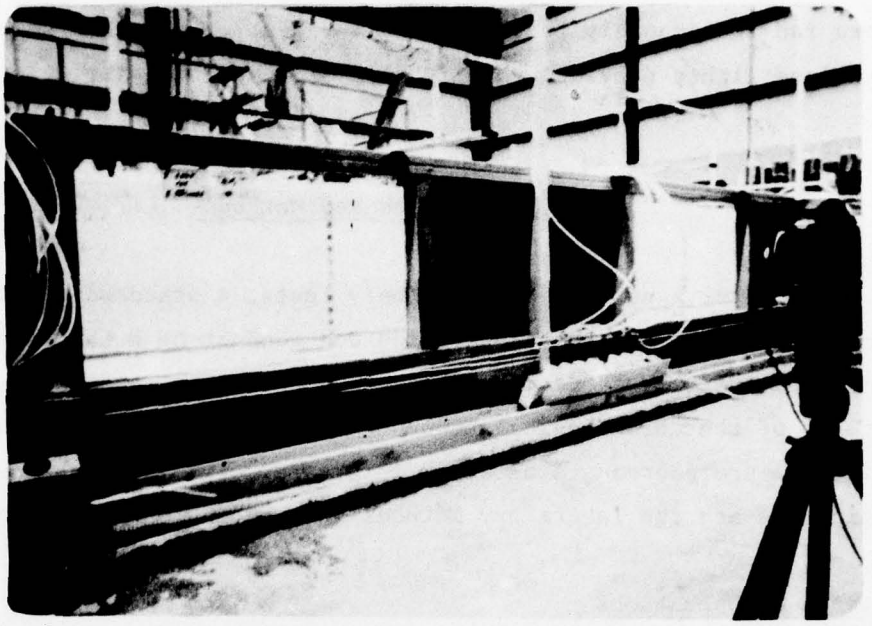

Figure 18. Motorized camera in position

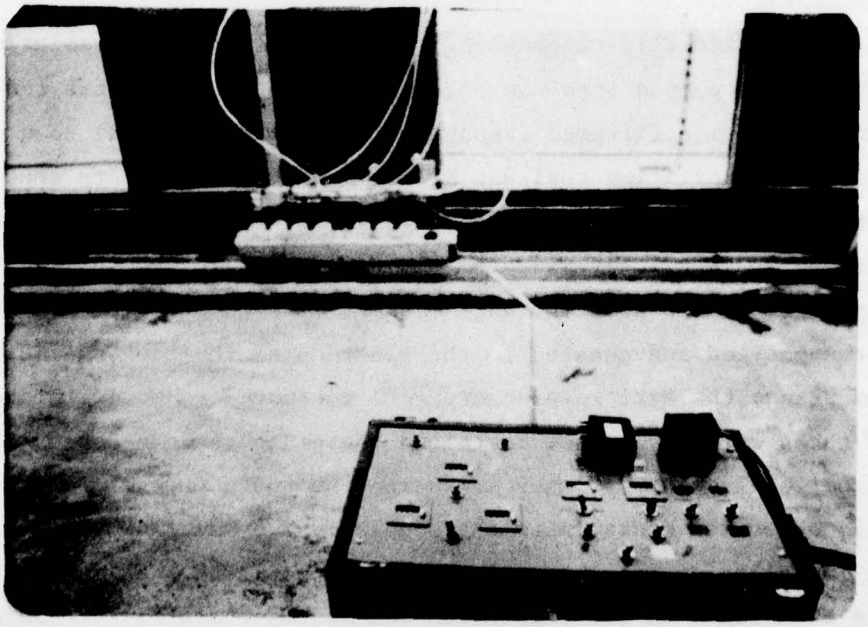

Figure 19. Camera timing control

camera ran continuously to the end of the test. A bank of high-intensity flood lights provided top lighting of the test tank.

Test Procedures and Methods

30. After a number of preliminary tests, a standard operating procedure evolved for the preparation and conduct of a test and for the laboratory analysis of test samples. The procedure is described below in terms of the chronological sequence of operations. Where warranted individual procedures are outlined in greater detail in subsequent sections as are the laboratory methods and procedures pertaining to test samples.

Sequence of Operations

31. Starting with the test tank and all ancillary equipment in a clean state, the operations were performed in the order given below. The sediment slurry was prepared according to the procedure described in paragraph 17 and was stirred and recirculated continuously to maintain the sediment in suspension. The 300 gals of brine solution was prepared and pumped into the empty test tank, and the test tank was then filled with filtered fresh water (see paragraph 16) to a depth of 24 in. The partition seal was pressurized, and the plate seals were installed in the troughs. The range yardsticks were then placed in position at 4-ft intervals from the origin, and the bottom sediment traps were placed at each range marker. The water sampler assemblies were submerged and secured to the tie rods of the tank. Prior to submergence the syringe plungers were retracted to purge the barrels and tubes with air. Once installed the plungers were depressed to the bottom leaving the syringes armed and the tubes free of water that would otherwise contaminate the samples. The mud flow generator box was installed on the bottom and suitably weighted. Salinity readings were then taken in the tank water and sediment slurry to ensure that each was in the range of 10 to 11 ppt. The slurry flow rate was then

set according to the procedure described in paragraph 18 after which a pretest slurry sample was taken for solids content. The connection between the slurry hose and the mud flow generator was made underwater to eliminate air pockets in the supply line. If the test were to be run with current, the recirculation system was then installed and the pump started. Water current speed was measured by timing the travel of a drogue. If the test required waves, the wave machine was set at the rpm corresponding to the prescribed wave period and the amplitude of the paddle was adjusted until the required wave height was obtained. After all tank preparations were completed the cameras were then loaded and mounted and the bank of flood lights was turned on. The test was started by first opening valve C followed by valve D in the mud supply system (Figure 7). Value B was immediately adjusted to bring the pressure gauge reading to the value recorded at the time of flow rate calibration. The cameras were started as the head wave discharged from the mud flow generator box. When the head wave passed through the first sampler array ("A" station) the AA sample set was taken. As it passed "B" station, AB and BB sample sets were taken. Sets AC, BC, and CC were obtained as the head wave passed the "C" station. The detailed locations of the sampling stations and tubes are given in Appendix C. Upon completion of the test the water samples were discharged from the syringes into coded sample bottles. The second side of the tank was then prepared for the next test by following the same setup and test procedure as for the first side.

32. After both sides of the tank were utilized, cleanup operations were carried out. The tank was emptied by first pumping down to a 6-in. water depth through the drain troughs. The remaining turbid water was carefully drained out by gravity in order not to disturb the bottom sediment. The bottom sediment traps were then lifted and their contents flushed into coded sample bottles with distilled water. The tank was then washed down and all hoses and plumbing flushed until clean. All water samples and bottom sediment samples were sent to the laboratory for analysis.

Sample Processing

33. Sediment slurry samples that were taken from the mud supply system before and after each test were analyzed for solids content. The sample was first analyzed for salinity using a conductivity-type salinometer with automatic temperature correction. It was then thoroughly mixed, and a volume of approximately 20 cc was poured into a drying dish (of known tare) and weighed. After drying at 106 deg C to a constant weight, the system was weighed again. The solids weight was corrected for salt content, and the solids content was determined by the following relation:

$$\frac{\text{Weight of solids}}{\text{Weight of mixture}} \times 100 = \text{percent solids (pcs)}$$

34. The water samples taken with the syringe assemblies were analyzed for suspended solids. Salinity of the sample was measured to enable correction for salt content. A measured volume of well-stirred sample mixture was filtered to remove excess liquid then weighed in the moist state. The filter and residue were then dried to constant weight at 106 deg C. The solids weight was corrected for salt content and ratioed to the measured volume to determine the g/l concentration of suspended solids in the mixture. The relatively few samples with high solids content were analyzed in the same manner except they were dried directly without filtering.

35. Bottom sediment samples were analyzed for suspended solids content per unit of bottom area. The salinity of the sample was measured for the purpose of salt content correction. The sample was allowed to settle and the clear supernatant was decanted. The sediment was transferred to a drying dish, settled, and decanted again. The sample was dried at 106 deg C to a constant weight. The solids content was determined by the ratio of solids weight over the sediment trap area and was expressed in the units of g/cm^2.

Timing Procedures

36. A time base was required in each test in order to determine the speed of the head wave and to establish the time relationship of events that occurred during the test. The primary standard was a Heyer

320 microsplit stopwatch that was manually operated by an observer who walked with the head wave and noted the time at which it intercepted each yardstick. The splitter function enabled these times to be read to 0.01 sec. As a backup for the stopwatch method, the movie film was used as a time base. The movie film was calibrated by filming a stopwatch for a period of 15 secs at the start of each roll. Time intervals between filmed events were determined by counting frames of the developed film (with the aid of an editing viewer and frame counter) and applying the calibrated speed in frames per second. A third timing base was provided in the form of a large-faced clock that was located in the start window of each test. The clock provided the day, date, hour, minute, and second timing information.

CHAPTER IV: EXPERIMENTAL PROGRAM

Purpose and Scope

37. The purpose of the experimental program was to explore the behavior of a fluid mud flow in the laboratory and to evaluate the influence of basic physical and dynamical parameters as well as certain environmental conditions on this behavior. In this chapter analytical relationships are outlined which aid in understanding the mechanism of a fluid mud flow, the test plan is presented, and the experimental results are presented and discussed.

Analytical Model of Mud Flows

38. Although the behavior of a mud flow is complex and the theory of its behavior not fully developed, simplifying assumptions can be made that permit an analytical solution and provide insight into the influence of various parameters on the results of the laboratory test program. The assumptions, while circumventing the exact conditions, still represent a reasonable approximation of the physical problem. The system is assumed to be two layered with the mud forming the denser bottom layer whose excess density is related to suspended sediment concentrations. The suspended sediment is uniformly distributed throughout the mud layer so that its density is constant. The less dense upper layer represents the saltwater column whose depth or thickness is large compared to the thickness of the mud layer. The analytical model incorporates a downsloping bottom and a steady, uniform, two-dimensional mud flow. The analysis outlined below follows that presented in Streeter[17] for two-layer flow.

39. When the mud is supplied at a constant flow rate to a sloping bottom, the bottom layer reaches a state of steady, fully developed flow in which the momentum is unchanging and forces along the stationary bottom surface and the moving interface between layers are just balanced

by the gravity force component acting parallel to the bottom. The flow condition is shown schematically in Figure 20 below. If a control volume is drawn around a length, $d\ell$, of the bottom layer, the momentum equation

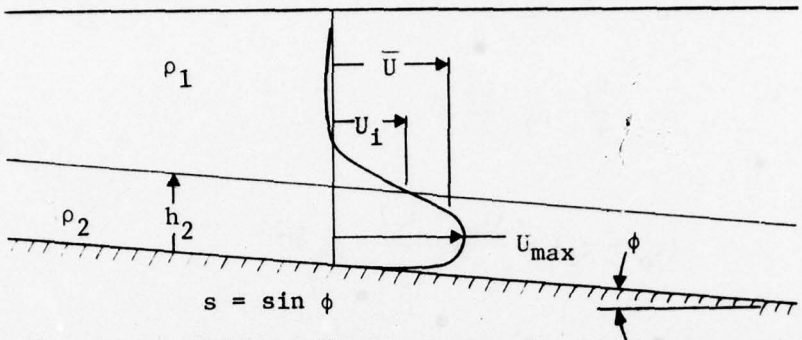

Figure 20. Steady uniform flow in bottom layer with bottom slope

can be written for the mud layer. Figure 21 shows the control volume and the forces acting on it. For two-dimensional flow

$$\Delta\rho g \sin\phi\, h_2\, d\ell - (\tau_o + \tau_i)\, d\ell = 0 \qquad (1)$$

where: $\Delta\rho = (\rho_2 - \rho_1)$

ρ_1 = density of upper layer

ρ_2 = density of mud layer

ϕ = slope angle

s = slope, sin ϕ

h_2 = thickness of bottom layer

ℓ = downslope distance

τ_o, τ_i = shear stress at bottom surface and upper interface, respectively

$\bar{U}$ = average velocity in the fluid mud layer

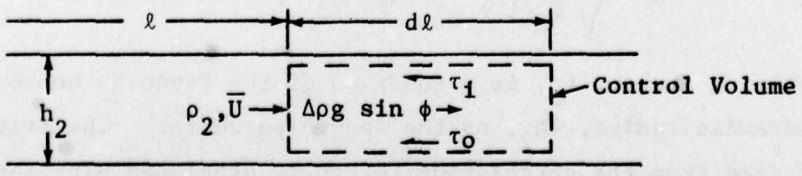

Figure 21. Control volume around bottom layer

The shear stress may be expressed in terms of a friction factor, f, according to

$$\tau_o = \frac{f_o}{4} \rho_2 \frac{\overline{U}^2}{2} \tag{2a}$$

$$\tau_i = \frac{f_i}{4} \rho_2 \frac{\overline{U}^2}{2} \tag{2b}$$

and $$(\tau_o + \tau_i) = \frac{(f_o + f_i)}{8} \rho_2 \overline{U}^2 \tag{3}$$

Substitution of equation 3 into equation 1 yields

$$\overline{U} = \sqrt{\frac{8}{(f_o + f_i)} (g' h_2 s)} \tag{4}$$

where: $$g' = \frac{\Delta\rho}{\rho_2} g \tag{5}$$

The shear stresses may be expressed in terms of their ratio as

$$\frac{\tau_i}{\tau_o} = \alpha = \frac{f_i}{f_o} \tag{6}$$

so that $$(f_o + f_i) = f_o(1 + \alpha)$$

and

$$\overline{U} = \sqrt{\frac{8}{f_o(1 + \alpha)} (g' h_2 s)} \tag{7}$$

The friction factor, f_o, is a function of the Reynolds number Re using the hydraulic radius, $4h_2$, as the length parameter. The friction factor is obtained from the correlation for fully developed pipeline or open-channel flow. According to Streeter,[17] α is 0.64 for laminar flow

(Re $\leq$ 1000) when the properties of the two layers are approximately the same. For turbulent flows up to Re = 10^5, α is 0.43.

40. The form of equation 7 makes no allowance for the fact that at zero slope the bottom layer flows away from a constant source. Since there is no gravitational force component to balance friction, the energy of the bottom layer is eventually dissipated and the flow never becomes steady and fully developed. Over short distances where degradation is small, it is expected that the form of equation 7 would apply for flat bottom conditions except that the slope, s, would disappear and the constant would change. The zero slope equation would be of the form

$$\overline{U} = c_1 \sqrt{g' h_2} \tag{8}$$

The motion of the head wave has been investigated by Migniot[11] who found that it followed a constant Froude number relationship. The velocity of the head wave, u , is therefore given by

$$\frac{u}{\sqrt{g' h_2 s}} = c_2 \text{ for a sloped bottom}$$

and

$$\frac{u}{\sqrt{g' h_2}} = c_3 \text{ for a flat bottom}$$

These rearrange to the form of equations 7 and 8

$$u = c_2 \sqrt{g' h_2 s} \text{ for sloped bottoms} \tag{9}$$

$$u = c_3 \sqrt{g' h_2} \text{ for horizontal bottoms} \tag{10}$$

41. The presence of sediment in the bottom layer changes the system for which equations 10 and 11 apply and somewhat alters the behavior of the bottom layer. Although it is initially distributed

throughout the bottom layer, the suspended sediment settles to the lower strata to create a pronounced concentration profile. When this layer of sediment particles sinks into the boundary layer, the flow slows down under the influence of bottom shear. If the bottom shear is below the resuspension threshold, the particles will stop on contact with the bottom surface or bed and be removed from the dynamic bottom layer. Since the settling out process is time dependent due to generally low settling velocities, and since large particles settle faster than small particles, the sediment that reaches and feeds the head wave is increasingly finer and its rate of delivery ever diminishing as the head wave travels further from the source. The concentration of sediment in the head wave falls as a result of the diminishing flow rate which according to equation 10 causes the head wave to slow down.

Test Plan

42. The plan for the laboratory test program was to generate a reproducible fluid mud systems, to impose variations of certain environmental parameters, and to measure the change in behavior of the mud system as a function of the parameter variations. The fluid mud test system was designed to simulate a two-dimensional mud flow whose behavior was controlled primarily through its thickness and the rate at which sediment slurry was pumped to sustain the mud flow. The environmental parameters were treated as independent test variables and the measured parameters as dependent variables. These are discussed in more detail below.

Independent Variables

43. The environmental parameters and mud system characteristics that were treated as independent variables included the following:

a. Sediment/water type.

b. Bottom slope.

c. Water current.

d. Surface waves.

e. Slurry concentration.

f. Discharge velocity.

g. Slot height (i.e. mud flow thickness).

44. Sediment/Water Type. The sediment type was felt to be significant because of the influence of saltwater flocculation on settling rates and subsequently on the behavior of the fluid mud system. Sediment and water types were combined into a single variable because this is typical of dredging operations where fluid mud flow is an important consideration. In the case of a hydraulic dredging operation with open-water discharge, the in situ material is diluted with local water before passing through the dredge pumping system. The sediment slurry is then discharged back into the same type water column from which it came. Particularly, the salinity of the sediment slurry and the lower water column will in most cases be the same. Despite the drawback of having to manufacture large quantities of saltwater, the saltwater system was used as the base reference condition because it typified dredging conditions in the coastal estuarine environment. The source of in situ sediment was local (Boston Harbor). The salinity of the sediment slurry and the tank water was established at 10 to 11 ppt to simulate the flocculant character of the estuarine environment. The saltwater system was tested against a freshwater sediment system.

45. Bottom Slope. Bottom slope exerts a strong influence on the behavior of the fluid mud flow because of its effect on the settling-resuspension process and subsequently the ability of the mud flow to sustain itself. Of particular interest was the downslope angle at which the fluid mud system flowed at constant velocity over the length of the test tank. Bottom slope was changed by installing a false bottom on each side of the test tank. Each of the two bottoms was set at a different slope and was tested in both upslope and downslope directions. The bottom texture was the hard smooth surface of the tank bottom.

46. Water Current. Current exists at virtually all dredging operations and consequently is of interest to determine how and to what

extent it interacts with a fluid mud flow. Specific points of interest included the extent of thickening of the mud system due to parallel and counter currents as well as indications of effects on the flow velocity of the fluid mud layer.

47. Surface Waves. The orbital motion of surface wave systems is transmitted throughout the water column to the bottom region where it can interact with the fluid mud flow. The plan was to obtain an indication of how the orbital motion interacted with the mud system, whether there was sufficient shearing action to drive turbidity higher in the water column, and the extent to which the overall motion of the fluid mud layer was affected by the presence of orbital motion.

48. Slurry Concentration. The density difference between the mud flow and the water column is one of the basic driving forces that establishes the dynamics of the fluid mud system. The slurry concentration determines the density difference between the mud flow and the water column. Increased or decreased values of slurry density cause the motion of the system to be enhanced or inhibited, respectively.

49. Discharge Velocity. This parameter was utilized as a control on the advance velocity of the fluid mud system (i.e., head wave velocity). Discharge velocity refers to the average velocity of the advancing mud wave as it exits from the discharge slot of the mud flow generator. Its value was altered by changing the slurry flow rate delivered through the discharge opening. The objective was to determine whether the discharge velocity affected the downstream behavior of the mud flow.

50. Slot Height. Slot height refers to the height of the discharge opening in the mud generator and was intended as the control parameter for head wave height and fluid mud layer thickness. The discharge velocity was held constant with changes in slot height by varying slurry flow rate proportionately. The interest was in whether the slot height would cause a change in the thickness dimensions of the downstream mud flow.

Dependent Variables

51. The dependent variables in the test program were measured during each test. These included the head wave velocity as it moved down the tank, the height of the top of the turbidity cloud above the bottom, the sediment concentration through the fluid mud and turbidity layers, and the mass of sediment that settled on the bottom during each test.

52. Head Wave Displacement Versus Time. Head wave displacement as a function of time was used to establish the linear velocity of the head wave as it travelled down the tank. The change in the velocity plot indicated the presence of settling activity and/or the influence of the gravity slope force.

53. Cloud Height. Cloud height in conjunction with fluid mud layer thickness was used to determine the thickness of the turbidity layer.

54. Sediment Concentration Profiles. The concentration profiles were used to establish the thickness of the fluid mud layer. The relationship between the profiles in space and time was helpful in correlating settling characteristics and head wave dynamics. In this report solids ratios are given in units of percent solids (pcs) by weight.

55. Bottom Sediment Deposits. Bottom sediment was monitored for the purpose of establishing settling characteristics as a function of distance from the source of the mud flow.

Test Matrix

56. The objective of the test program was to evaluate the influence of the selected independent system variables on the geometry and behavior of the fluid mud system. In order to accomplish this with a reasonable number of tests, each variable was assessed separately with respect to the mud flow system characteristics under a standard test condition. The "standard" condition (given below) was determined by matching scaled-down field conditions (by Froude number) with the capabilities of the test facility, especially the mud supply system.

Sediment	
type	saltwater
source	Boston Harbor
Water	
type	salt
salinity	10 ppt
depth	14 in.
Sediment slurry	
solids ratio	15 pcs
salinity	10 ppt
flow rate	22 gpm
Bottom slope	0.0 (horizontal)
Discharge velocity	0.11 fps
Slot height	2 in.
Water current	0.0 fpm (still)
Surface waves	none (calm)

In Table 1 the independent variables and their values are arranged in matrix form with respect to the standard configuration. The total number of tests was 25 including a full factorial matrix of three slurry densities and five bottom slopes that was used to scrutinize more closely the relationship between these two variables.

Test Results

57. The experimental program utilized twenty-five (25) tests to evaluate the influence of the six (6) independent variables on the behavior of the mud flow system as "standardized" by the baseline or reference condition. Although approximately two (2) additional tests were run for each of four (4) of the independent variables, a complete factorial test matrix was conducted for the combination of three (3) slurry concentrations and five (5) slopes. Exclusive of the above tests, an additional nine (9) shakedown tests were necessary to develop the mud flow generator, to establish compatibility between saltwater sediment and the water column, and to implement the current-generating system.

58. The test conditions and primary results are summarized in Table 2 for the group of twenty-five (25) tests. The test conditions are given by the six (6) independent variables of the system; i.e.,

Table 1

Test Matrix for Fluid Mud Studies

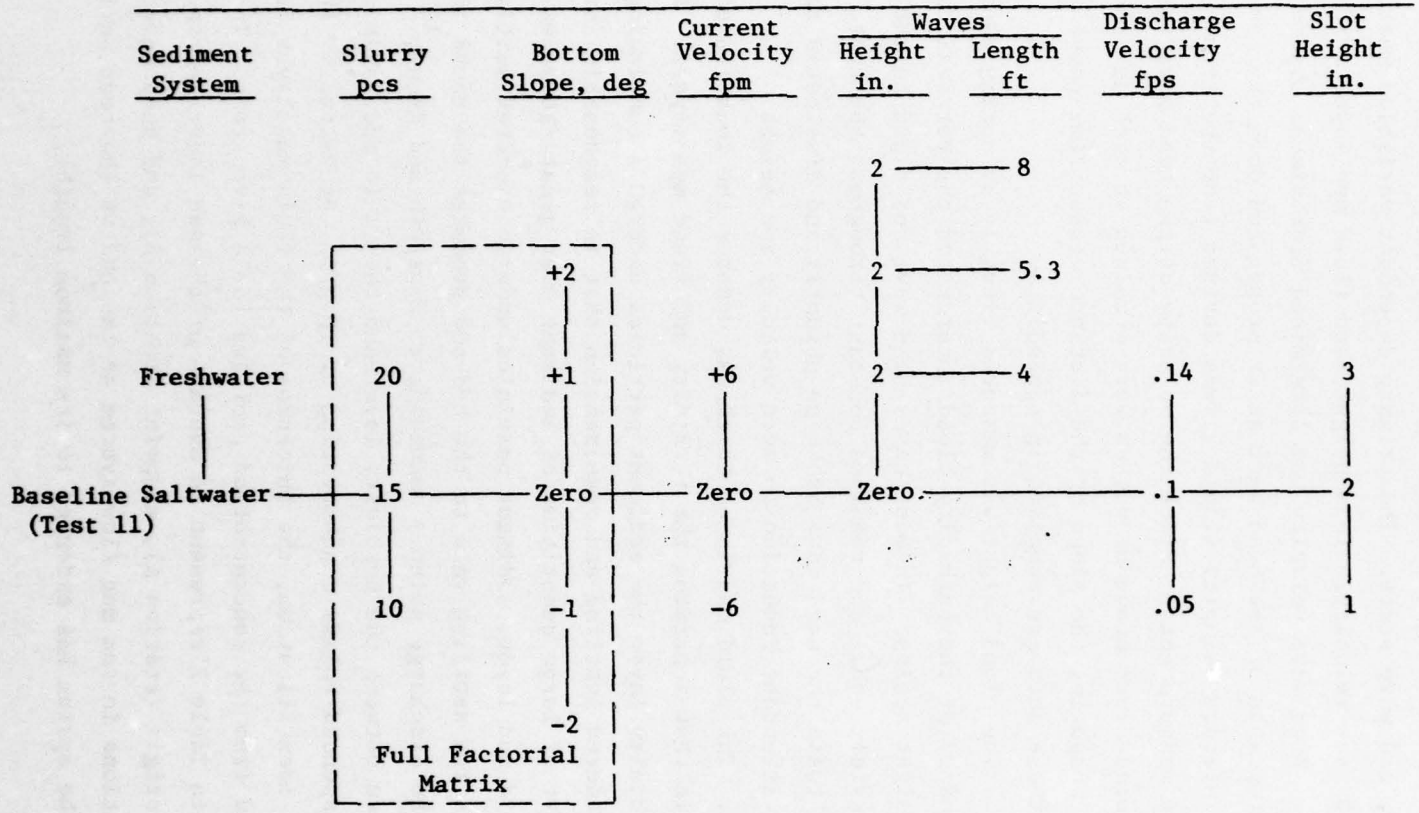

Note: Freshwater sediment source was Michigan City; saltwater source was Boston Harbor. Total number of tests was 25.

water/sediment type, sediment concentration, bottom slope, discharge velocity from the mud flow generator, height of the discharge slot, current, and wave state. The primary dependent variables measured are head wave velocity, cloud height, and fluid mud layer thickness.

59. Head wave velocity was determined from visual observations and photographs of the head wave as it propagated down the tank. The overall average velocity (Table 2) was derived from the total distance and time measurements. Since the velocity of the head wave varied as it advanced, instantaneous values were obtained at each downrange station by measuring the slope of the distance versus time curve for each test. These data are compiled in Appendix A.

60. The cloud height was measured visually by noting where the top boundary of the turbidity cloud intercepted the vertical color-coded height scales. In most cases head wave and cloud height were approximately equal and remained constant throughout the test. In certain tests the head wave broke up abruptly and dissipated to a wisp with an attendant reduction to zero velocity and height.

61. The fluid mud layer thickness denotes the location of the interface that separates the turbidity and fluid mud layers. Within the turbidity layer the sediment particles undergo a continuing cycle of unhindered settling and resuspension that is responsible for the transport of large quantities of sediment over great distances. Within the fluid mud layer, sediment particles undergo hindered settling which enhances the settling rate to the bed and produces the mound that grows under the discharge point. According to Einstein and Krone,[12] the interface between the turbidity layer and the fluid mud layer occurs at a suspended solids concentration of 10 g/ℓ. By virtue of this density identification, the thickness of the fluid mud layer is obtained from the concentration profiles for a given test. The values listed in Table 2 represent an average of the mud layer thicknesses at the origin (station A), midpoint (station B), and head wave (station C) locations in the mud flow system at the end of the test period (i.e., after the system has extended to its maximum length).

Table 2

Test Conditions and Results

Test No.	Water		Sediment		Botton Slope*	Discharge Velocity	Slot Height	Current	Wave		Cloud Height	Fluid Mud Layer Thickness	Head Wave Velocity Overall Average
	Type	Salinity ppt	Type	Concentration pcs	deg	fps	in.	fpm**	Height in.	Length ft	in.	in.	fps
11	Salt	11.0	Silty Mud	9.6	0	0.10	1	0	0	0.0	2.5	0.80	0.062
12		9.5		12.2			3				3.0	1.58	0.216
13				14.2		0.14	2				3.0	1.09	0.123
14				14.5		0.05					3.0	1.03	0.107
15		10.0		15.1		0.10			2	4.0	2.5	1.08	0.192
16		10.5		17.6					2	8.0	4.0	0.94	0.155
18		10.0		16.2				-6	0	0.0	4.0	0.76	0.235
19	Fresh	0.0	Clayey Silt	19.5				0			3.0	1.04	0.127
20	Salt	9.5	Silty Mud	16.5	+2						2.0	0.81	0.078
21					+1						2.0	1.07	0.090
22		9.0		13.9	-1						3.0	0.97	0.279
23				14.3	-2						3.0	0.85	0.329
24		13.0		17.9	+2						2.0	0.95	0.054
25				19.7	+1						2.5	0.97	0.108
26		9.0		19.8	0						3.0	1.11	0.136
27		13.0		21.3	-1						2.5	1.21	0.290
28				21.2	-2						3.0	0.91	0.414
29		10.0		8.7	+2						2.5	0.89	0.086
30				7.4	+1						2.5	0.81	0.097
31				10.3	0						3.0	0.73	0.140
32		9.5		8.6	-1						3.5	0.80	0.218
33				9.9	-2						3.5	0.73	0.247
35		10.0		13.1					2	5.3	2.0	1.09	0.152
36				16.6				+6	0	0.0	12.0	1.03	0.210
37				17.3				0			2.5	1.04	0.161

Note: No entry indicates preceding value applies.
* + slope up; - slope down, in direction of flow.
** + current with mud flow; - current counter to mud flow.

Concentration Profiles

62. The concentration profiles were developed for each test from the water sample data. These were taken at heights of 3/16, 1/2, 1, and 1-1/2 in. above the bottom of the tank, at three stations (A,B,C) located 8 ft apart, and at three times as the head wave passed (6 in.) each sample station. A series of profiles is illustrated in Figure 22 which is the data for test 37, the baseline or reference condition. In Figure 22 the height above the bottom is plotted against sediment concentration in g/ℓ. All profiles converge at low concentrations to the visually determined cloud height (Table 2) at an arbitrarily selected concentration of 0.01 g/ℓ. This estimate established the approximate density gradients at low concentrations.

63. The time sequence of the profile was established according to the progress of the head wave. As the head wave passed the first sample station, A (approximately 4 ft from the origin), profile AA was taken; when it passed station B (8 ft from A, midtank), profiles AB and BB were taken; when the head wave reached station C (8 ft from B, end of tank), profiles AC, BC, and CC were taken.

Bottom Sediment Profiles

64. Bottom sediment samples were taken after each test and were reported in terms of the mass of sediment in the tray divided by its area (g/cm^2). The samples sat on the bottom for as long as 1 hour before the draining of the tank started and another hour during the draining operation before they could be retrieved. It is felt that the data are biased by draining effects and excessive settling time but that relative properties are maintained. The bottom sediment profiles for each test are presented in Appendix B.

Mud System Behavior

65. Several characteristics of the mud system came to light with further scrutiny of the concentration profiles for the baseline test (Figure 22). The location and sequence of samples indicated the variation in sediment concentration with time and space from which inferences

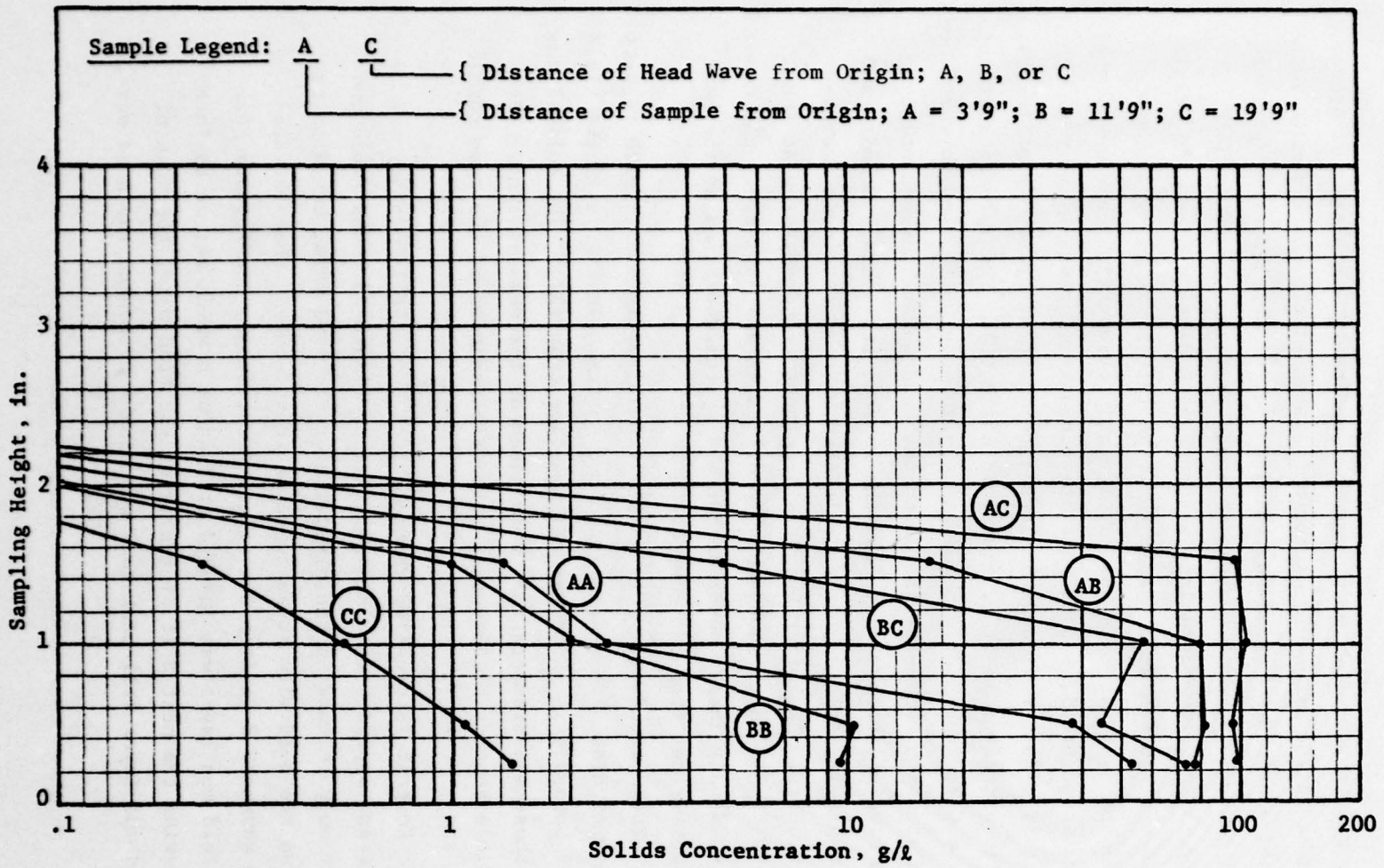

Figure 22. Concentration profiles, test 37

could be made concerning the movement of sediment within the mud system. Differences in the structure of the mud system at the three sample locations were assessed by examining the last set of samples after the head wave had passed station C. These included profiles CC, BC, and AC. Generally, solids concentration decreased with distance from the origin. The cause of this was undoubtedly the high rate of settling along the length of the system. This was particularly evident in the case of the head wave whose profiles show that its concentration was highest at the start (profile AA), was somewhat less after 8 ft of travel (profile BB), and was lowest after 16 ft of travel (profile CC). The rate of settling over the entire length of the mud system from source to head wave reduced the rate at which sediment was fed to the head wave. Consequently, as the head wave progressed away from the source, its average density and hence its gravity driving force diminished with an attendant decrease in its velocity. A similar but less prominent trend appeared at the location 8 ft behind the head wave (profiles AB and AC); i.e., the concentration at a relative point in the mud system decreased as the head wave moved further from the source.

66. These trends are more easily visualized if viewed with respect to the moving head wave of the fluid mud system. In Figure 23 the fluid mud layer boundary is shown for the baseline test (37). The solid lines connect those measurements that were taken at the same instant. The dashed lines connect measurements that were recorded at the same sample station.

67. Several interesting characteristics of the laboratory mud system became apparent from the profiles of Figure 23. The fluid mud layer not only thinned in the direction of the head wave, but also receded from the head wave at an appreciable velocity. When the head wave had advanced 8 ft from the origin (station B), the forward edge of the fluid mud layer was located at station B which was at the head wave. During the next 8 ft of travel of the head wave, the edge of the fluid mud layer fell back to a position 4 ft behind the head wave.

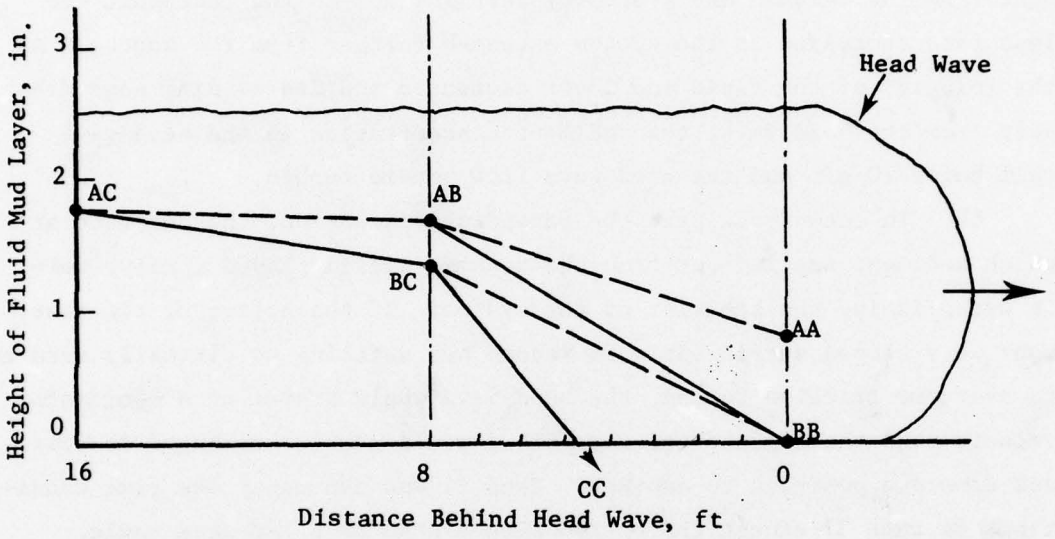

Figure 23. Fluid mud layer profiles, test 37

In other words the average absolute velocity of the fluid mud layer dropped to half that of the head wave. At this rate of deceleration the fluid mud layer would have come to a virtual stop within another tank length (i.e., the recession velocity of the fluid mud layer equals the head wave velocity). The thinning of the fluid mud layer and its recession from the head wave were both attributable to the loss of sediment from the dynamic mud system by settling and to the fact that the loss rate increased as the system extended further from the source. As the velocity of the fluid mud layer decreased and its leading edge drew away from the head wave, the sediment concentration in the head wave fell below 10 g/ℓ and the head wave flow became turbid.

68. In accordance with the foregoing discussion, the net rate at which sediment settled out from the dynamic system played a major role in establishing the behavior of the system. If the bottom of the test tank were sloped sufficiently to reduce net settling to virtually zero and to overcome friction forces, the head wave would travel at a constant velocity and the concentration profiles would remain unchanged in time and from one position to another. Test 22 was run under the same conditions as test 37 except the bottom sloped down at a 1-degree angle. The velocity of the head wave actually increased slightly as it moved down the tank, and the concentration profiles (Figure 24) bore the same relationship to each other as in test 37 (Figure 22) except that differences were noticeably less pronounced. The concentration profiles appeared to fall closer to each other and approach a single profile. The fact that the trends of Figure 22 were still discernible, though less pronounced, in Figure 24 indicated that the net settling rate was considerably reduced by the sloping bottom. The residual settling was undoubtedly associated with the coarse-grained sand fraction.

69. The bottom sediment samples for tests 37 and 22 (Figure 25) supported the conclusion that less settling occurred during the -1-degree sloped run. In the case of the baseline test with horizontal bottom, the deposit (i.e., settling rate) was greatest at the origin and decreased approximately linearly to near 0 at the 24-ft range marker.

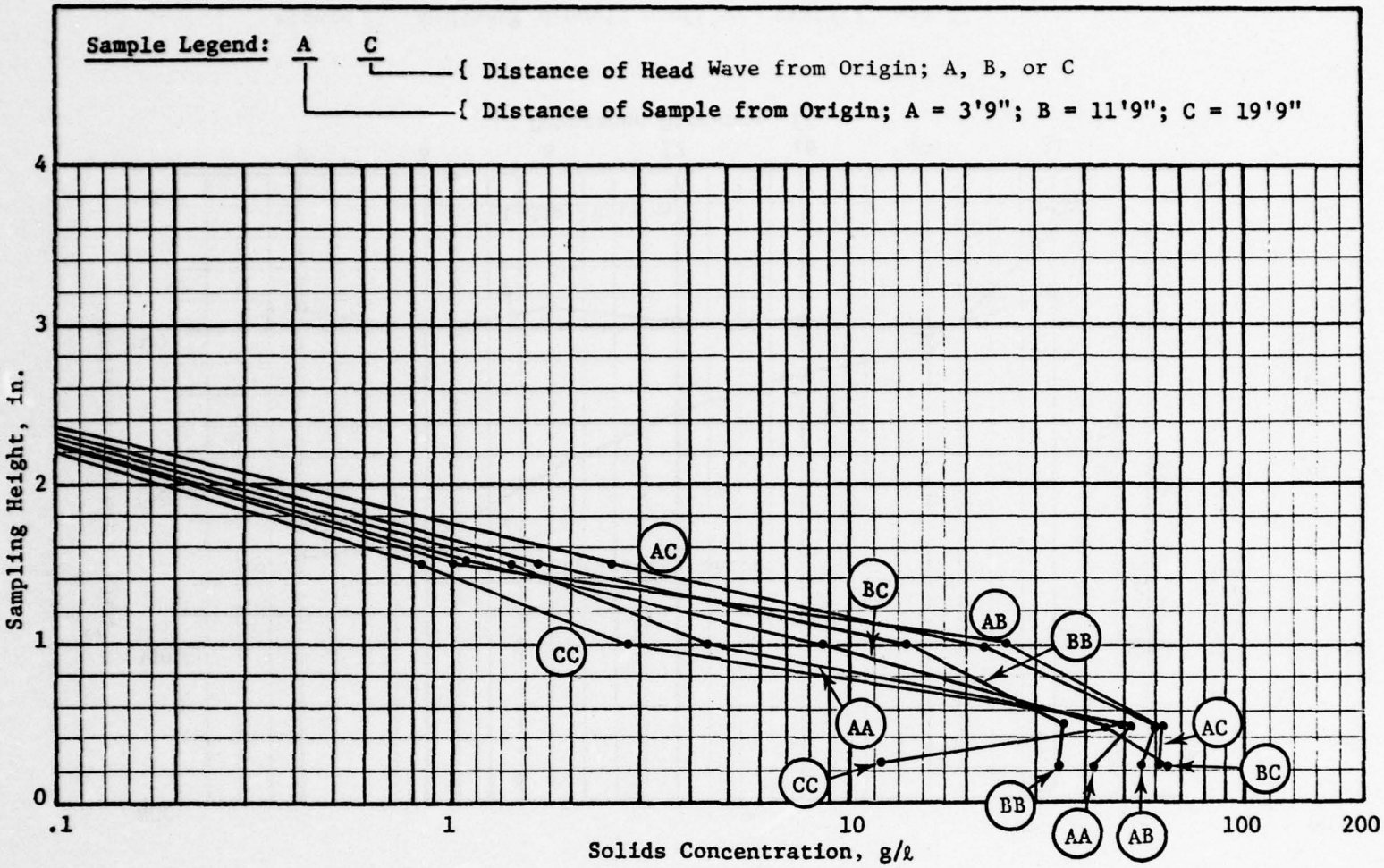

Figure 24. Concentration profiles, test 22

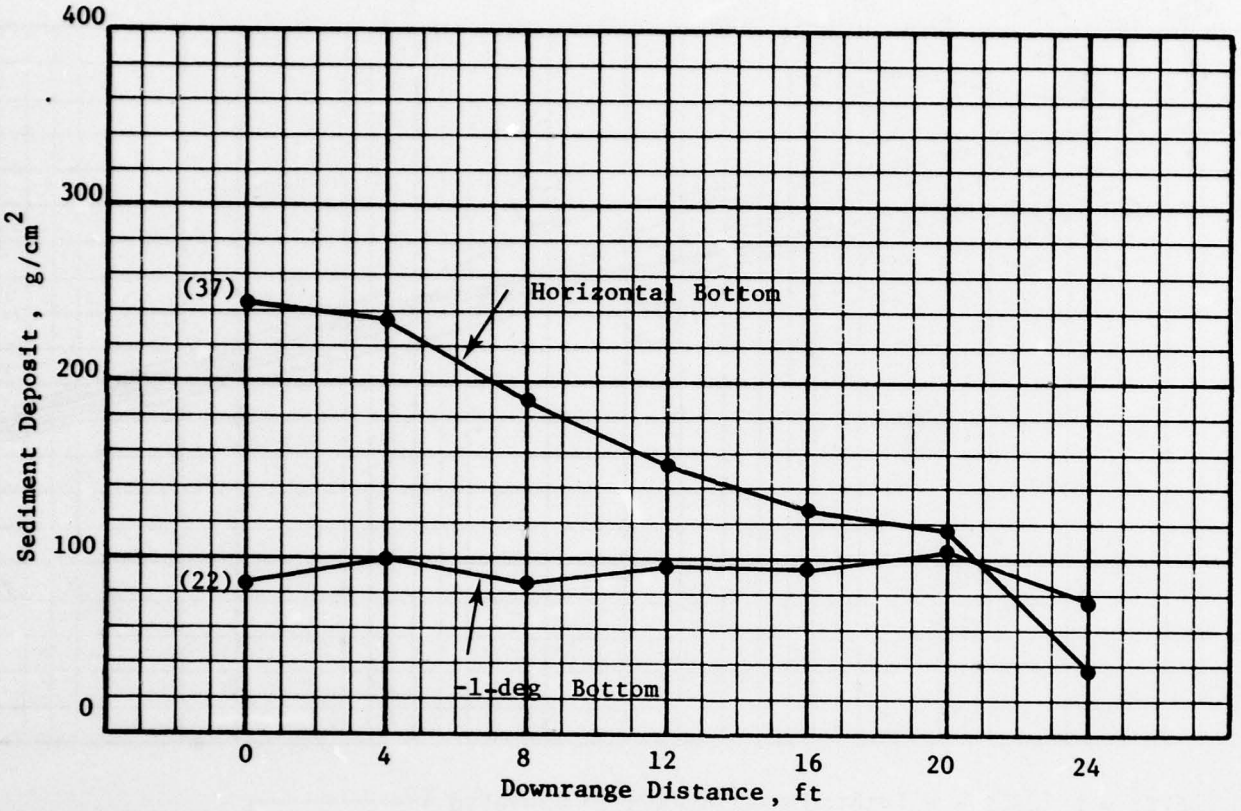

Figure 25. Sediment deposit profiles, tests 22 and 37

The -1-degree bottom slope test indicated a uniformly thick deposit (settling rate) over the length of the tank bottom at a level that approached the minimum for the horizontal bottom.

70. The mass flow rate of solids (conc. x vel.) through a vertical section cannot be determined exactly without a velocity profile; however, a reasonable estimate can be made by combining the concentration profile and qualitative knowledge of the velocity profile. (The test plan did not provide for matching velocity and concentration profiles because the added cost and complexity of the former were beyond the scope of the program.) The general relationship between the concentration and velocity profiles at a point in the mud system (shown schematically in Figure 26) is such that the higher concentrations and velocities occur in the lower levels of the mud profile well within the fluid mud layer (solids concentration >10 g/ℓ). In the turbidity layer sediment density and velocity

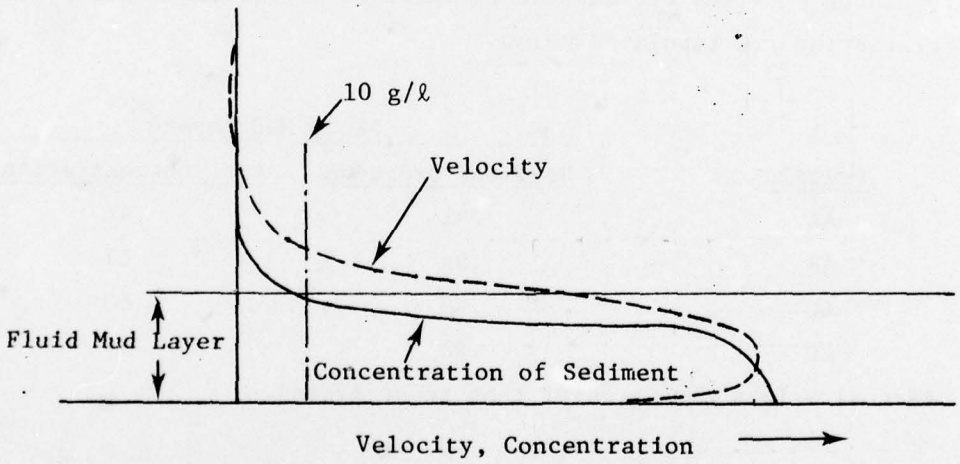

Figure 26. Generalized concentration and velocity profiles

are both relatively low. If concentration is integrated over height above the bottom, the fluid mud layer fraction of sediment can be obtained by taking the ratio of $\int cdA$ in the fluid mud layer to that over the entire profile (fluid mud layer + turbidity layer). If the concentration is additionally weighted according to velocity (i.e., $\int cdA$), the higher velocities in the fluid mud layer will cause its sediment fraction

to be greater than that given by the areal fraction. It can therefore be concluded that the actual sediment distribution between the fluid mud and turbidity layers can be estimated from the areal fractions; however, the mud layer fraction is actually greater than the corresponding areal value, while the turbidity layer fraction is actually less. The average concentration of the fluid mud layer is estimated in the same fashion by reference to the area value. The latter is obtained by dividing the value for $\int cdA$ over the fluid mud layer by its height.

71. Referring back to the concentration profiles for the baseline test, Figure 22, the fraction of sediment in the fluid mud layer as well as its average concentration can be estimated. Head wave profiles BB and CC fall below the fluid mud layer threshold concentrations (10 g/ℓ), which means that a fluid mud layer does not exist at these locations. The remaining profiles reflect the presence of a fluid mud layer; their characteristics are tabulated below:

	Fluid Mud Layer*	
Profile	Sediment Fraction	Avg. Concentration, g/ℓ
AA	.91	41
AB	.96	67
BC	.95	53
AC	.98	94

*Actual values were greater than those listed.

72. In accordance with the profiles for the baseline test (Figure 22), the fluid mud layer contained over 90 percent of the sediment and its average concentration was at least 2/3 of the maximum value for the profile. By the time the last set of samples was taken, the concentration profile at the station nearest the origin (profile AC) was fully developed (i.e., a steady-state condition existed). At this point more than 98 percent of the sediment was contained within the fluid mud layer. The concentration was virtually constant over the height of the fluid mud layer so that average and peak concentrations were approximately equal. It is noteworthy that the average concentration at station A

was 94 g/ℓ compared to 190 g/ℓ (17.3 pcs) as delivered at the discharge of the mud flow generator box. The dilution ratio of 2 is attributable to water entrainment and settling effects over the 6-ft distance from generator box to sampling station A.

Data Presentation

73. The test results are presented graphically in terms of the behavior of dependent variables as a function of independent variables. The dependent variables included head wave velocity, cloud height, height of the fluid mud layer, amount of deposited sediment, and concentration profiles. The independent variables include slot height and discharge velocity, both of which reflect the performance of the mud flow generator, sediment type as characterized by salinity, solids ratio (by weight) of the sediment, bottom slope, current, and waves as measured by bottom orbital velocity. The sediment deposit profiles are compiled in Appendix B and the concentration profiles in Appendix C. To facilitate reference to these data the sediment profiles are grouped in separate figures and the concentration profiles are positioned in sequence for each independent variable.

Slot Height

74. In this group of tests the height of the discharge slot in the mud generator box was varied in order to determine its influence on mud flow behavior. The box was tested with openings of 1 in., 2 in. (baseline), and 3 in. while all other variables were maintained at baseline values. Since discharge velocity was held at .1 fps, the flow rate was varied proportionately with slot height; i.e., 11, 22, and 33 gpm for heights of 1, 2, and 3 in., respectively.

75. The head wave velocity characteristics are shown in Figure 27 for each slot height as a function of downrange distance from the origin (test numbers in parentheses). At the origin the velocities of the 3-in. and 2-in. head waves were nearly the same at 0.28 fps, while the 1-in. head wave travelled at about half this velocity. This can be verified through the theoretical expression for head wave velocity

as a function of the density differential and the height of the sediment wave. If the density difference is based on the sediment concentration shown in Table 2 and if the height of the sediment cloud is given by the slot height, the head wave velocities, u , at the origin are approximated by the equation

$$u = 0.34\sqrt{\frac{\Delta\rho}{\rho} gh_2} \qquad (11)$$

which predicts the values of .141, .271, and .275 fps for 1-in., 2-in. (baseline), and 3-in. slot heights, respectively. These approximate very closely the head wave velocities at the origin which indicates that the relationship of the curves of Figure 27 in the origin region conforms to theory and therefore reflects differences in slurry density as well as in slot height.

76. The tendency of the head wave to move at a velocity higher than the specified discharge velocity created the impression that the mud flow was established within the mud generator box. If the head wave wanted to travel faster than the discharge velocity, as in the 2- and 3-in. slot height tests (37 and 12, respectively), the mud layer would thin down to less than the slot height. On the other hand if the match was closer, as in the 1-in. slot height test, the head wave velocity would approach the design velocity and the mud layer would just fill the discharge opening. Figure 28 shows that only for the 1-in. slot did the mud layer thickness approach the opening; in the other two tests the mud layer filled only one half of the discharge opening.

77. Beyond the origin region the effects of settling caused the head wave to slow down in each case. The velocity decay with distance was the same for the 1- and 2-in. slot height tests (11 and 37, respectively). The 3-in. test (12) showed signs of less sediment settling in the first 8 ft during which the velocity was sustained. This was undoubtedly due to the higher velocity which tended to keep the sediment in suspension. Beyond the origin region the velocity decay increased until it approached that for the baseline test.

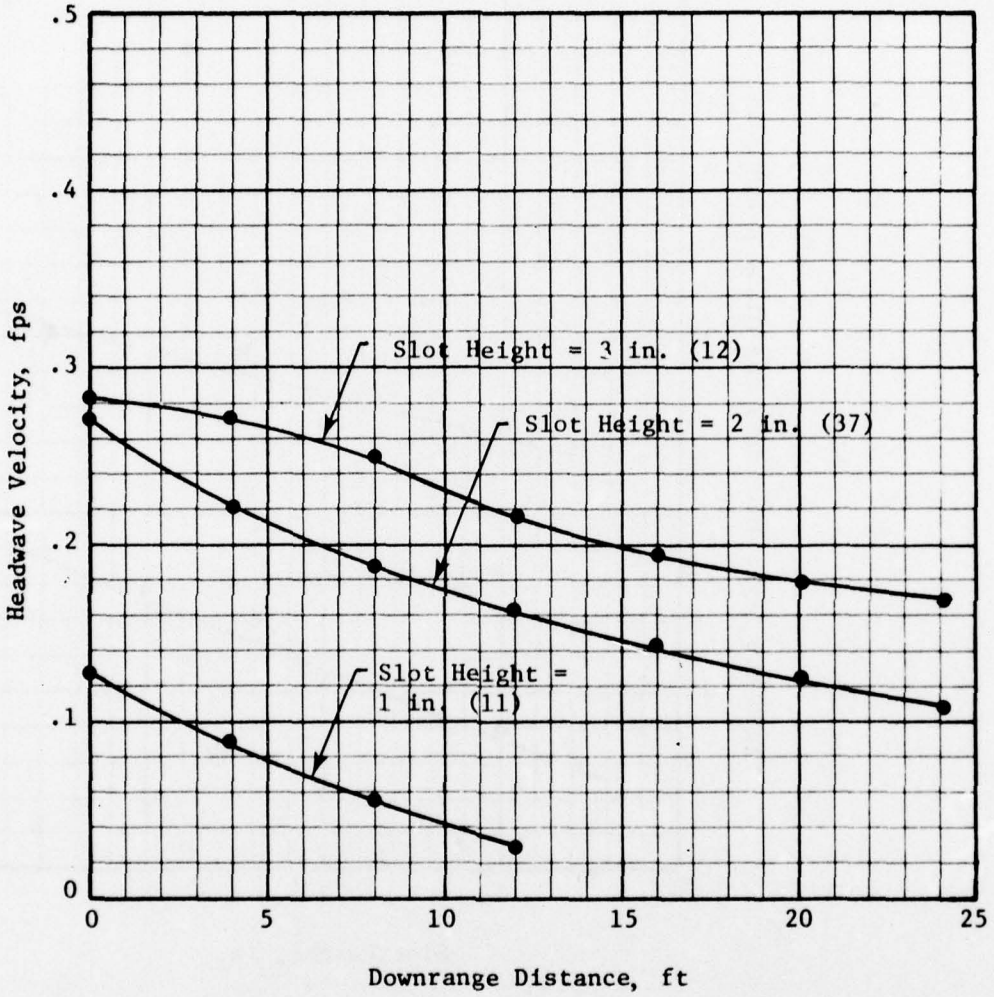

Figure 27. Head wave velocity versus distance for discharge slot height parameter

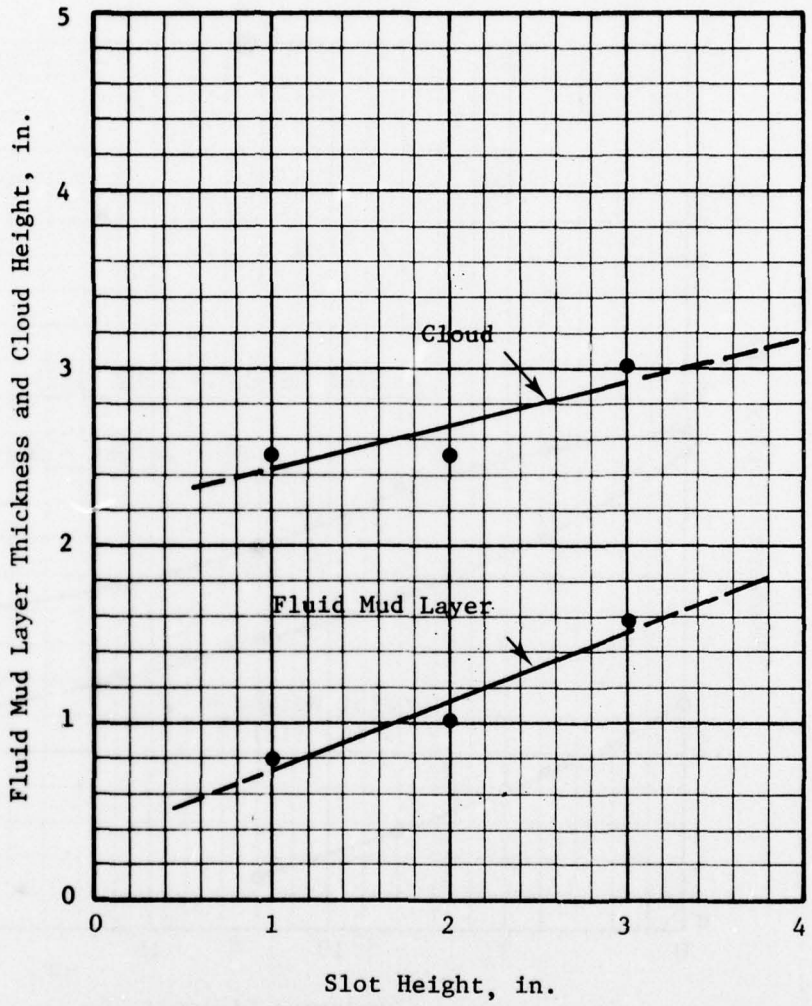

Figure 28. Cloud height and fluid mud layer thickness versus slot height

78. The concentration profiles and amount of deposited bottom sediment for these tests support the trends described above. The concentration profiles for the 1- and 2-in. slot height tests (Figures C1 and C2, Appendix C) were quite widely spaced, thus denoting significant sediment settling. The profiles for the 3-in. slot height test (Figure C3, Appendix C) were noticeably more consolidated, which indicates smaller changes in time and space and hence less sediment settling. The accumulation of bottom sediment for the 1- and 2-in. openings (Figure B1, Appendix B) reflected high settling rates by the strong linear distribution of sediment from the origin (where the sediment layer was thick) to the downstream end of the tank (where it was thin). The profiles for the 3-in. slot height test showed only a slight gradient from one end of the tank to the other, which indidates that a small amount of sediment settled out during the test and that the settling rates were therefore low.

79. Both the cloud height and the fluid mud layer thicknesses increased with slot height as is shown in Figure 28. According to the foregoing discussion the trend was not so much a function of slot height as it was of increased slurry flow rate since the mud flow did not fill the slot opening. A higher mud flow rate out of the source increased the fluid mud layer thickness which caused the head wave and mud layer to travel at a higher velocity. The higher velocity of the mud system increased friction and turbulence at the upper interface, thus generating more turbidity and forming a thicker cloud.

Discharge Velocity

80. The slurry was delivered on the bottom of the tank through the mud generator box from which it was designed to discharge at .1 fps through a 2-in.-high x 36-in.-long slot. If the mud system naturally moved out of the box faster than the design speed, it would do so with an attendant reduction in the mud layer thickness. If the delivery conditions matched the characteristics of the unrestrained mud flow

system, the fluid mud layer would fill the slot and the head wave would move at the design speed before settling effects interfered.

81. The objective of these tests was to determine the effect of discharge velocity on the behavior of the mud system as represented by the baseline configuration. With all other variables set at baseline values, test 13 was run at a discharge velocity of .05 fps and test 14 at .14 fps in order to bracket the baseline value of .10 fps. These velocities were obtained by adjusting the slurry flow rate in proportion to the desired velocity. Inasmuch as the baseline velocity (.1 fps) required 22 gpm, the .05- and .14-fps conditions were obtained with 11 and 31 gpm, respectively.

82. The results of these tests are presented in Figures 29 and 30 where they are compared to the data for the baseline test. The head wave velocity profiles show that at the start of each test the natural speed of the head wave greatly exceeded the design discharge velocity. Consequently, the fluid mud layer did not fill the discharge slot, and hence its thickness was not controlled by the height of the opening (i.e., 2 in.). According to Figure 30, the fluid mud layer was about 1 in. thick and therefore occupied only one half of the slot. Under these conditions the behavior of the mud system was controlled by the slurry flow rate rather than the design discharge velocity. Thus, the head wave profile for the lower flow rate condition (test 14) fell below that for the baseline test 37, and the profile for the high flow rate test 13 should have fallen above the baseline profile but did not. The concentration profiles for this set of tests (Figures C4-C6) show that test 13 did not fit the trend. Its profiles (Figure C6) were too widely spaced for such a high flow rate, whereas they should have been more closely grouped as in test 12 (Figure C3), a nearly identical test. The mud layer thickness and the cloud height should have been greater than the indicated values (Figure 30). A likely explanation of these discrepancies is that the slurry level in the 400-gal reservoir tank ran low during the test and caused the supply system to deliver considerably less than the maximum flow rate.

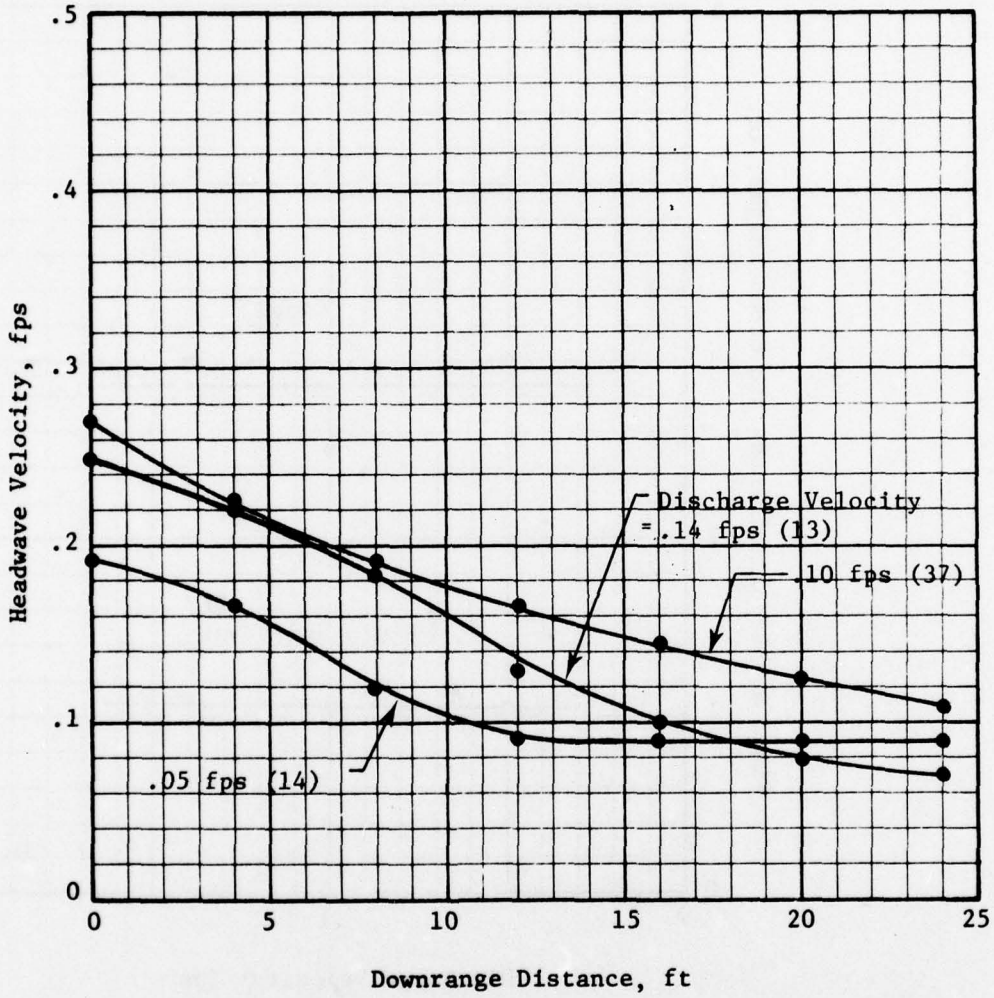

Figure 29. Head wave velocity versus distance for discharge velocity parameter

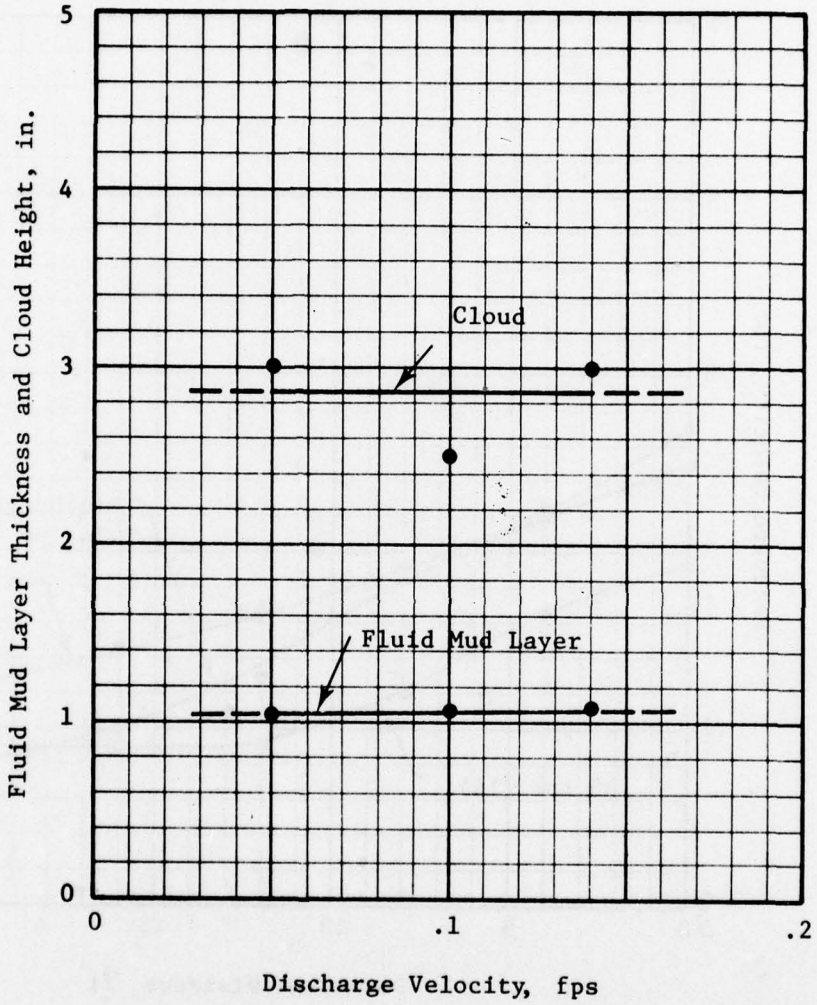

Figure 30. Cloud height and fluid mud layer thickness versus discharge velocity

Sediment System

83. A freshwater sediment system was tested for comparison with the saltwater baseline system particularly to ascertain the effects of flocculation on the settling process. The freshwater sediment was obtained from Trail Creek in Michigan City on the shore of Lake Michigan. The properties of the two sediments are presented in Table 3 for comparison.

Table 3

Properties of Test Sediments

Sediment Source	Boston Harbor	Michigan City
Type	Saltwater	Freshwater
Salinity, ppt	10	0
Sand Fraction, percent	24	6
Silt Fraction, percent	45	69
Clay Fraction, percent	31	25
Median Grain Size, dispersed, mm	0.018	0.014
Total Organic Carbon, percent	6.0	3.2

The Boston Harbor sediment had a higher sand content and a larger median grain size; the fluid mud was black and turbidity wisps were gray. The Michigan City sediment contained considerably more silt than the Boston Harbor material; it was brown in color while its turbidity wisps were tan.

84. A comparison of the results for the freshwater (test 19) and saltwater (test 37) tests is presented in Figures 31 and 32. The freshwater head wave started at a higher velocity than the saltwater head wave, but by the end of the test it had slowed to half the velocity of the saltwater wave and was several feet behind. The freshwater mud slurry had a slightly higher density driving force which explains the initially greater speed of its head wave. The greater deceleration of the freshwater head wave after the first 5 ft of travel was probably

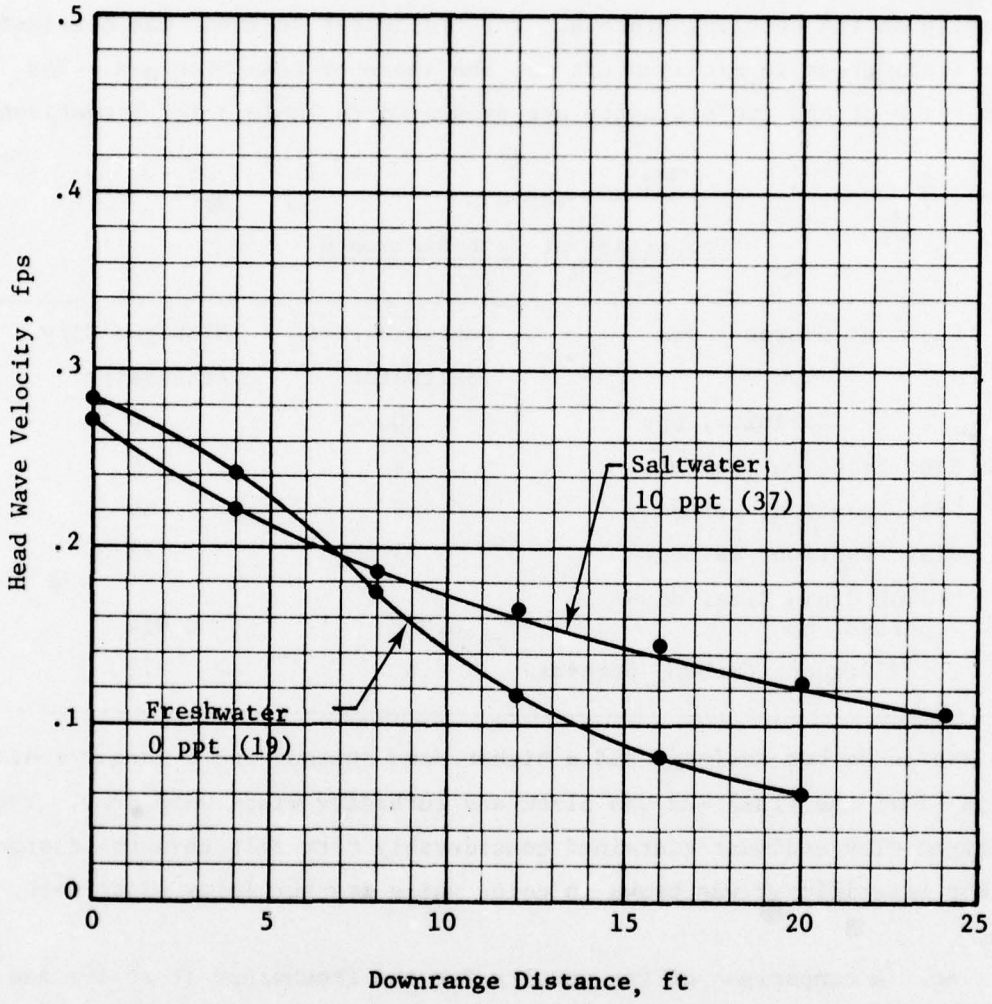

Figure 31. Head wave velocity versus distance for fresh and saltwater sediment systems

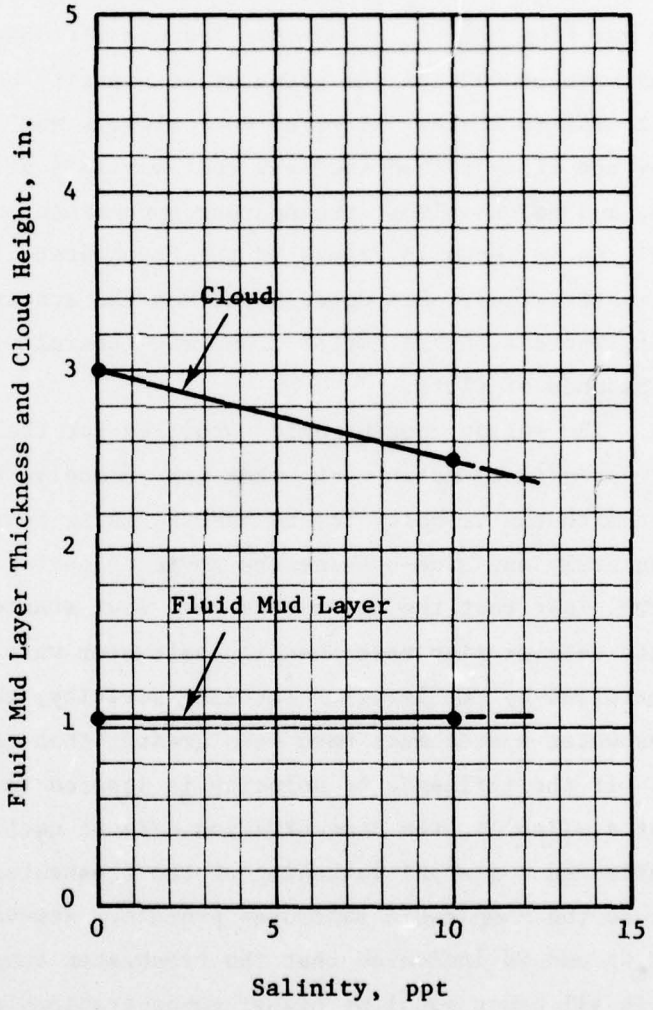

Figure 32. Cloud height and fluid mud layer thickness versus salinity

due to higher settling rates particularly in the early stages of the test. The sediment deposit profile for test 19 (Figure B3) shows a high level plateau over the first 12 ft of travel which indicates that most of the settling occurred in this region, thus promoting a low-density head wave in the flow beyond. The movie footage corroborated this in that the head wave showed all the signs of low-density behavior by the time it had travelled 20 ft. It moved very slowly, was light tan in color denoting the fine-grained sediment that was left after the coarser material settled, and had an almost transparent appearance due to low sediment density. As is shown in Figure 32 the freshwater cloud was higher than the saltwater cloud. Its upper layer had the appearance of a thick layer of fluff, whereas the saltwater cloud was generally smooth with relatively sparce patches of fluff.

85. The solids concentration profiles for these tests (Figures C7 and C8, Appendix C) match each other very closely, but they are in conflict with the velocity trends and the movie records. By projecting simultaneously and side-by-side the movie clips for these two tests, it became clear that the freshwater head wave started faster and showed a greater deceleration rate than the saltwater wave. Since this behavior was controlled by the level of settling activity, the settling rate in the freshwater system must have been greater than that in the saltwater system. If the influence of velocity is ignored (since velocity profiles were not available), the concentration data at each sample station should have reflected a gradual weakening of the freshwater profile with respect to the comparable saltwater profile. However, an overlay of Figures C7 and C8 indicated that the freshwater concentration profiles showed in all cases equal or higher concentrations than the saltwater profiles.

86. The explanation of this anomaly could be (a) the deviation of the concentration data was large enough to mask the anticipated trend due to flocculation, (b) the velocity profiles were sufficiently different so that the decreasing concentration trend was not revealed in the concentration profiles, and (c) the sampling data were completely

erroneous. It is noteworthy that the concentration data would be correct if flocculation played a significant role in the settling process in the saltwater system. Since the timing data and photographic evidence were indisputable, the trends derived from the head wave velocity profiles (Figure 31) were honored.

87. In accordance with the above, the results of the sediment system tests may be summarized as follows:

a. The starting head wave velocities exceeded the design discharge velocity by a factor of almost three so that the mud layer did not fill the slot but rather acted under the influence of natural forces. The thickness of the fluid mud layer was approximately 1 in. in each test so that it filled only half the slot opening (2 in.). The height of the freshwater cloud was greater than that of the saltwater cloud. Since the fluid mud layers were of equal thickness, the turbidity layer was thicker in freshwater (2.1 in.) than in saltwater (1.5 in.). This was probably due to the higher percentage of fines in the freshwater sediment. The starting velocities were in proportion to the densimetric driving force $\sqrt{\frac{\Delta\rho}{\rho}}$ (Equation 11).

b. The deceleration of the freshwater head wave was noticeably greater than that for the saltwater wave. This indicates that the settling rate was greater in the freshwater system than in the saltwater system.

c. Any signs of enhanced settling due to flocculation in the saltwater system were masked by the higher settling rate of the freshwater sediment.

d. The concentration profiles for the sediment tests matched each other closely. In every case the freshwater profile displayed a higher average density than the corresponding saltwater profile.

Slurry Density and Bottom Slope

88. Slurry density and bottom slope variables were combined in a factorial test matrix comprised of three (3) densities and five (5) slopes. The objective was to study upslope and downslope mud flow behavior as a function of not only bottom slope but also slurry density. Slurry densities were selected on either side of the baseline value (15 pcs) at 20 pcs and 10 pcs. The corresponding slurry properties are shown in Table 4 for a liquid salinity of 10 ppt.

Table 4

Slurry Properties for 10 ppt Salinity

Dry Weight, pcs		Actual Slurry*	
Target	Measured Average	Density g/cc	Sediment Concentration g/ℓ
10	9.0	1.070	96
15	15.7	1.118	170
20	20.0	1.150	224

*Solids density = 2.66 g/cc.

As can be seen from Table 4 the measured solids ratios varied somewhat from the target values of 10, 15, and 20 pcs because the dilution process was based on estimated mud properties and the measured value was not available until after each test was completed. The average of the five (5) measured values is listed in Table 4 opposite the corresponding target value. In the remaining test the target values are used to reference these data.

89. Bottom slope values were based on a 2-degree maximum since this was the limit that the tank could provide and still maintain at least a 12-in. water depth at the high end of the false bottom. The slope angles were therefore selected as 0, 1, and 2 degrees. The slope values were 1:57 for 1 degree and 1:29 for 2 degrees. The upslope was denoted by a plus (+) sign and the downslope by a minus (-) sign.

Since at a given angle the behavior of the mud system was quite different in the two directions, each was counted as a discrete angle. Thus, the test angles were +2, +1, 0, -1, and -2 degrees. The 0-degree angle was the baseline condition.

90. The dynamic characteristics of the fluid mud systems can be seen from the plots of head wave velocity as the wave propagates down the tank. These are shown in Figures 33, 34, and 35 for the 10-, 15-, and 20-pcs slurries, respectively. In all tests the starting head wave velocity was well above the design discharge velocity for the mud flow generator (i.e., 0.10 fps). Since the fluid mud layer was essentially 1 in. thick for each of these tests (Figures 36-38), it filled only half the slot height and its dynamics were determined by natural forces. The influence of bottom slope is shown clearly in the 15-pcs slurry test (Figure 34). As the bottom sloped down from the horizontal position, the head wave moved down the tank at a higher speed. At 1 degree downslope (test 22) the head wave actually accelerated over the test length; at 2 degrees downslope (test 23) the acceleration was more pronounced and the head wave appeared to approach a terminal velocity value. These effects were due to the gravity component, $\frac{\Delta\rho}{\rho}gs$, acting parallel to the bottom surface in the downslope direction (vector relationships are shown in the sketch below).

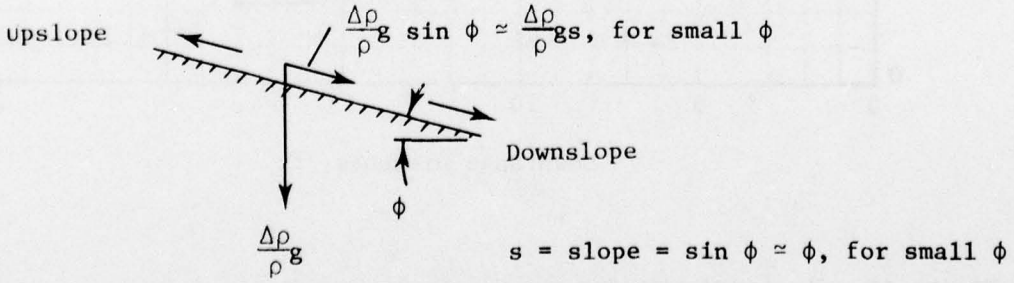

In the downslope direction the gravity component counteracted friction forces at the top and bottom interfaces of the sediment wave. Its action on the fluid mud layer increased the shear stress applied to the sediment bed and thereby increased resuspension activity and rates and reduced

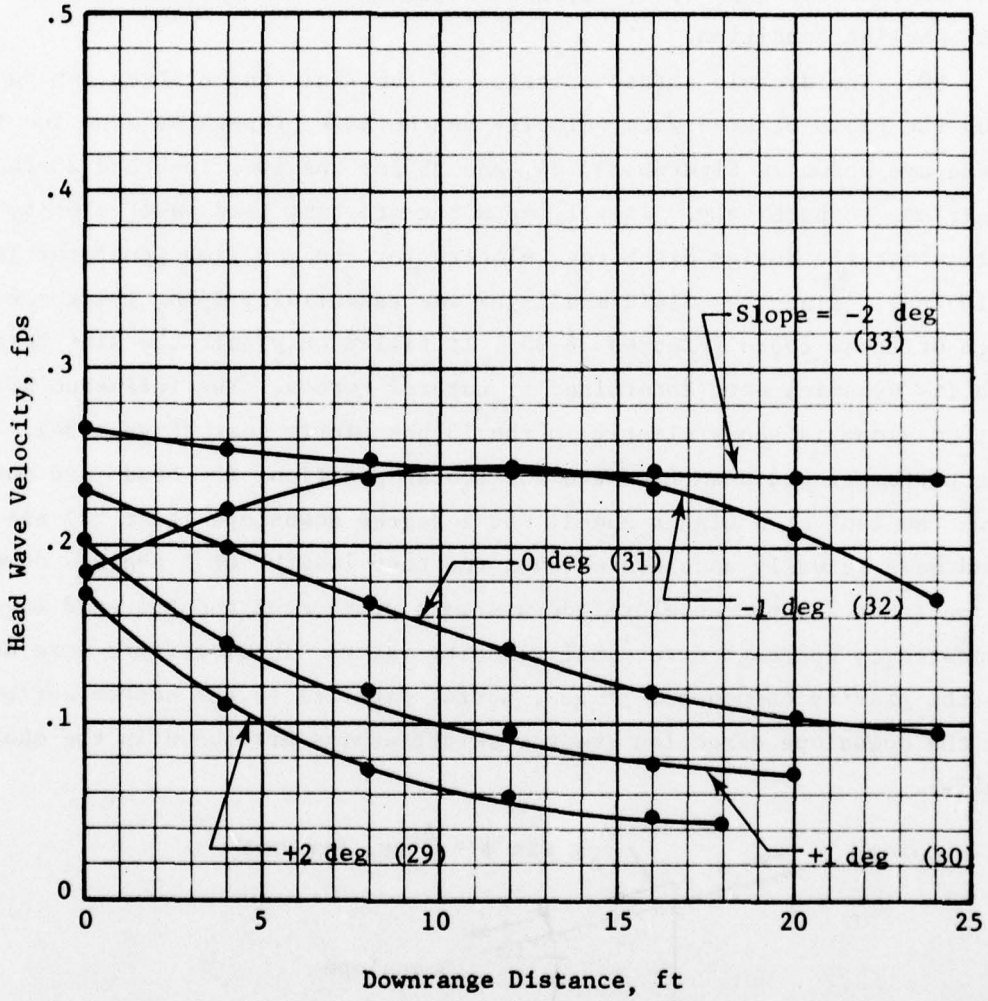

Figure 33. Head wave velocity versus distance for slope parameter, 10-pcs slurry

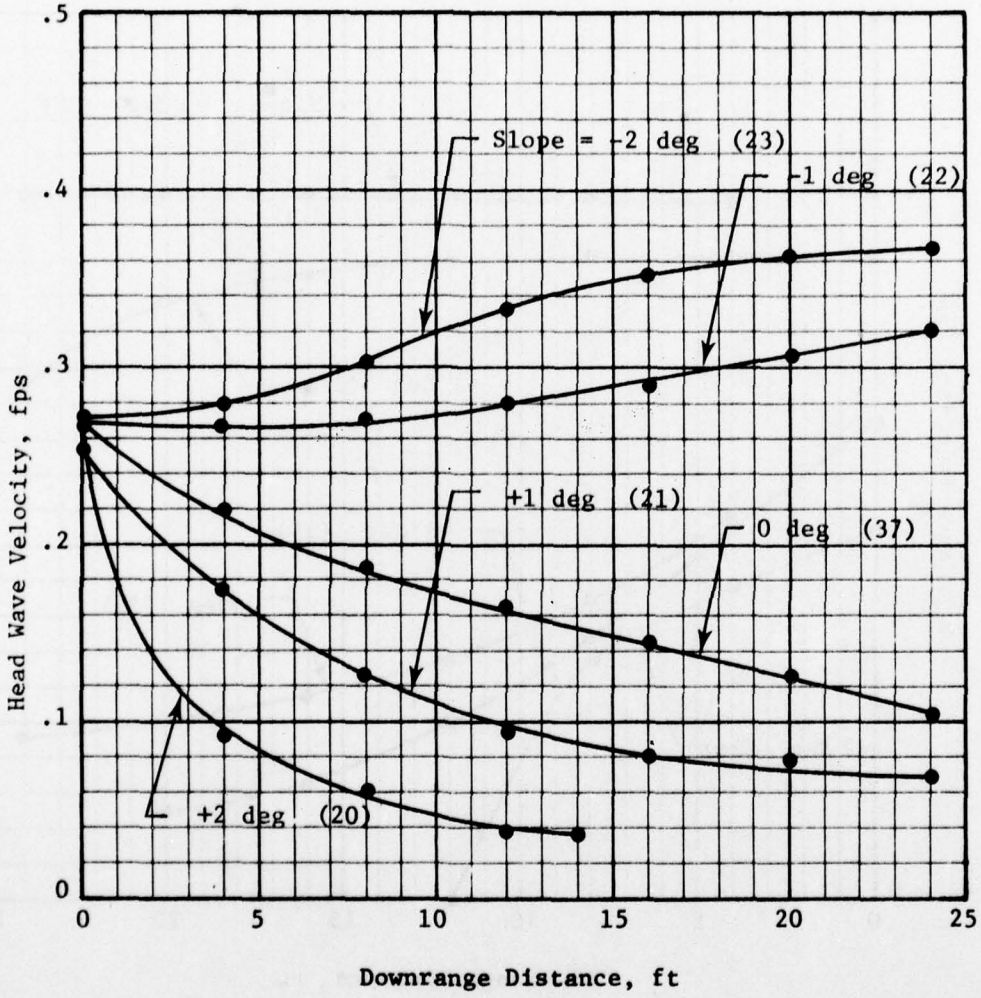

Figure 34. Headwave velocity versus distance for slope parameter, 15-pcs slurry

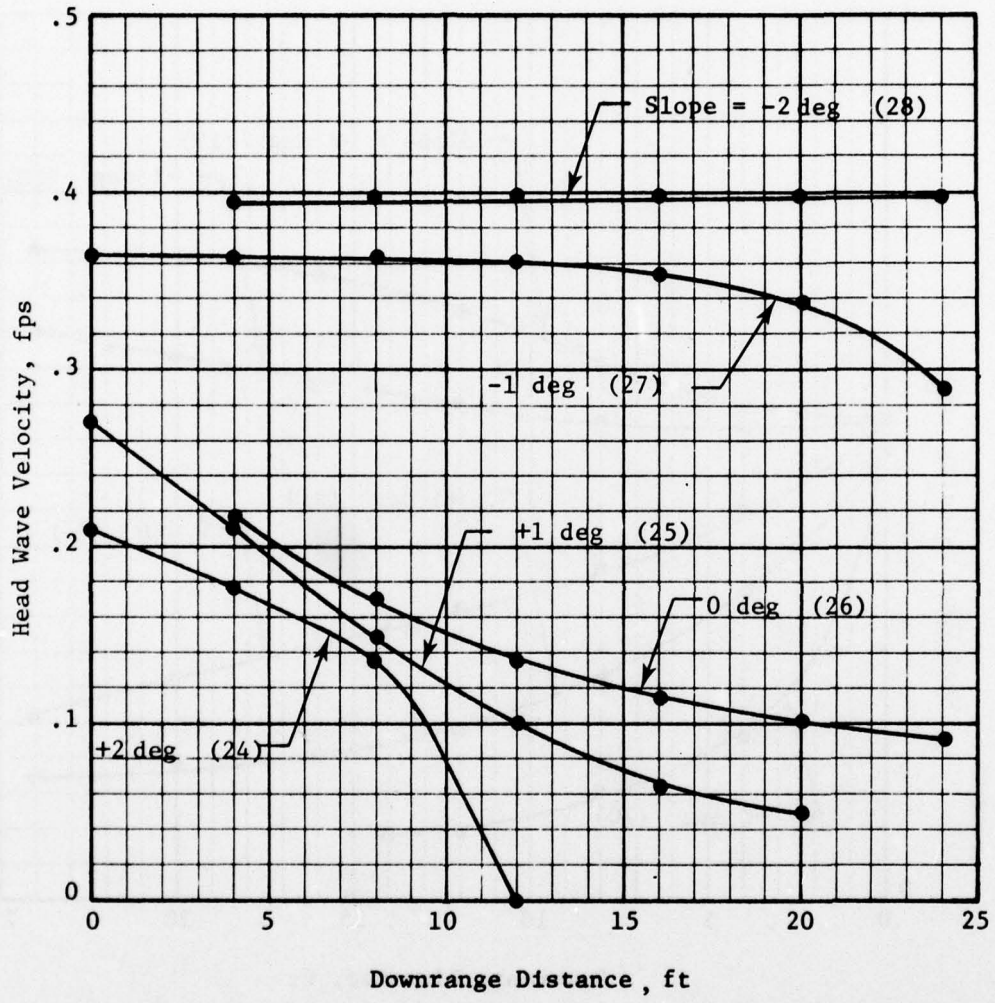

Figure 35. Headwave velocity versus distance for slope parameter, 20-pcs slurry

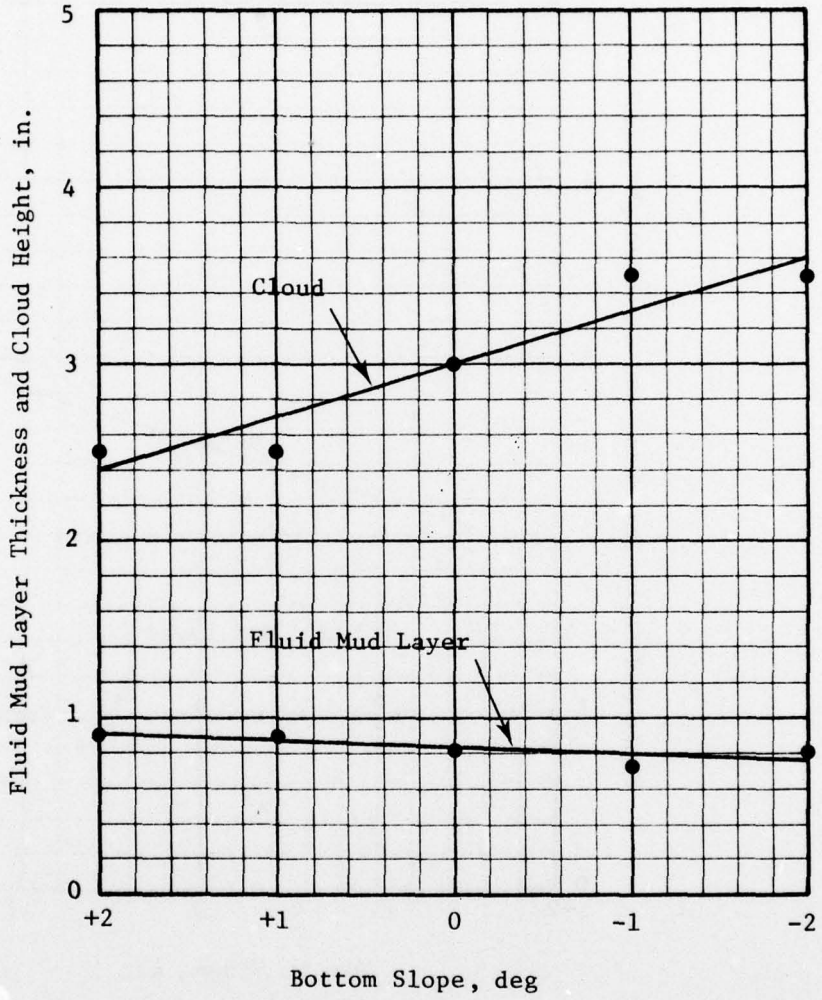

Figure 36. Cloud height and fluid mud layer thickness versus bottom slope for 10-pcs slurry

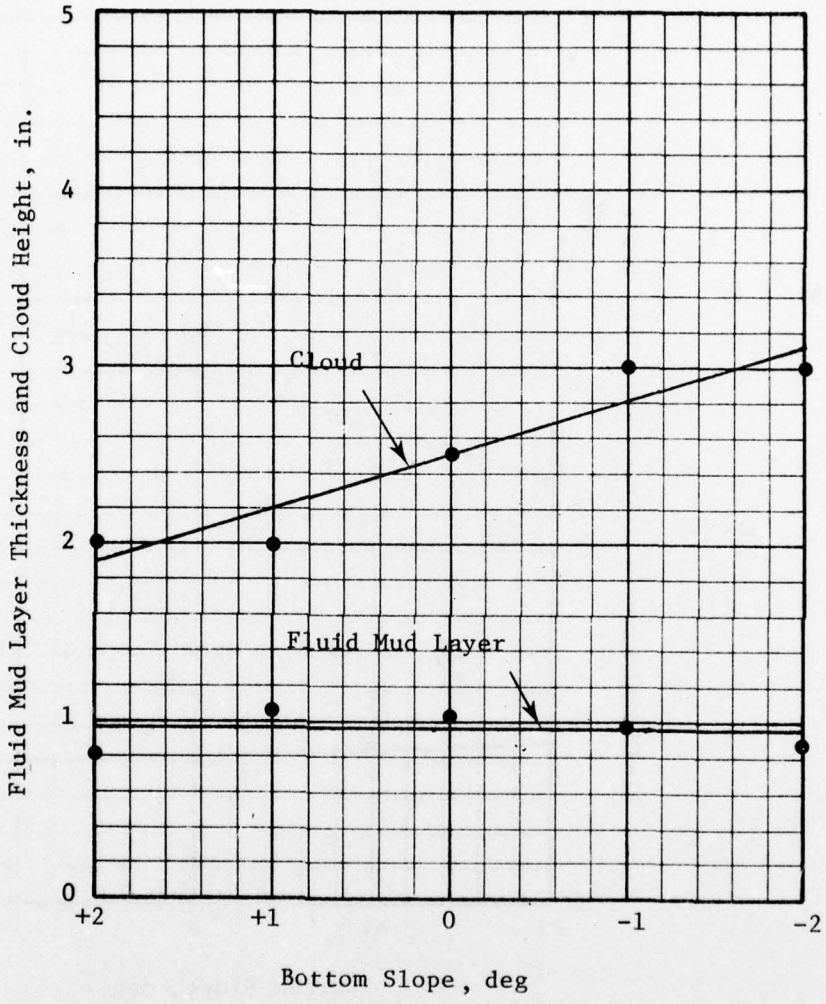

Figure 37. Cloud height and fluid mud layer thickness versus bottom slope for 15-pcs slurry

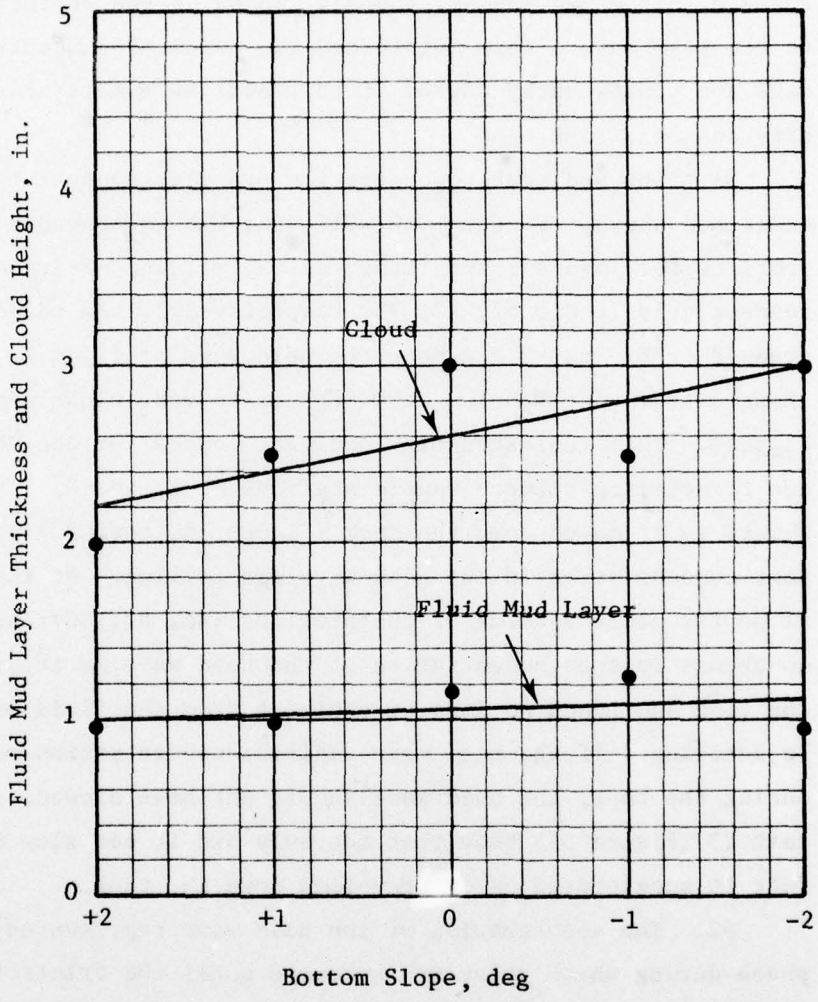

Figure 38. Cloud height and fluid mud layer thickness versus bottom slope for 20-pcs slurry

the net settling of sediment from the fluid mud layer. The reduction in settling losses increased the rate at which sediment was transported forward in the mud system, thereby improving the sediment supply rate to the head wave. This reinforced the sediment concentration in the head wave and consequently caused it to travel at a more nearly constant velocity down the tank.

91. The sediment concentration profiles support the behavior described above. Figures C16, C17, and C18 in Appendix C show the profiles for 15-pcs slurry tests at 0-, -1, and -2-degree slopes, respectively (tests 37, 22, 23, respectively). As the downslope increased from 0 to -2 degrees, the head wave profiles AA, BB, and CC changed from wide spacing at 0 degrees to very close spacing at -2 degrees. This indicates high sediment losses for the horizontal bottom due to settling between sample stations A, B, and C. The head wave slowed as it moved down the tank (Figure 34, test 37) because the sediment concentration in the head wave was falling. At the -2-degree slope the close spacing of the profiles (AA, BB, CC) indicates virtually no change in the concentration of the head wave as it progressed down the tank and hence no loss of sediment from the fluid mud system due to settling. If the head wave sediment concentration was constant during the test, the head wave should not have slowed. The data for test 23 (Figure 34) show that not only did it not slow down but in fact it accelerated as it travelled down the tank.

92. The acceleration of the head wave represented a transient phase during which velocity increased until the friction and drag forces just balanced the gravity forces associated with the height of the mud layer and the slope of the bottom. In tests 22 and 23 the terminal velocity was not achieved within the length of the tank. The head wave velocity for the -2-degree slope appeared to approach a higher terminal value than that for the -1-degree slope. This is valid since the gravity force due to the slope was greater for the steeper angle.

93. In accordance with the above results the bottom slope may be set at a value such that the fluid mud system is in a steady-state condition wherein the concentration profiles are the same and unchanging and the head wave velocity is constant. This represents the slope at which the fluid mud will flow continuously without slowing down or stopping. From Figure 34 this value is approximately 0.75 degree for the 15-pcs slurry system.

94. In the upslope tests the gravity component along the slope acted counter to the direction of fluid mud flow and was noticeably effective in retarding the flow. As the fluid mud layer slowed, the shear force on the bed lessened, which reduced resuspension and increased the net rate of settling. Consequently, less sediment reached the head wave so its concentration weakened and the head wave slowed down. The head wave velocity plots (tests 20 and 21, Figure 34) reflect this deceleration trend and show it to be clearly dependent upon the upslope angle. The sediment concentration profiles (Figures C14, C16, Appendix C) provide evidence of the severely decreasing concentration in both the head wave and the fluid mud layer as a function of distance travelled and increasing upslope angle.

95. The observed behavior of the fluid mud systems under upslope conditions was compatible with the reasoning presented in the preceding discussion. Although the head wave started up the slope with reasonable speed and momentum, it slowed down perceptibly under the force of the gravity slope component. After approximately 12 ft of travel for the 1-degree upslope and 10 ft for the 2-degree upslope, the lower fluid mud layer appeared to stop abruptly as though the mud supply to the head wave was suddenly cut off. At the same time the head wave was transformed into a turbidity wisp that moved ahead of and separated from the denser lower layer. The leading edge of the dense layer was obscure, and a head wave was not present, and the dense layer decelerated to a barely discernible velocity. This phenomenon was peculiar to

each upslope test. Visual observations gave the impression that the momentum of the fluid mud layer decreased as it came to a near stop, while the turbid head wave still had enough momentum to gradually move ahead of the mud layer. Figure 39 shows the head wave of test 21 as it reached the 16-ft mark 2 ft ahead of the mud layer after initial separation occurred at 12 ft.

96. Although no hard evidence is available, the recession and separation of the fluid mud layer from the head wave are probably due to the high settling rate that was promoted by the gravity slope component. As recession proceeded, the head wave was fed a low-concentration mixture at a diminishing rate. When the fluid mud layer slowed to a near stop (recession velocity ≈ head wave velocity), the head wave supply was cut off and the head wave consisting of low-concentration fines separated from the fluid mud layer and travelled on under its own power. Most of its kinetic energy was converted to potential energy as it moved up the slope, and the remainder was dissipated through friction.

97. Slurry concentration influenced most of the dependent variables of the study. The concentration profiles (Figures C9-C23, Appendix C) for each bottom slope, when viewed in sequence according to slurry concentration, indicate that as slurry concentration increased from 10 to 20 pcs, maximum sediment concentration in the fluid mud layer likewise increased. The fluid mud layer thickness, as derived from the concentration profiles, showed only slight sensitivity to slurry density (Figures 36-38). The straight-line plots of mud layer thickness are superimposed in Figure 40 to illustrate the relationship more clearly. The trend is in the direction of thicker layers with denser slurries, which is logical since the concentration profiles tend to be geometrically similar and their peak values increase with slurry density.

98. Slurry density showed some influence over the behavior of the head wave as can be seen by scanning in sequence the velocity plots for 10-, 15-, and 20-pcs slurries (Figures 33, 34, and 35, respectively). The +2-, 0-, and -2-degree velocity plots are superimposed in Figure 41

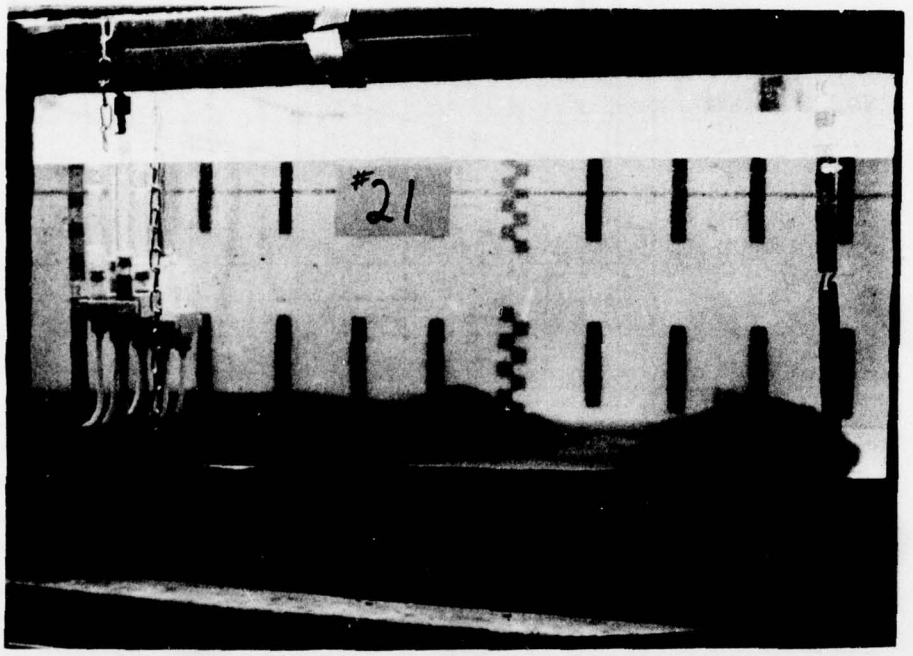

Figure 39. Separated head wave, +1-degree slope, test 21

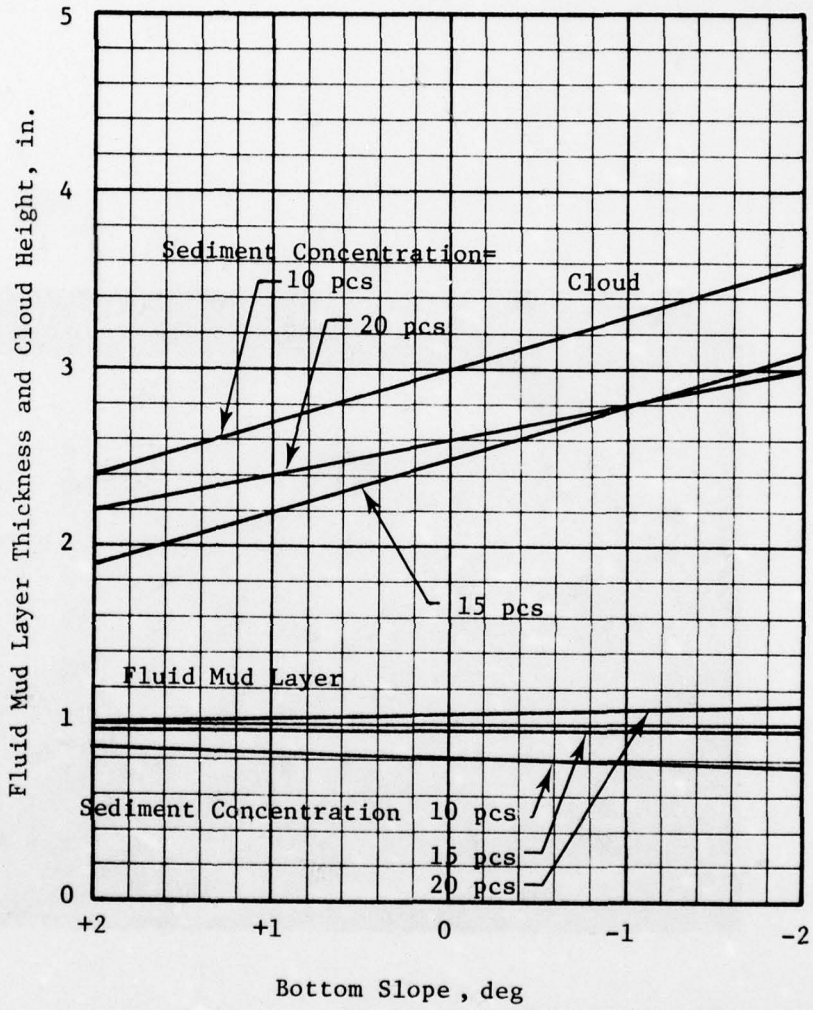

Figure 40. Cloud height and fluid mud layer thickness versus bottom slope for 10-, 15-, and 20-pcs slurries

AD-A062 480 J B F SCIENTIFIC CORP WILMINGTON MA F/G 13/3
LABORATORY INVESTIGATION OF THE DYNAMICS OF MUD FLOWS GENERATED--ETC(U)
AUG 78 G HENRY, R W NEAL, S H GREENE DACW39-76-C-0173
UNCLASSIFIED WES-TR-D-78-46 NL

2 OF 2
AD
A062480

END
DATE
FILMED
3-79
DDC

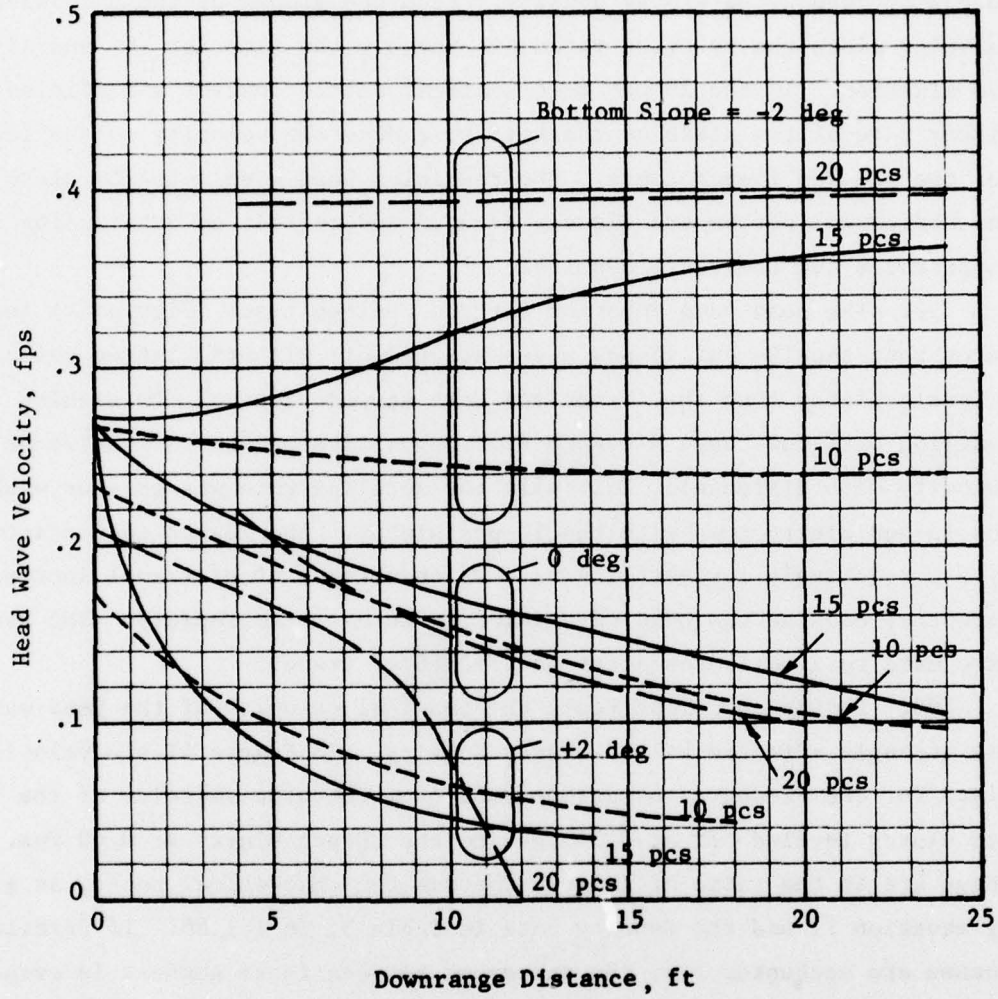

Figure 41. Head wave velocity versus downrange distance for +2-, 0-, and -2-degree bottom slopes and 10-, 15-, and 20-pcs slurries

in order to show their differences more clearly. In the 0-degree slope tests the starting velocities are in approximately the correct relationship with respect to slurry density. From the slopes of the head wave velocity plots the settling rates are roughly the same for 10- and 15-pcs slurries. In the 20-pcs test sediment settled out at a sufficiently higher rate at the start of the test to reduce the velocity to the levels for the 10- and 15-pcs tests. The resulting head wave velocity plots for the horizontal bottom are closely grouped and reflect no outstanding differences due to slurry density.

99. The head wave behavior for the upslope tests (Figure 41) indicates that the 10- and 15-pcs waves started off with the latter velocity properly higher than the former and both showed signs of diminishing settling with downrange distance (i.e., positive second derivative of velocity with distance). Initially the settling rate was greater with the 15-pcs slurry than with the 10-pcs slurry. The 20-pcs test started with a relatively low settling rate which after 6 ft of travel increased abruptly, causing the head wave velocity to decrease rapidly. The head wave came to a full stop after only 12 ft of travel.

100. In the downslope tests the terminal velocity of the head wave was strongly affected by the slurry density. In Figure 41 the velocity plots for the -2-degree downslope test show that the velocity of the 10-pcs slurry leveled off at 0.24 fps and the 20-pcs slurry at 0.40 fps. These are in the ratio of 1:1.67, whereas the theoretical ratio, as given by equation 11 and the density data in Table 3, is 1:1.86. If friction losses are accounted for, the agreement between these numbers is even closer so that the velocity shift is attributable to the change in slurry density. In the 15-pcs test (-2-degree slope, Figure 41), the head wave was in a transient state although its velocity appeared to approach an asymptotic value of 0.38 fps. It is not clear why the 10- and particularly the 20-pcs head waves were in a steady-state condition from the start and the 15-pcs wave was in a transient state throughout the test. The asymptotic velocity value, however, does bear

the correct relationship to the 10-pcs value (actual ratio = 1.58, theoretical = 1.50). Thus, in all three tests at -2 degrees slope the steady-state head wave velocity was proportional to $\sqrt{\Delta\rho}$.

101. The dependence of the critical slope on slurry density is indicated by the head wave velocity plots in Figures 33, 34, and 35. The critical slope is the minimum downslope angle at which the fluid mud system just reaches a steady state of motion. This condition is characterized by constant head wave velocity and identical concentration profiles in space and time. The critical slopes were estimated to be 2.4, 0.75, and 2.0 degrees for 10-, 15- and 20-pcs slurries, respectively. These values are plotted below in Figure 42.

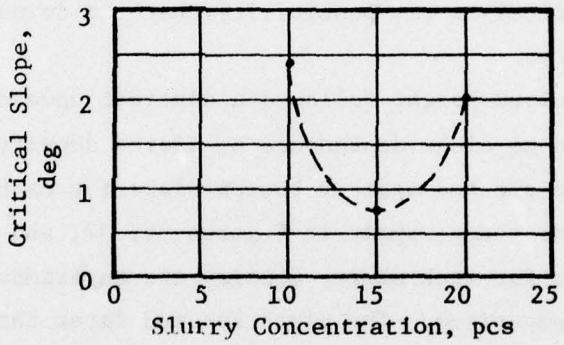

Figure 42. Critical slope versus slurry concentration

The critical slope adjusts the gravity force component (along the bottom) so that it just overcomes those forces acting to cause the sediment grains to settle out. If the settling characteristic is weak (i.e. low settling rates), the critical slope will be small. As the settling characteristic becomes stronger (unstable mixture), the critical slope must increase. According to Figure 42 the settling characteristic was strongest at 10 pcs, slightly less at 20 pcs, and it fell to one third strength at 15 pcs. This trend indicates that net settling, as measured by critical slope, lessened as the slurry concentration increased from 10 to 20 pcs. This trend cannot be attributed to flocculation because

the large mean grain size of the Boston Harbor sediment as well as high sediment concentration suppressed flocculation activity so that its role was at most minor. The strong influence of sediment concentrations in the range 50 to 200 g/ℓ on the viscosity of the slurry[11] might have created conditions in the boundary layer that influenced the settling characteristics of the sediment. For instance, in the region from 10 to 15 pcs increasing viscosity might have had an insulating effect that slowed down particle motion and reduced the settling rate. From 15 to 20 pcs the increased viscosity might have caused the boundary layer to grow so thick that it acted as a sediment trap and effectively increased the loss of sediment from the fluid mud layer. The foregoing explanation is only conjecture and is not supported directly by hard evidence. Equally hypothetical is the possibility that the downslope data were all or in part faulty.

102. The cloud height followed a distinct upward trend with downslope but showed no clear dependence on slurry density. The cloud height data were plotted against bottom slope for each of the three slurry densities; these appear in Figures 36, 37, and 38. The linear regression plots for each slurry density are superimposed in Figure 40 for direct comparison. The plots for mud layer thickness are also included in Figure 40 so that turbidity layer thickness can be viewed along with cloud height (i.e., turbidity layer thickness = cloud height - fluid mud layer thickness). For each slurry density the cloud height and the turbidity layer thickness both increased as the bottom slope changed from upslope to downslope angles. The explanation of this result lies with the head wave velocity which showed the same trend (Figures 33, 34, and 35). Head wave velocity established the turbulence state at the upper interface between cloud and water column. The turbulence level in turn determined how much fine-grained sediment was stirred up to form the cloud and hence how thick the turbidity layer would be. The height of the cloud and the thickness of the turbidity layer were approximately 0.5 in. greater for the 10-pcs tests than for the 15-pcs tests, and the 20-pcs data fell in between the two sets (Figure 40).

Current

103. The behavior of the fluid mud layer was investigated in currents that ran in the same direction as and in the opposite direction to the motion of the flowing mud. In this section the test in the same direction is referred to as the parallel flow condition and that in the opposite direction the counter flow condition. A single test was conducted in each direction at a current velocity of 6 fpm (0.1 fps) which was approximately one third of the starting velocity of the head wave. These tests had less than the full tank length available because the mud generator box had to be placed beyond the turbulence region of the header box in the parallel flow test and far enough upstream of the recirculation suction so that mud was not ingested and recirculated during the counter flow test.

104. Visual observations of these tests revealed several peculiarities of the mud system behavior in the presence of currents. The motion of the head wave was not noticeably affected by either the parallel or counter flow currents. The head wave did not appear to move faster in the parallel flow test nor slower in the counter flow test than in the zero current (baseline) test. The general level of turbidity was notably higher in the current tests than in the baseline test. Under counter flow conditions turbidity was generated at an increased rate at the upper interface of the mud layer, and it was transported rearward from the head wave by interfacial waves that broke to form cylindrical vortices. These appeared to rise from the interface in the form of sporadic puffs which then moved solely under the influence of the current. The puffs extended 2 to 3 in. above the main turbidity cloud but were sparse enough not to add to the height. In the parallel flow test as much turbidity was generated as in the counter flow case. In the zero current test the mud flowed to the head wave along the bottom and then up and over through the head wave where it virtually came to rest in the upper strata of the mud layer. When parallel current was superimposed on this motion it appeared to apply a shearing action on the upper strata that created turbulence and

generated turbidity at the upper interface. This turbidity was initiated at the head wave as the sediment mixture reached the upper levels of the mud layer after rotating through the head wave. The resulting puffs of turbidity extended along the entire length of the mud layer from head wave to mud generator box and they moved with the current. As the head wave slowed down and approached the current velocity the turbidity moved along with it.

105. The quantitative data for the current tests corroborate the observed behavior of the mud system. The head wave characteristics (Figure 43) indicate that the parallel flow head wave (test 36) started at about the same velocity as in the zero current (test 37). It held its velocity for several feet before it slowed down abruptly and approached the characteristic for the zero current test. At the start the shearing action of the current on the upper interface of the mud layer possibly inhibited the settling process momentarily which caused the head wave velocity to be sustained. After a few feet of travel the mud layer stabilized and the sediment dropped out at an accelerated rate. In the counter flow test the head wave started at a higher velocity but with a greater rate of deceleration than in either the zero or parallel current tests. It then leveled off parallel to the zero current characteristic at a slightly higher velocity. In this case the shearing action of the current possibly accelerated the settling rate at the start of the test by slowing the mud flow.

106. The concentration profiles for the current tests (Figures C24, C25 and C26, Appendix C) are not widely different and they do not indicate prominent differences in settling rates. There is a peculiarity however in the peak concentration of the head wave. Whereas in virtually every other test the peak concentration of the head wave decreased as the head wave moved down the tank, in the counter flow test the peak at station B after 8 ft of travel was greater than that at A, the first sampling station. This would normally indicate an increase in the sediment content of the head wave which could have been realized by a

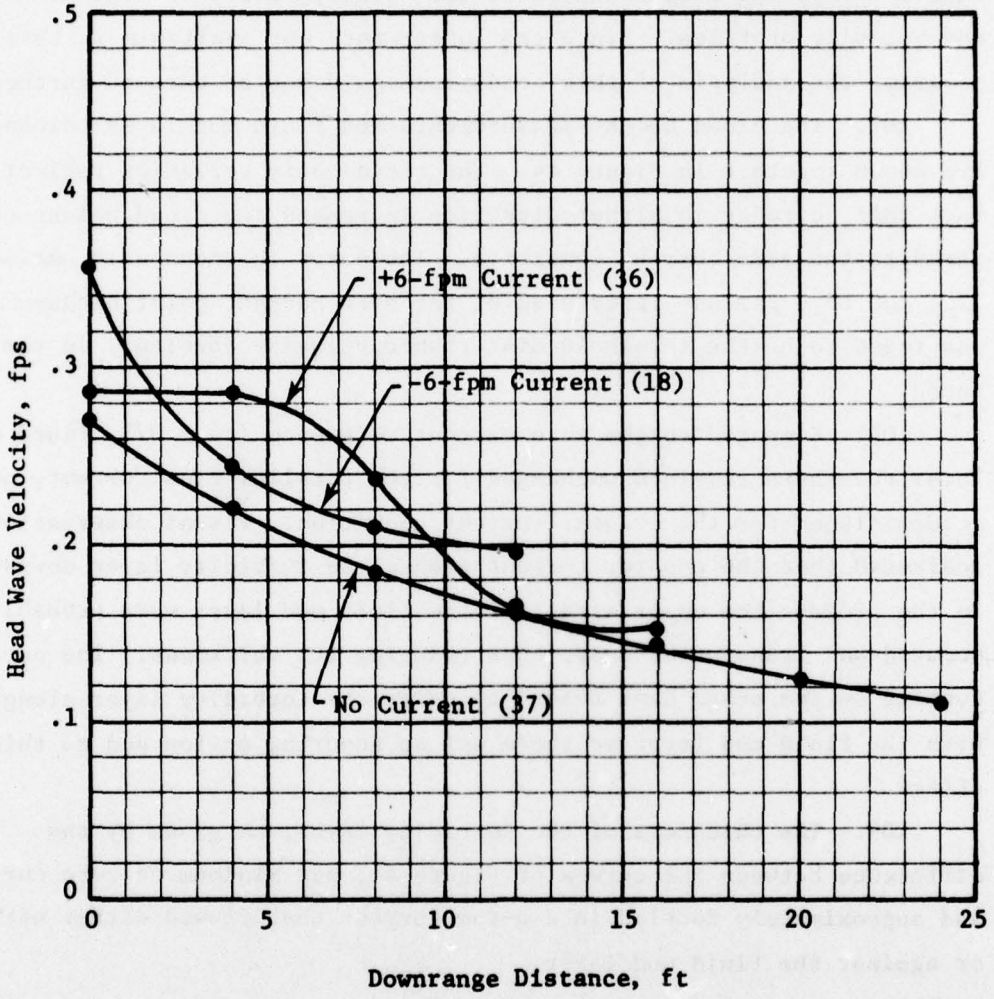

Figure 43. Head wave velocity versus distance for current conditions

fluctuation in the rate that sediment was supplied to the head wave, presumably caused by the counter flowing current. This could be verified by comparing mass balances at each station based on concentration and velocity profiles. Since the latter were not available in this program, the analysis of this condition could not be pursued further.

107. The cloud height measurements and fluid mud layer thicknesses are shown together in Figure 44. The cloud characteristics reflect the fact that currents in either direction increased the cloud height compared to the zero current condition. The curve is shown as a horizontal line out to 3 fpm on either side of the zero current point because this was found to be the threshold disturbance velocity (orbital) in the wave tests.

108. Compared to the zero current reference (test 37), fluid mud layer thickness remained unchanged for the parallel flow current, and it diminished for the counter current condition. Visual observations indicated that the counter current washed the turbidity layer downstream. In the process the upper strata of the fluid mud layer were probably scoured and transported away, thus reducing its thickness. The parallel current on the other hand tended to carry the turbidity layer along with the fluid mud layer so there was no scouring action and no thinning effect.

109. The thickness of the turbidity layer, as given by the difference between the curves of Figure 44, was minimum at zero current and approximately doubled in a 6-fpm current that flowed either with or against the fluid mud layer.

Waves

110. The interaction of waves on the fluid mud system was demonstrated by a series of three wave tests. The tank waves were prescribed by postulating a typical full-scale wave system that might be encountered in the field and scaling that system by Froude number down to tank scale. Since the interaction between waves and mud was generated by the orbital motion of the water column, particularly in the region of the mud flow,

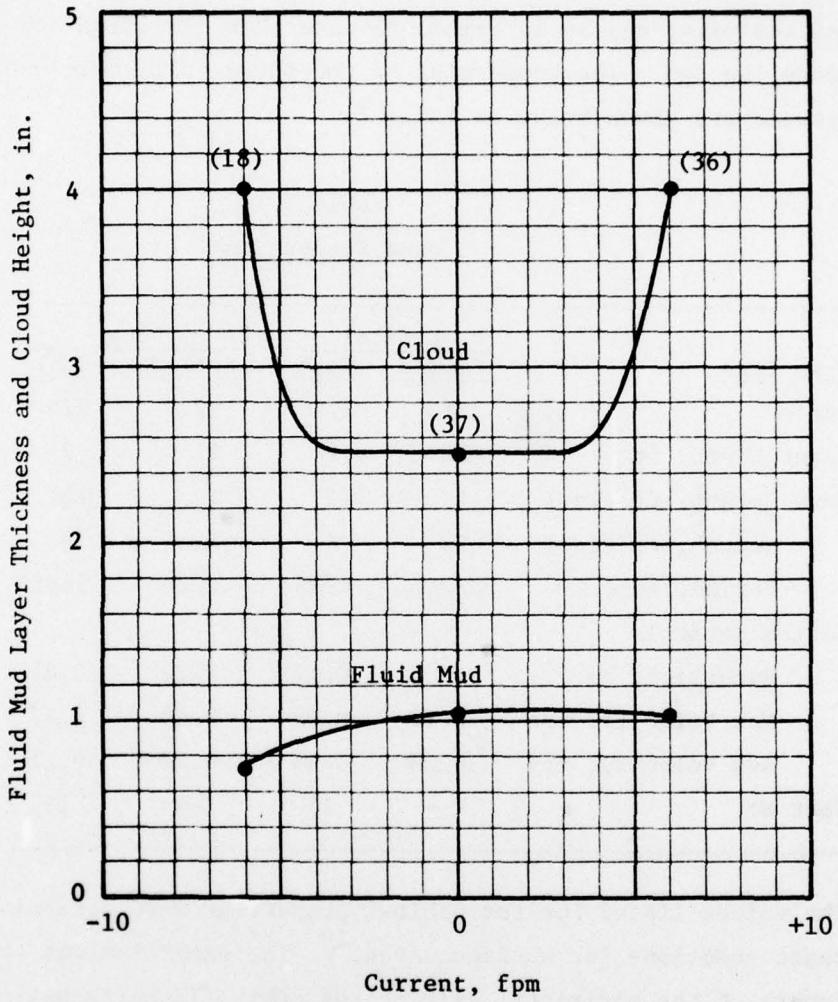

Figure 44. Cloud height and fluid mud layer thickness versus current

the bottom orbital velocity and particle excursion were used as indicators of orbital activity. The selected wave systems represented the typical wave which had a low orbital activity, a longer wave of more intense orbital activity, and an intermediate wave that clarified any threshold between the two. The properties of the three full-scale and tank-scale wave systems are given below in Table 5.

Table 5

Wave Properties

	Typical		Long		Intermediate	
Wave Type	Scaled	Tank	Scaled	Tank	Scaled	Tank
Scale	1/1	1/6	1/1	1/6	1/1	1/6
Water Depth, ft	12	2	12	2	12	2
Wave Height, ft (in.)	1	(2)	1	(2)	1	(2)
Length, ft (in.)	24	4	48	8	32	(64)
Period, secs	2.17	0.88	3.20	1.30	2.52	1.02
Bottom Orbital						
Excursion, in.	1.04	0.17	5.22	0.87	2.30	0.38
Max Velocity, fps	0.12	0.05	0.43	0.17	0.24	0.10
Avg Velocity, fps	0.08	0.03	0.27	0.11	0.15	0.06
Test No.	--	15	--	16	--	35

The values listed for the orbital properties were determined from the basic equations for surface waves.[18] The excursion was the total length of the horizontal axis of the orbit (2X horizontal amplitude), maximum velocity was given by the product of angular velocity and horizontal amplitude, and average velocity was the ratio of total distance travelled in an orbit (2X excursion) divided by the orbit period. The bottom orbit excursion and period were checked for each wave system that was generated in the test tank. These agreed closely with the theoretical values in Table 5.

111. Visual observations indicated that the mud flow was unaffected by the "typical" wave system (i.e., 2 in. high x 4 ft long x 0.03 fps,

test 15). The bottom orbital motion was barely perceptible in the clear water column before the mud was released, and its perceptibility did not improve in the presence of the mud flow. The head wave moved smoothly and was not impeded by orbital motion during its transit of the tank. The turbidity layer remained stable, and the low level of orbital motion did not stir sediment into the upper levels of the water column. After 14 ft of travel, the head wave started to separate slowly from the body of the fluid mud layer, and the two elements continued to move down the tank at nearly the same speed. There was no apparent connection between the separating head wave and the orbital motion, and the phenomenon did not occur in either of the other two wave tests. However, it was the only case of head wave separation with zero-slope bottom; all other incidents occurred with upsloping bottoms.

112. The "long" wave generated a strong orbital motion that was superimposed on the motion of the mud system with no visible diminution of either motion. At any instant the entire flowing mud system from head wave to generator box was undergoing oscillatory motion in the form of travelling compression and expansion waves. The motion of the mud system was induced by the orbital motion of the water column which near the bottom had a horizontal component but virtually no vertical component. The travelling surface wave system imparted the same travelling characteristic to the bottom motion which was made visible by the presence of the mud system. The mud system was therefore acting as a tracer fluid that sensed the presence of compression and expansion waves on the bottom as well as their propagation in the same direction and at the same speed as the surface waves. The observed excursion of mud particles was approximately 1 in., which is in close agreement with the value in Table 5.

113. The shear and turbulent conditions associated with the 1-in. bottom excursion of the "long" wave were intense enough to drive fine-grained sediment into the upper water column. From all appearances the sediment flowed up and over the head wave and was deposited on top at

zero velocity where it formed the normally stationary upper strata of the mud flow. The visible upper layers were taken up by the orbital motion and a very fine, transparent cloud moved slowly upward in the water column into regions of greater orbital motion. By the end of the test this nearly transparent cloud had risen to a height of 9 in. at the mud generator box, tapering to zero at the head wave at the downstream end of the tank. The linear variation in cloud height suggests that the height to which the fine-grained sediment was driven depended upon the length of time the upper strata of the mud system were exposed to the orbital motion of the water column.

114. The intermediate wave system resembled the "typical" wave, and the fluid mud system oscillated through an excursion of approximately 0.5 in. as it moved down the tank. Although a light wisp of turbidity formed over the top of the fluid mud layer, it did not migrate higher in the water column during the period of the test. The head wave thinned down toward the end of the test, but it showed no signs of separating.

115. The head wave velocity plots are presented in Figure 45 for the three wave conditions and the baseline test which represents no waves and zero orbital velocity. The plots for the intermediate (test 35) and long wave (test 16) systems agree very closely with that for no waves (test 37), which indicates that these wave systems did not interfere with the gross motion of the head wave. The uniformity of the plots and their slopes also indicates that the orbital motion near the bottom did not alter the settling characteristics of the sediment (by increasing resuspension). This might be due to the fact that in the bottom region the orbital motion has virtually no vertical component and it is also damped by the viscosity of the fluid mud.[11]

116. Under typical wave conditions (test 15) the head wave behavior ran counter to that of the other wave tests in the series. In this test the head wave maintained its velocity out to 16 ft before it started to decrease. This was also the test in which the head wave

separated after 14 ft of travel at the end of the constant velocity phase (Figure 45) after which the separated head wave slowed at an increasing rate. The implication of this is that the barely perceptible orbital motion on the bottom inhibited the settling rate and caused the head wave velocity to remain steady. Yet in the other two wave tests where the orbital motion was considerably greater this influence over settling was conspicuously absent. Neither the concentration profiles (Figure C27 - C30, Appendix C) nor the bottom sediment data (Figure B11, Appendix B) shed any light on this apparent anomaly. This inconsistency along with the separated head wave renders the results of test 15 somewhat suspect.

117. Orbital motion had a significant influence on the cloud height and the thickness of the fluid mud layer. As shown in Figure 46, their values remained constant up to an orbital velocity of 0.06 fps (intermediate wave). Beyond that the influence of orbital motion increased these dimensions so that at 0.11 fps their values had risen by approximately 60 percent as did the thickness of the turbidity layer. The threshold velocity beyond which orbital motion disturbed the fluid mud system was therefore set at 0.06 fps.

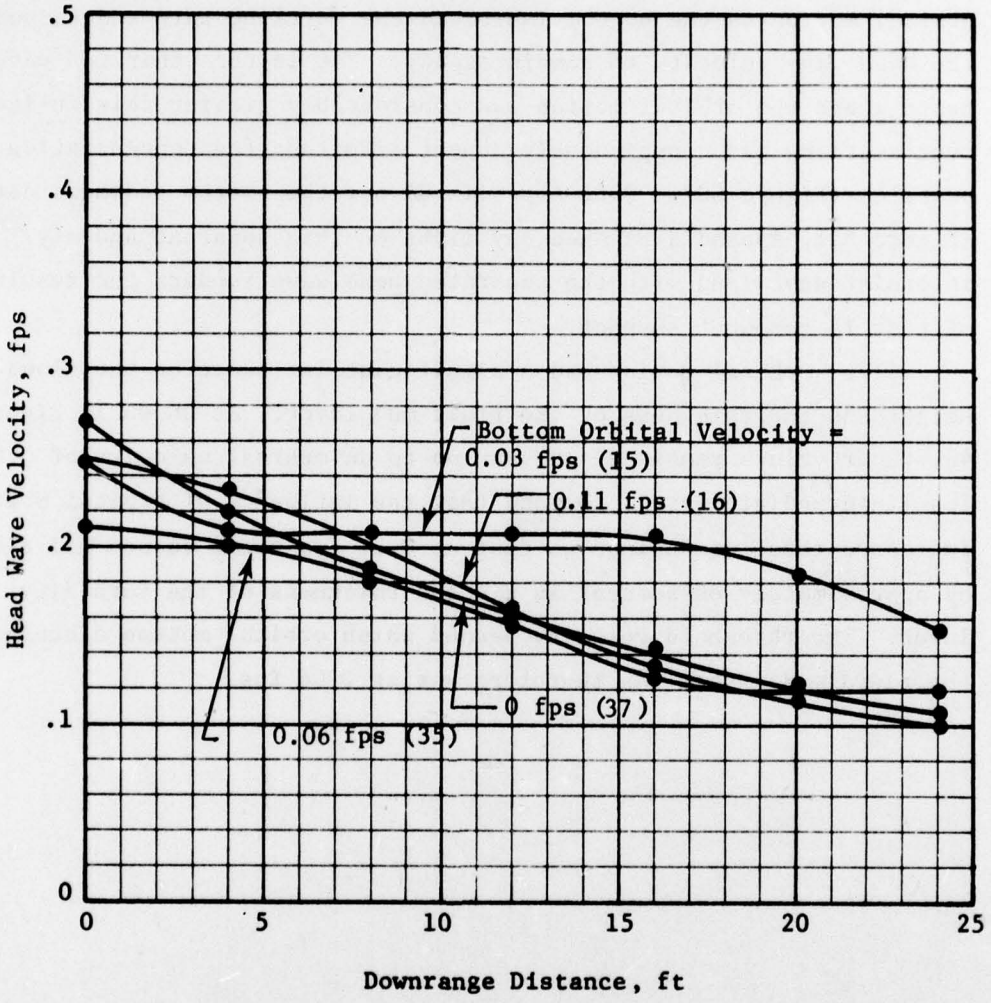

Figure 45. Head wave velocity versus distance as a function of bottom orbital velocity

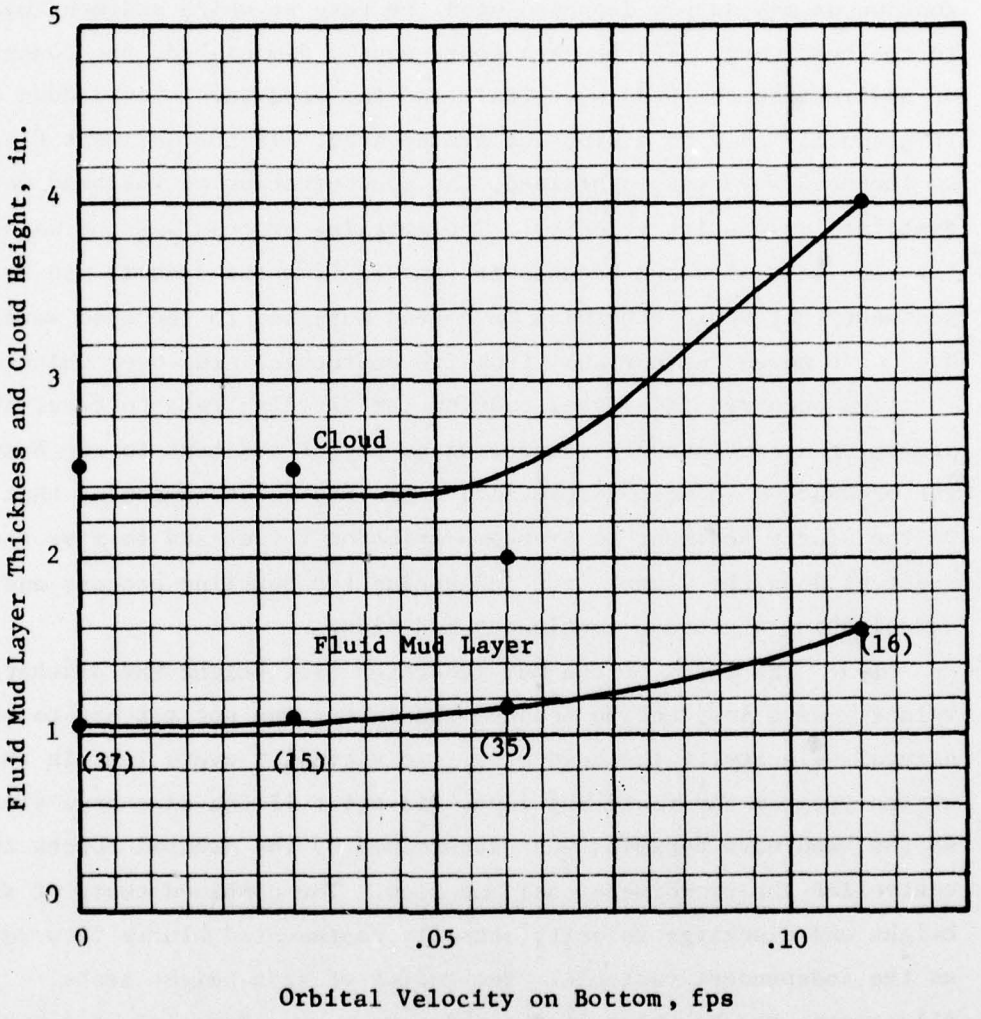

Figure 46. Cloud height and fluid mud layer thickness versus bottom orbital velocity

CHAPTER V: CONCLUSIONS

118. The behavior of a two-dimensional fluid mud system with continuous mud supply depended upon the rate at which sediment was fed to the head wave. If the rate continuously diminished, the concentration of sediment in the head wave fell, and the head wave slowed down until it gradually came to a stop and disappeared. If the sediment flow rate to the head wave was maintained, the concentration of the head wave was sustained as was its velocity. The settling process was the major cause for head wave slowdown because it removed from the dynamic mud system sediment that would otherwise have been supplied to the head wave. As the head wave moved further away from its source the area over which settling occurred increased, causing the settling rate to rise, thereby promoting a continuously decreasing supply of sediment to the head wave. The presence of downslope provided a gravity force component that acted on the slurry sediment to overcome friction forces and to move the sediment down the slope, thus inhibiting the settling process and establishing a steady, continuous mud flow.

119. The tests of the mud generator slot height and discharge velocity were ineffective because the latter was not matched to the natural velocity of the head wave. In virtually every test in the entire program the fluid mud layer did not fill the discharge slot so the head wave dynamics were determined by the natural forces that controlled the two-dimensional mud flow. The combined tests of slot height and discharge velocity actually represented slurry flow rate as the independent variable. The series of slot height tests illustrates the behavior of the mud system as a function of slurry flow rate. (Note in Figures 27 and 28, slot heights of 1, 2, and 3 in. were equivalent to slurry discharge rates of 11, 22, and 33 gpm, respectively.) The conclusions that can be drawn from these results are as follows:

a. The effects of settling diminished as the slurry flow rate increased. This is indicated in the head wave velocity plots (Figure 27) which reflect higher average head wave velocity and less deceleration of the head wave over the test range with higher slurry flow rates.

b. The fluid mud layer thickened as the slurry flow rate increased (Figure 28). This is logical in light of equation 11 since a greater flow rate would promote a higher solids concentration in the head wave and mud layer which would increase the density difference and hence the head wave velocity and height. Qualitatively, the behavior of the fluid mud layer was predicted by equation 11.

c. Cloud height increased with slurry flow rate at the same rate as fluid mud layer thickness so that the thickness of the turbidity layer remained constant over the range of slurry flow rates. The velocity of the fluid mud layer established the turbulence level at the upper interface, which in turn determined the amount of turbidity that was generated and consequently the thickness of the turbidity layer. The average velocity in the fluid mud layer, as given by the ratio of slurry flow rate and fluid mud layer thickness, was the same for the 22- and 33-gpm tests, which explains the constant turbidity layer thickness in this flow rate range. At 11 gpm the average fluid layer velocity was 70 percent of the value at 22 and 33 gpm. Accordingly, the turbidity layer should have been thinner at 11 gpm but was not (Figure 28). This trend might have been masked by the scatter of the data at the lower slurry flow rates.

120. The conclusion to be drawn from the single test on the salt and freshwater sediment systems is that the influence of flocculation was completely masked by mechanisms whose influence was opposite to that of the flocculation process. Any flocs that might have formed in the saltwater slurry during recirculation through the delivery system were almost certainly broken up by wall shear and high turbulence levels as the slurry was pumped through the delivery system. The slurry was therefore quite free of flocs as it exited from the mud generator box. The mean grain size of the Boston Harbor mud was approximately 0.020 mm (20 microns), which, according to Migniot,[11] has a very low flocculation factor, F, as defined by the ratio of the mean free sinking rate in a flocculent water medium and the mean free sinking rate of elementary particles in the deflocculated state. The value of F for Boston Harbor mud was 1.8, whereas the average for Migniot's estuarine muds was approximately 400. Migniot also noted that flocculation was not perceptible with grain sizes greater than 0.03 mm (30 microns). Accordingly, the Boston Harbor sediment most likely did not undergo flocculation to the extent that it influenced the behavior of the fluid mud system. The most reasonable conclusion to be drawn concerning the greater apparent settling rate in the freshwater system is that it was caused by differences in the properties of the two sediments although which properties and why are not readily apparent. The freshwater sediment had 24 percent more of its solids in the silt range (Table 2), but the saltwater sediment had 18 percent more of its solids in the sand range which would account for greater initial settling. The total organic carbon content may have enhanced the settling rate,[19] and since the TOC for the saltwater sediment was almost twice the value for the freshwater sediment, this factor favored a higher settling rate for the saltwater sediment. Even the median grain size was larger in the saltwater sediment, which is also synonymous with a higher settling rate.

121. Bottom slope exerted a strong influence on the behavior of the fluid mud system through the generation of a gravity force component

that acted parallel to the bottom in the downslope direction. With uphill flow of the fluid mud, the gravity force acted in phase with friction and drag forces to retard the mud flow and enhance settling. With downhill flow of the fluid mud, the gravity force counteracted friction and drag forces and stimulated resuspension to the extent that net settling was virtually eliminated. The condition of zero settling was characterized by no deceleration of the head wave and uniform sediment concentration profiles. The critical downslope angle at which the head wave maintained constant velocity fell between 0.75 and 2.0 degrees over the range of slurry densities tested. At angles greater than the critical value, the head wave accelerated until an equilibrium velocity was reached at which friction and drag forces were just balanced by the gravity slope component. The thickness of the fluid mud layer was virtually insensitive to the bottom slope over the range +2 to -2 degrees. The turbidity layer thickened as the bottom slope increased in the downslope direction. This reflected the greater turbulence level at the upper interface with higher head wave velocities.

122. Slurry density was found to influence the mud flow parameters in the starting region of each test and in the terminal phase of the downslope tests. The starting head wave velocities related approximately as $\sqrt{\Delta\rho}$ (as expressed in equation 11) in tests where all other parameters were held constant. Beyond the starting region settling effects determined the dynamics of the mud flow as it travelled down the tank. In those slope tests at or beyond the critical angle, the terminal velocity of the head wave was found to be related to $\sqrt{\Delta\rho}$. This agrees with theory based on the balance of friction and drag forces by the gravity slope force at the terminal condition. The thickness of the fluid mud layer displayed a weak trend with slurry density in that the layer thinned slightly with the 10-pcs slurry and thickened with a 20-pcs slurry as the downslope angle increased. The thickness of the turbidity layer was generally greater for the lower density mixture over the range of bottom slope angles.

123. Current was found to affect the fluid mud system in several respects. The turbidity layer doubled in thickness in the presence of a current (6 fpm) that was one third the level of the head wave velocity. The turbidity condition was not dependent on flow direction. It was equally intense for parallel flow and counter flow conditions. The counter current scoured the turbidity layer and thinned down the fluid mud layer. The parallel current transported the turbidity layer in the direction of mud flow with no apparent scouring or thinning of the fluid mud layer.

124. Large surface waves interacted with the fluid mud system to drive turbidity into the upper water column. The wave system generated orbital motion throughout the water column, and as the mud system flowed along the bottom it took on the oscillatory motion of the water column near the bottom. The orbital motion imposed on it did not interfere with the net forward motion of the mud flow. Up to an orbital velocity of 0.60 fps, the wave motion did not promote turbidity generation. Beyond this value, turbidity was driven upward in the water column such that its vertical advance was time dependent. Up to the threshold velocity the fluid mud layer and the turbidity layer were not affected. Beyond the threshold value, both layers thickened at a significant rate with increased orbital velocity.

REFERENCES

1. May, E.B., "Environmental Effects of Hydraulic Dredging in Estuaries," Alabama Marine Resources Bulletin No. 9, Apr 1973, Dauphin Island, Ala.

2. Nichols, M.M. et al, "A Field Study of Fluid Mud Dredged Material: It's Physical Nature and Dispersal," Technical Report (in preparation), U.S. Army Engineer Waterways Experiment Station, CE, Vicksburg, Miss.

3. Johanson, E.E., "Analysis of the Functional Capabilities and Performance of Silt Curtains," Technical Report (in preparation), U.S. Army Engineer Waterways Experiment Station, CE, Vicksburg, Miss.

4. Dunbar, C.O. and Rogers, J., Principles of Stratigraphy, John Wiley and Sons, New York, 1957, pp 13-17.

5. Kuenan, P.H., "Experiments in Connection with Daly's Hypothesis on the Formation of Submarine Canyons," Leidsche Geological Meded., Deel 8, pp 327-351.

6. Gould, H.R., "Some Quantitative Aspects of Lake Mead Turbidity Currents," Society of Economic Paleontologists and Mineralogists, Special Publication 2, 1951, pp 34-52.

7. Heezen, B.C. and Ewing, M. "Turbidity Currents and Submarine Slumps, and the 1929 Grand Banks Earthquake," American Journal of Science, Vol 250, 1952, pp 849-873.

8. Neal, R.W. and Henry, G., "Evaluation of the Submerged Discharge of Dredged Material Slurry During Pipeling Dredge Operations," Technical Report (in preparation), U.S. Army Engineer Waterways Experiment Station, CE, Vicksburg, Miss.

9. Tesaker, E., "Uniform Turbidity Current Experiments," International Association of Hydraulic Research Proceedings, Vol 2, 1969, pp 1-8.

10. Partheniades, E. and Mehta, A.J., "Deposition of Fine Sediments in Turbulent Flows," EPA Project No. 16050 ERS, University of Florida, Gainesville, Fla., 1971.

11. Migniot, C., "A Study of the Physical Properties of Various Very Fine Sediments and Their Behavior Under Hydrodynamic Action," la Houille Blanche, Vol 23, No. 7, 1968, pp 591-620.

12. Einstein, H.A. and Krone, R.B., "Experiments to Determine Modes of Cohesive Sediment Transport in Salt Water," Journal of Geophysical Research, Vol 67, No. 4, Apr 1962, pp 1451-1464.

13. Masch, F.D. and Espey, W.H., Jr., "Shell Dredging: A Factor in Sedimentation in Galveston Bay," Technical Report HYDO6-6702 CRWR-7, Nov 1967, University of Texas at Austin, Austin, Tex.

14. American Society for Testing and Materials, "Standard Method for Particle Size Analysis of Soils," Designation D 422-63 (Reapproved 1972), 1972 Annual Book of ASTM Standards, Part II, 1972, Philadelphia, Pa.

15. Shepard, E.P., "Nomenclature Based on Sand-Silt-Clay Ratios," Journal of Sediment Petrology, Vol 24, 1954, pp 151-158.

16. American Public Health Association et al., Standard Methods for the Examination of Water and Wastewater, 14th edition, EPHA, Washington, D.C., 1975, Part 505, pp 532-534.

17. Streeter, V.L., Handbook of Fluid Dynamics, Chapter 26, McGraw-Hill, New York, 1961.

18. McCormack, M.E., Ocean Engineering Wave Mechanics, Chapter 2, John Wiley and Sons, New York, 1973.

19. Wechsler, B.A. and Cogley, D.R., "Laboratory Study of the Turbidity Generation Potential of Sediments to be Dredged," Technical Report D-77-14, Nov 1977, U.S. Army Engineer Waterways Experiment Station, CE, Vicksburg, Miss.

APPENDIX A: INSTANTANEOUS HEAD WAVE VELOCITY

1. The head wave velocity was determined at each of the marker stations along the tank as an indicator of the settling activity taking place in the fluid mud layer through the change in the dynamics of the wave. Thus, as settling occurred, less material reached the wave so that its average density decreased with an attendent drop in velocity.

2. The instantaneous head wave velocity was obtained from the displacement vs. time data. A smooth curve was drawn through the plotted points, and its slope was measured at each marker station. Invariably, the curves were smooth and matched the data closely. The velocity values so obtained are presented in Table A1.

Table A1

Head Wave Velocities at Downrange Distances from Origin

Test Number	Downrange Distance, ft						
	0	4	8	12	16	20	24
11	.128	.090	.057	.031			
12	.282	.273	.249	.217	.193	.178	.168
13	.248	.223	.191	.128	.100	.0800	.073
14	.191	.166	.118	.091	.091	.091	.091
15	.248	.208	.208	.208	.208	.186	.156
16	.248	.234	.204	.158	.134	.114	.104
18	.360	.245	.210	.196			
19	.283	.240	.175	.117	.083	.063	
20	.268	.092	.061	.039	.035[a]		
21	.253	.176	.128	.093	.080	.078	.070
22	.268	.268	.271	.280	.288	.305	.320
23	.268	.278	.302	.332	.350	.361	.364
24	.216	.178	.138	.005			
25	.268	.213	.150	.100	.067	.053	
26		.218	.173	.138	.113	.103	.092
27	.364	.364	.364	.360	.352	.318	.289
28		.396	.396	.396	.396	.396	.396
29	.174	.110	.074	.060	.050	.043[b]	
30	.201	.145	.118	.097	.078	.072	
31	.231	.200	.167	.141	.120	.104	.094
32	.183	.210	.235	.245	.230	.208	.172
33	.266	.254	.248	.243	.241		.238
35	.212	.202	.180	.157	.130	.120	.120
36	.286	.286	.237	.162	.15		
37	.270	.220	.186	.166	.144	.126	.108

Note: a = value at 14 ft; b = value at 18 ft.

APPENDIX B: SEDIMENT DEPOSIT PROFILES

1. Bottom sediment samples were collected for each test for the purpose of exploring the influence of the test variables on settling characteristics as determined by the sediment patterns. The trays were located at each range marker (4-ft intervals, 0- to 24-ft range) and were shaped to minimize their disturbance of the mud flow. The trays sat for as long as an hour before the tank draining operation started and an additional hour while the tank was drained. The trays were then removed and the samples collected. The sediment was then filtered from each sample, dried, and weighed. The sediment weight was divided by the area of the tray to convert the data into sediment mass per unit area. The data so obtained are presented in this appendix in plots of sediment deposit (g/cm^2) versus downrange distance (ft) for each test (Figures B1-B11).

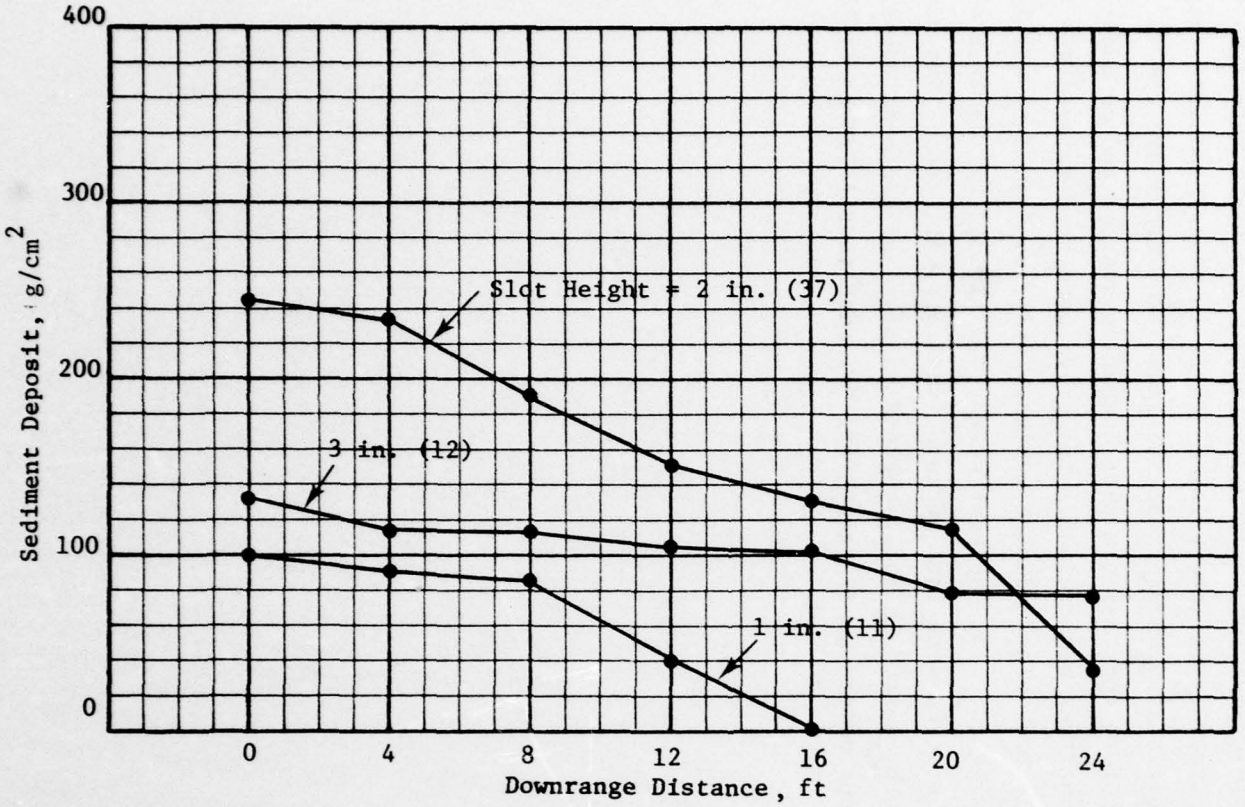

Figure B1. Sediment deposit profiles for slot height tests

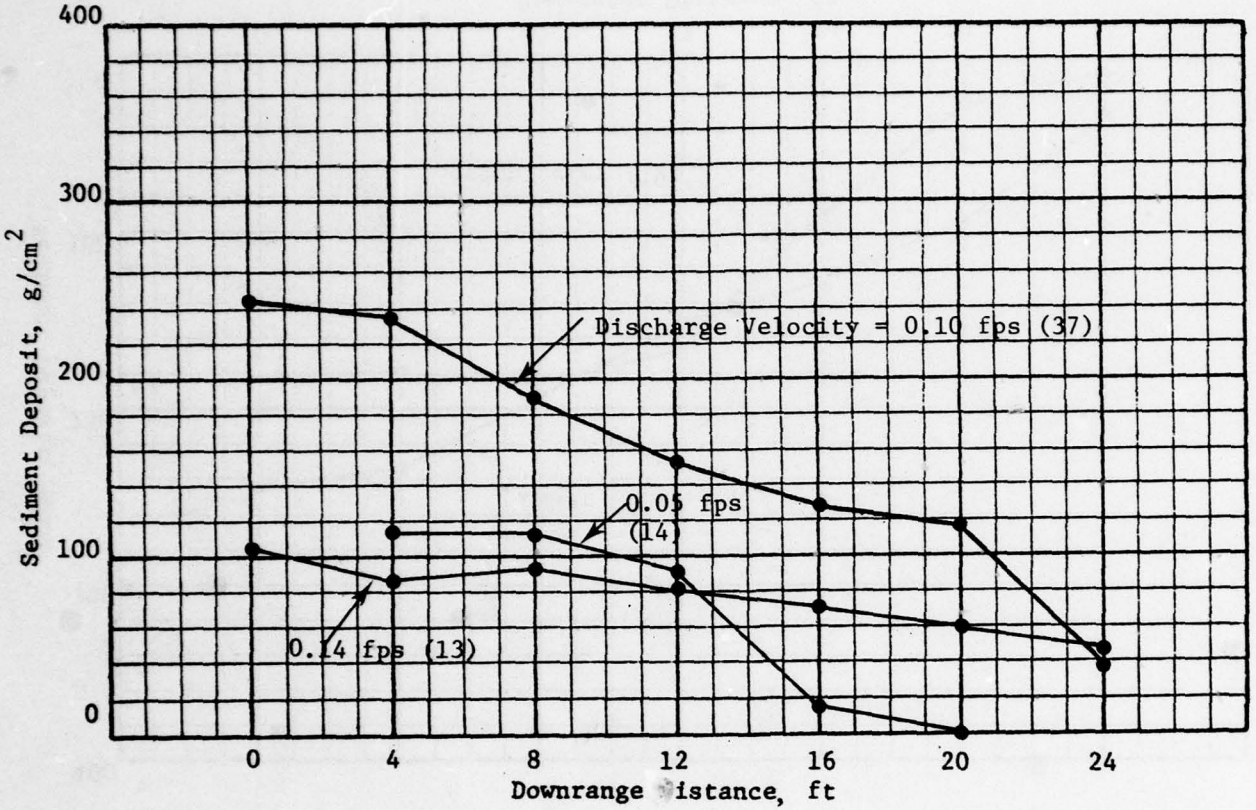

Figure B2. Sediment deposit profiles for discharge velocity tests

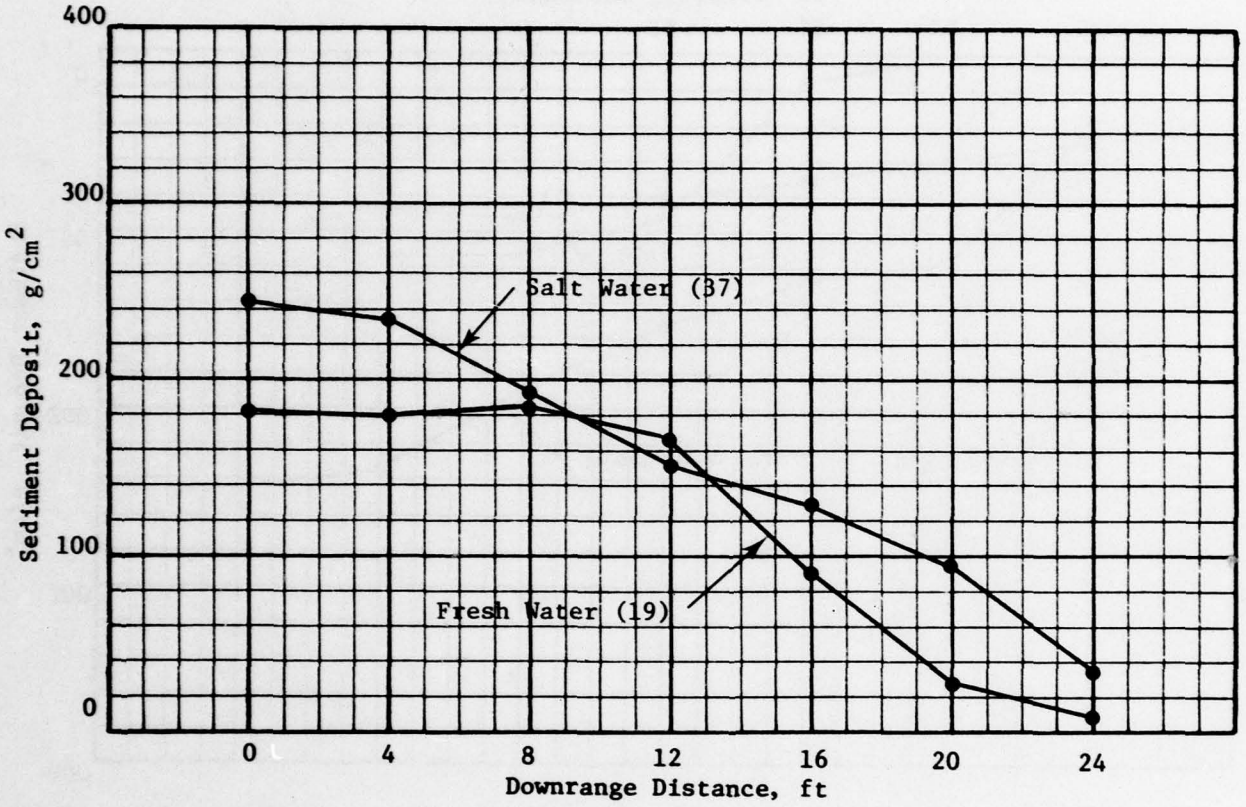

Figure B3. Sediment deposit profiles for sediment system tests

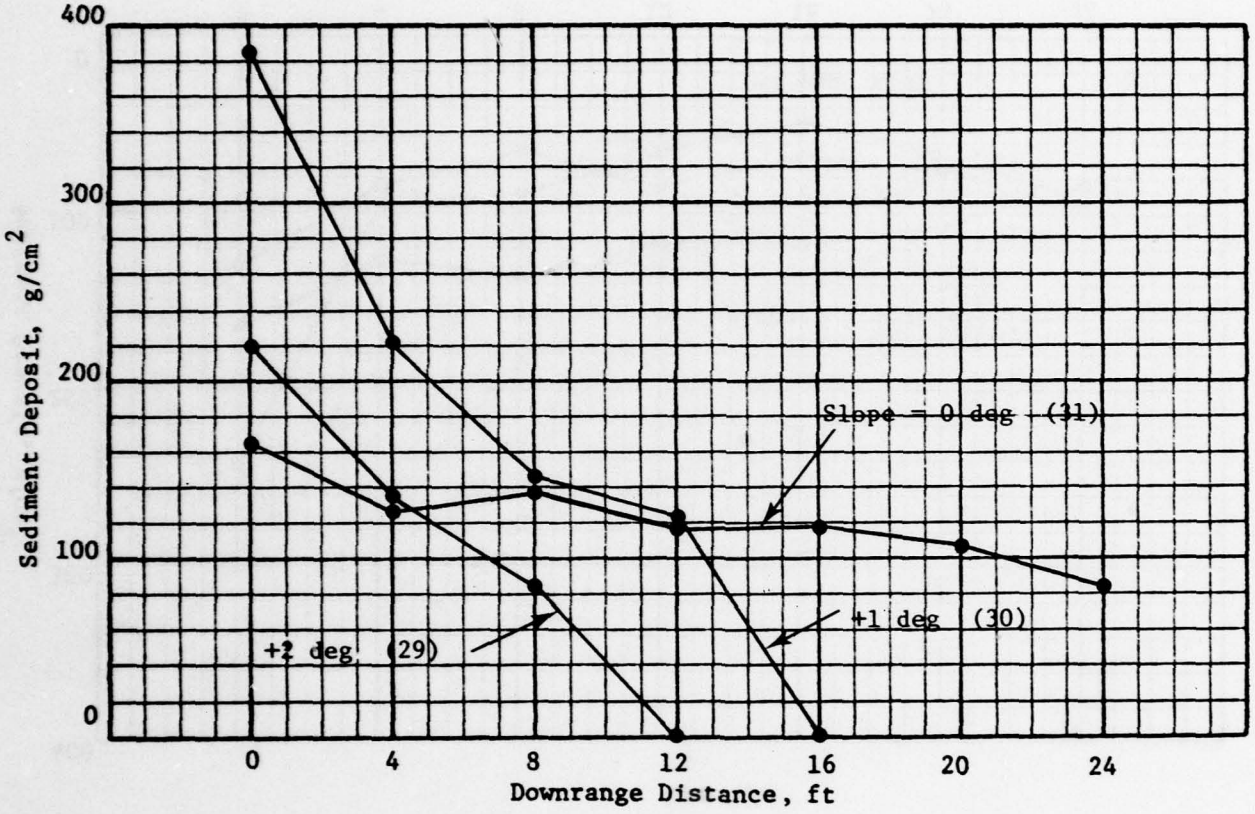

Figure B4. Sediment deposit profiles for positive slopes, 10-pcs slurry

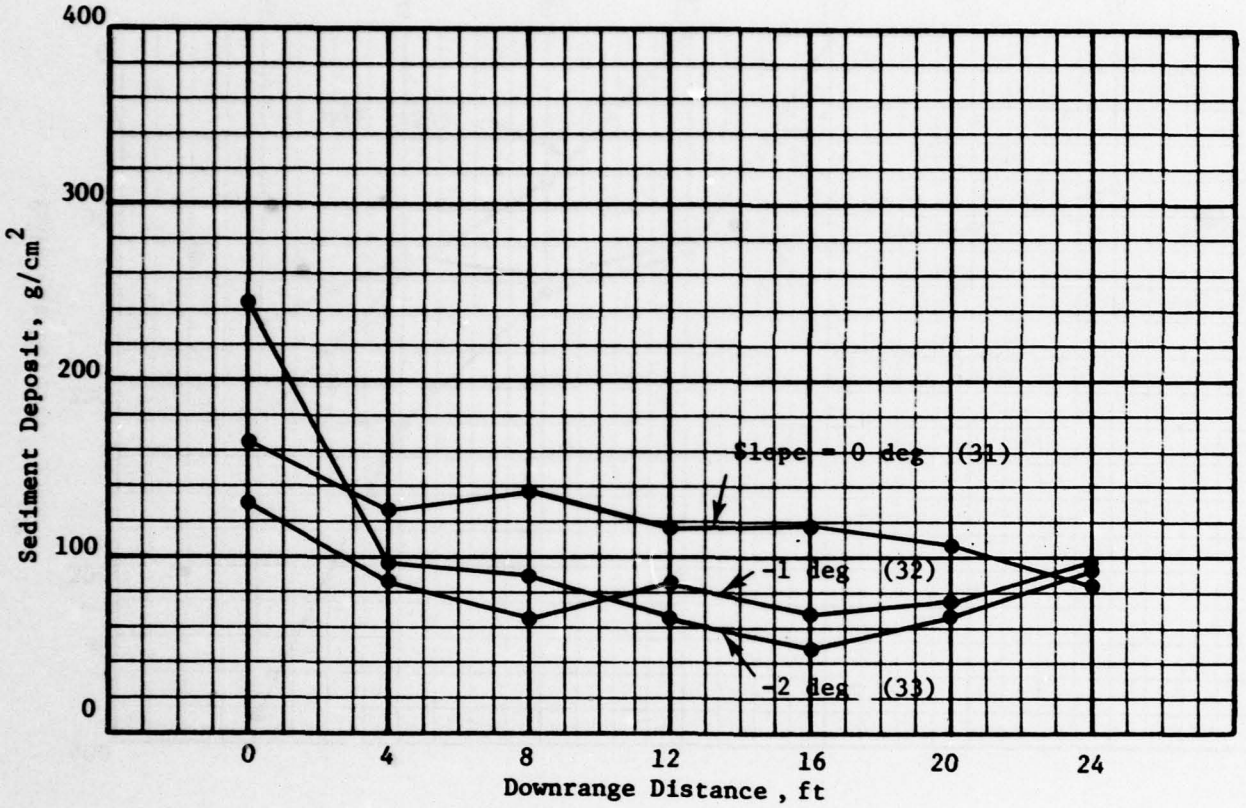

Figure B5. Sediment deposit profiles for negative slopes, 10-pcs slurry

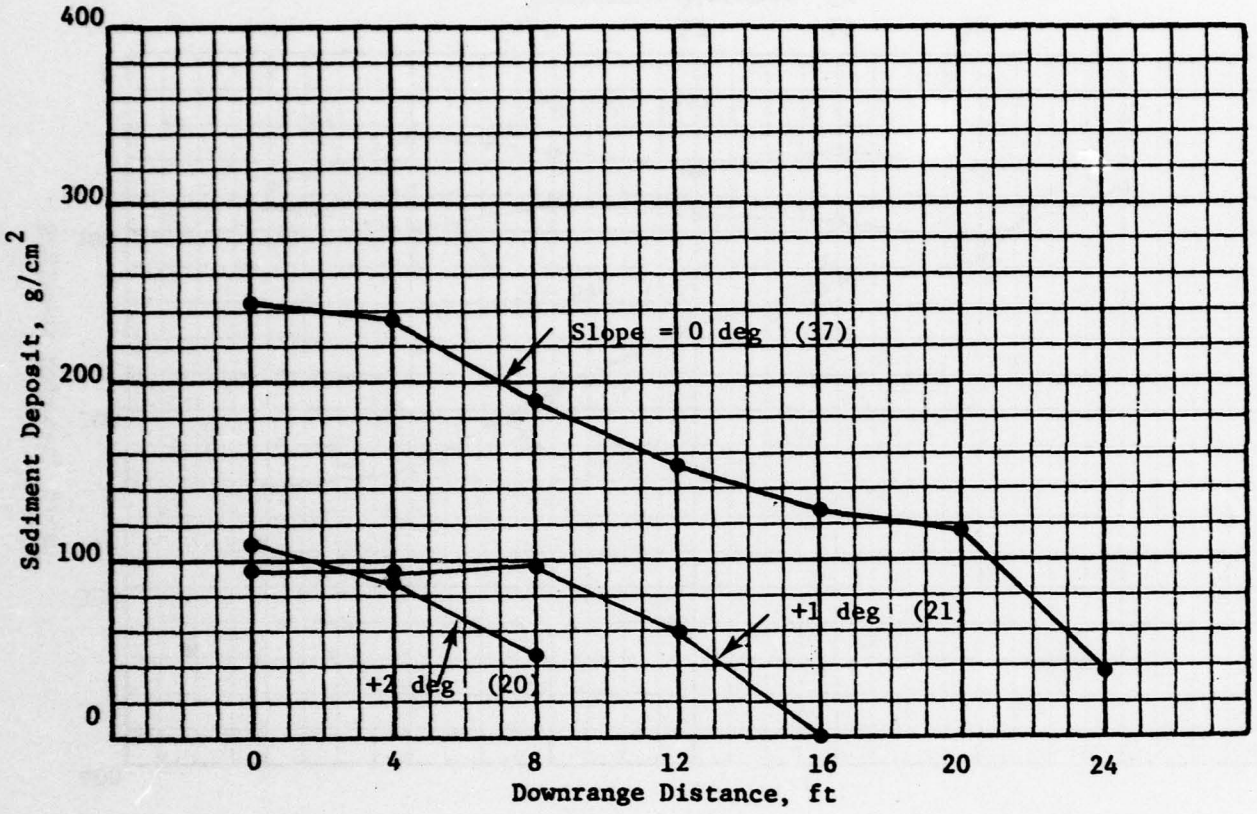

Figure B6. Sediment deposit profiles for positive slopes, 15-pcs slurry

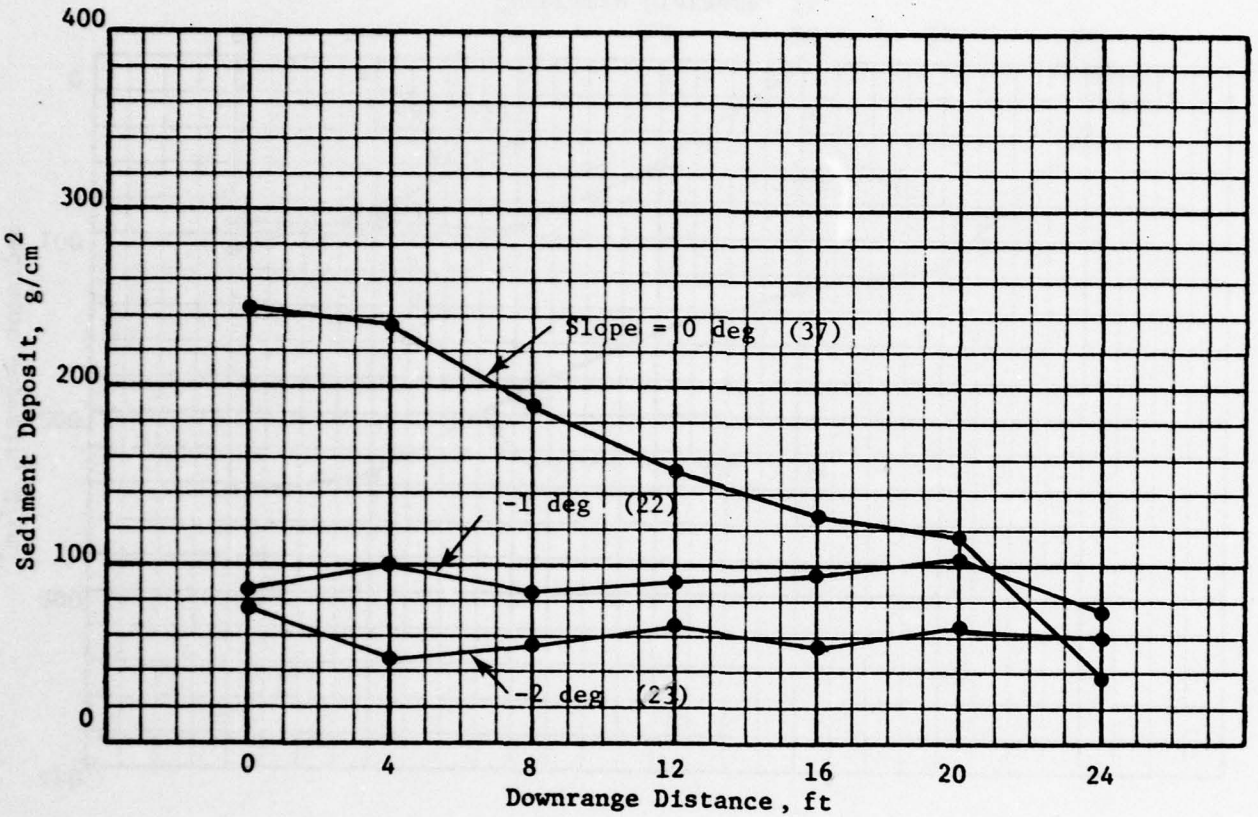

Figure B7. Sediment deposit profiles for negative slopes, 15-pcs slurry

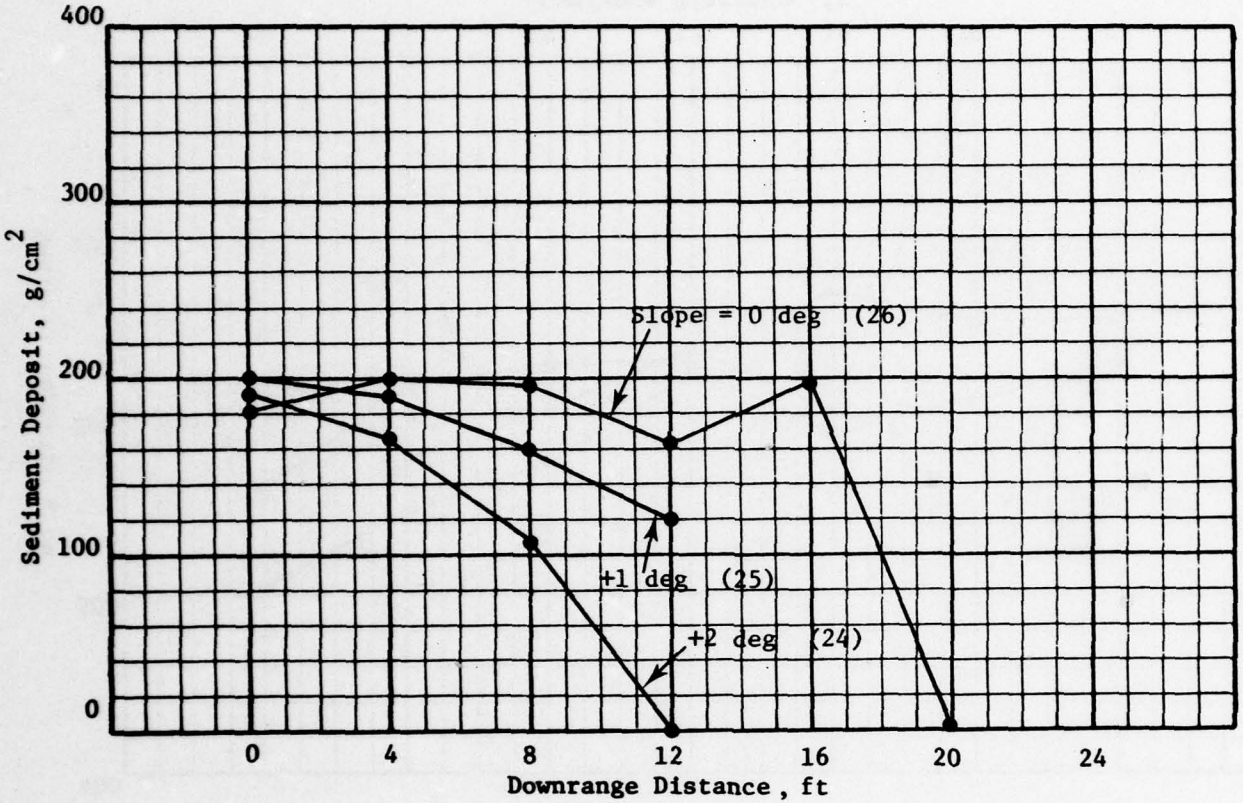

Figure B8. Sediment deposit profiles for positive slopes, 20-pcs slurry

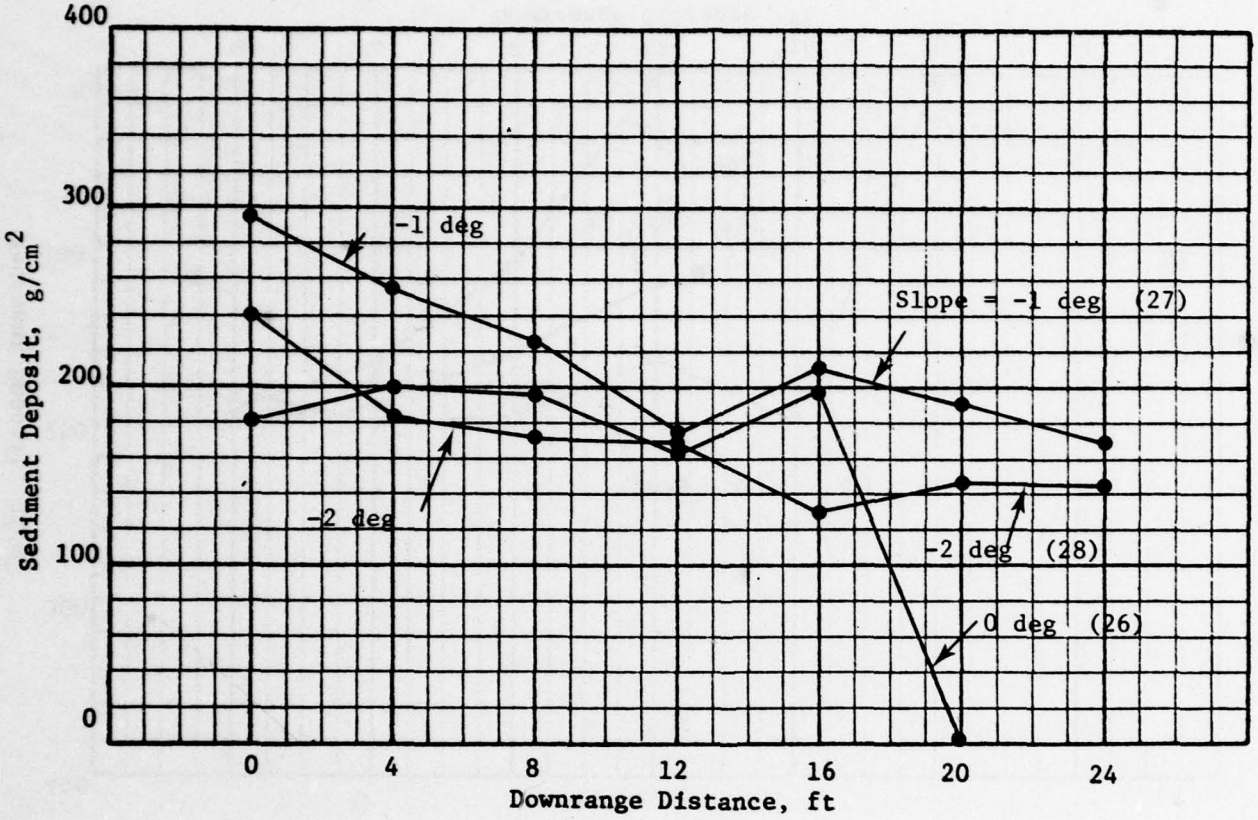

Figure B9. Sediment deposit profiles for negative slopes, 20-pcs slurry

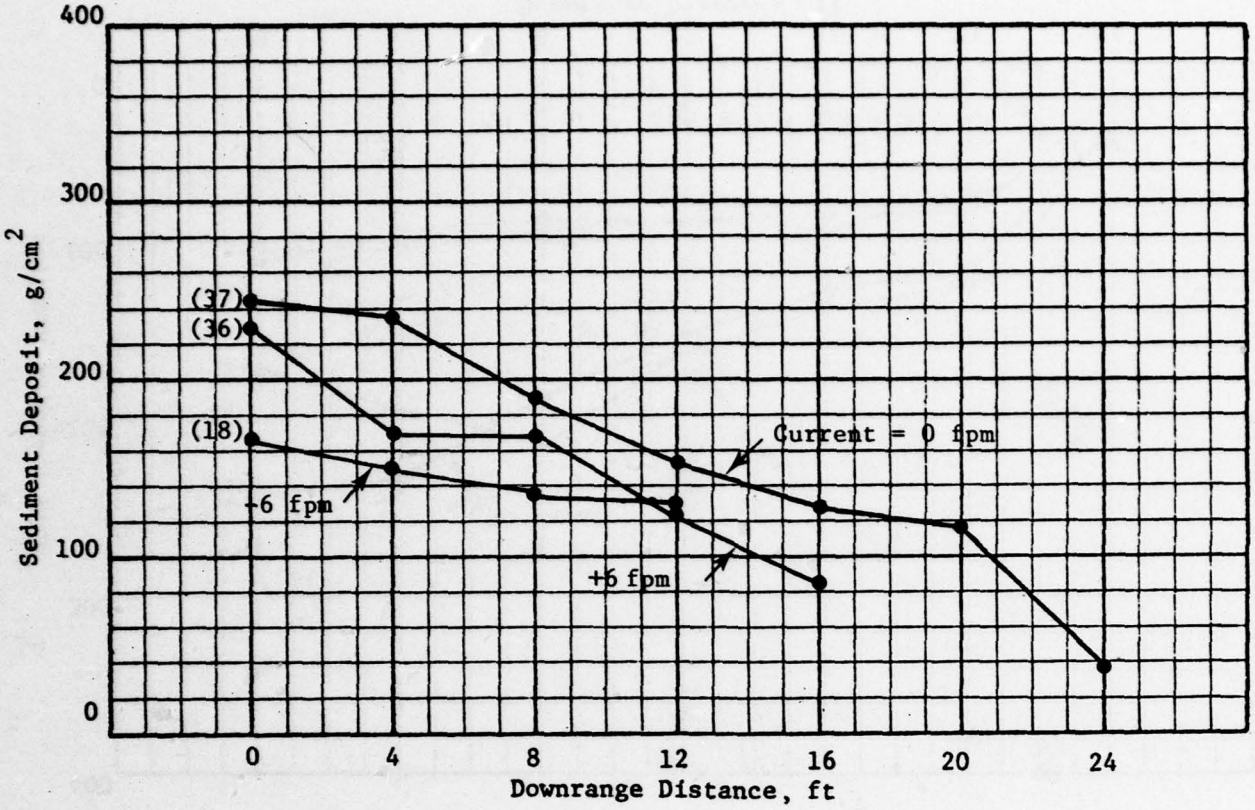

Figure B10. Sediment deposit profiles for current conditions

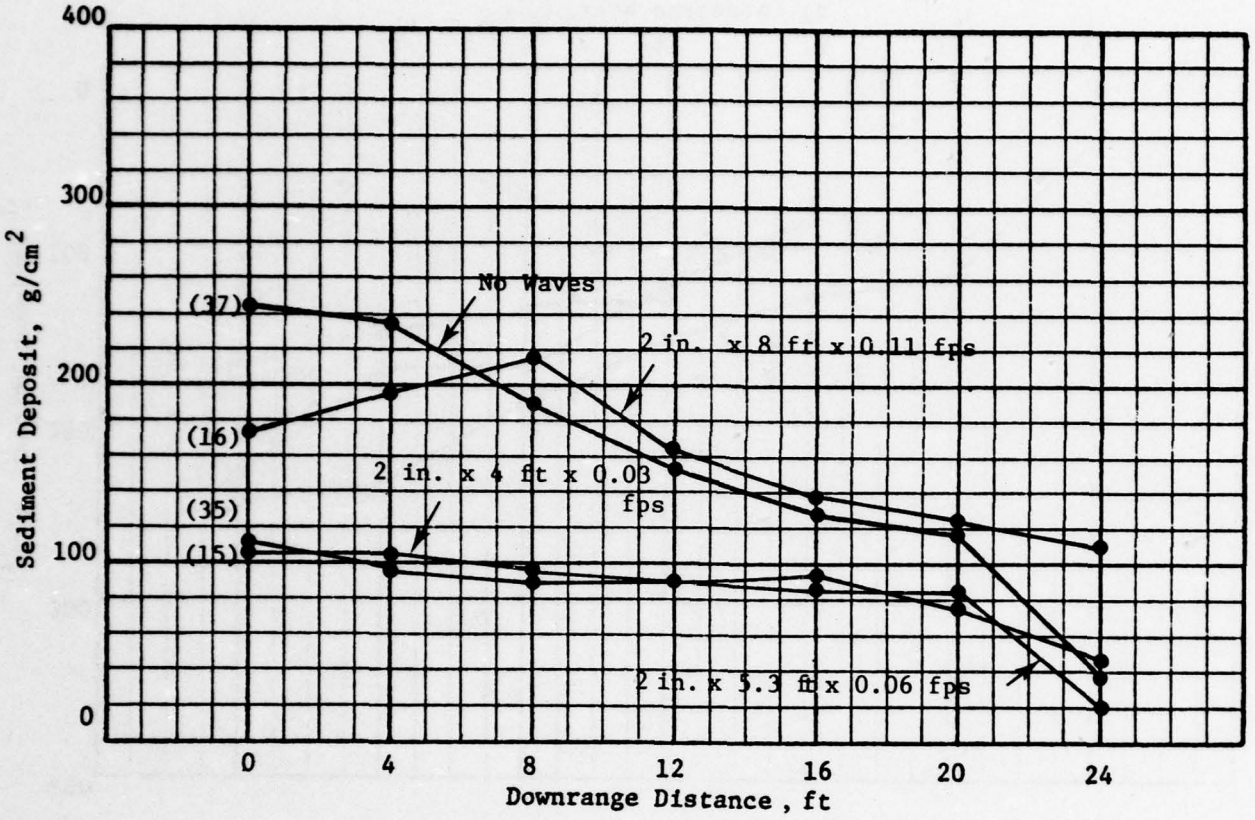

Figure B11. Sediment deposit profiles for wave conditions

APPENDIX C: SEDIMENT CONCENTRATION PROFILES

1. The sediment concentration profiles were compiled from the water sample data that were collected during each test. The sampling stations were located at three positions along the length of the test tank, each 8 ft apart with the first station positioned 3.75 ft downrange from the origin marker (0 ft). The origin marker was approximately 2 ft downrange from the discharge opening of the mud generator box. The locations of distance markers and sampling stations are illustrated in the sketch below.

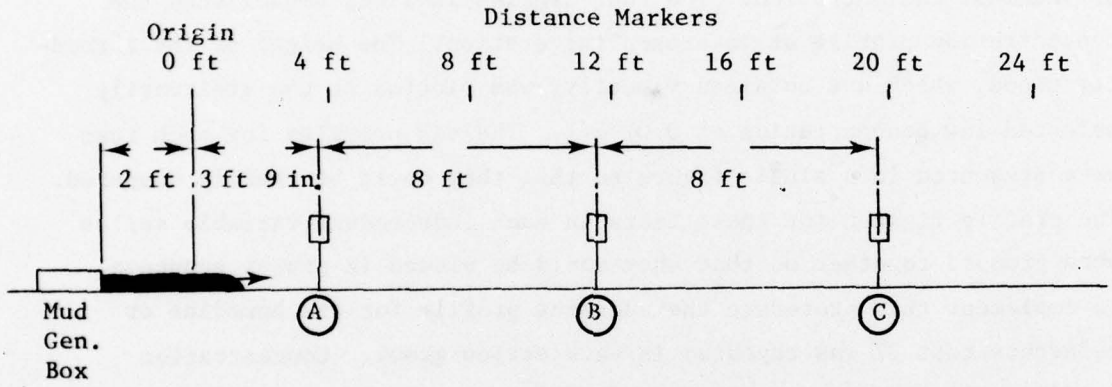

Sampling Stations

2. The timing of the water samples was triggered on the advance of the head wave. When the head wave had moved approximately 6 in. beyond station A, the first set of samples was taken. When the head wave passed station B, a set of samples was taken simultaneously at stations A and B. When the head wave passed station C, sample sets were taken simultaneously at all three stations. Each of the resulting six sets was designated by two letters; the first identified the station A, B, or C at which the set was taken, and the second letter specified the location of the head wave when the set was taken. Thus, sample set BC was taken at station B when the head wave had reached station C. Each set included four samples

that were taken at 5/16, 1/2, 1, and 1-1/2 in. above the bottom of the test tank. The total number of water samples taken during each test was therefore 20.

3. The water samples were analyzed in the laboratory to determine the weight of sediment per unit volume of mixture. A measured volume of well-stirred sample mixture was filtered, and the residue on the filter was dried to remove all remaining moisture. The residue was then weighed and its weight divided by the measured volume of mixture to determine the grams/litre concentration of sediment in the mixture.

4. The height of the sample above the bottom was plotted as a function of sediment concentration. The four samples in a set established the concentration profile at each sampling station. The height of the turbidity cloud, which was obtained visually, was plotted at the arbitrarily selected low concentration of 0.01 g/ℓ. The six profiles for each test were presented in a single figure so that they could be readily compared. The profile figures for those tests in each independent variable series were grouped together so that they could be viewed in proper sequence. To implement this procedure the sediment profile for the baseline or reference test 37 was repeated in each series group. Concentration profiles are presented in Figures C1-C30.

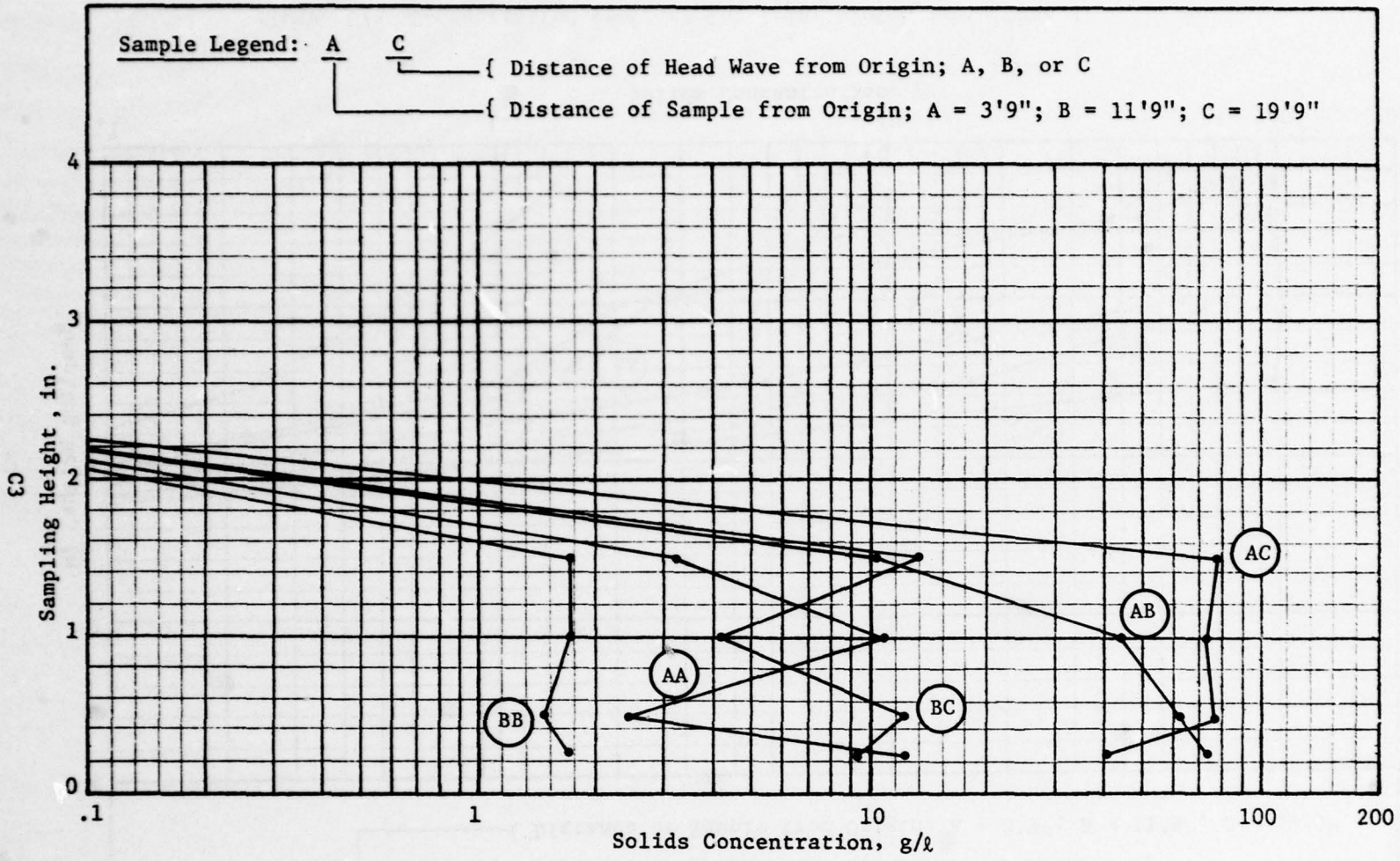

Figure C1. Concentration profiles for 1-in. slot height, test 11

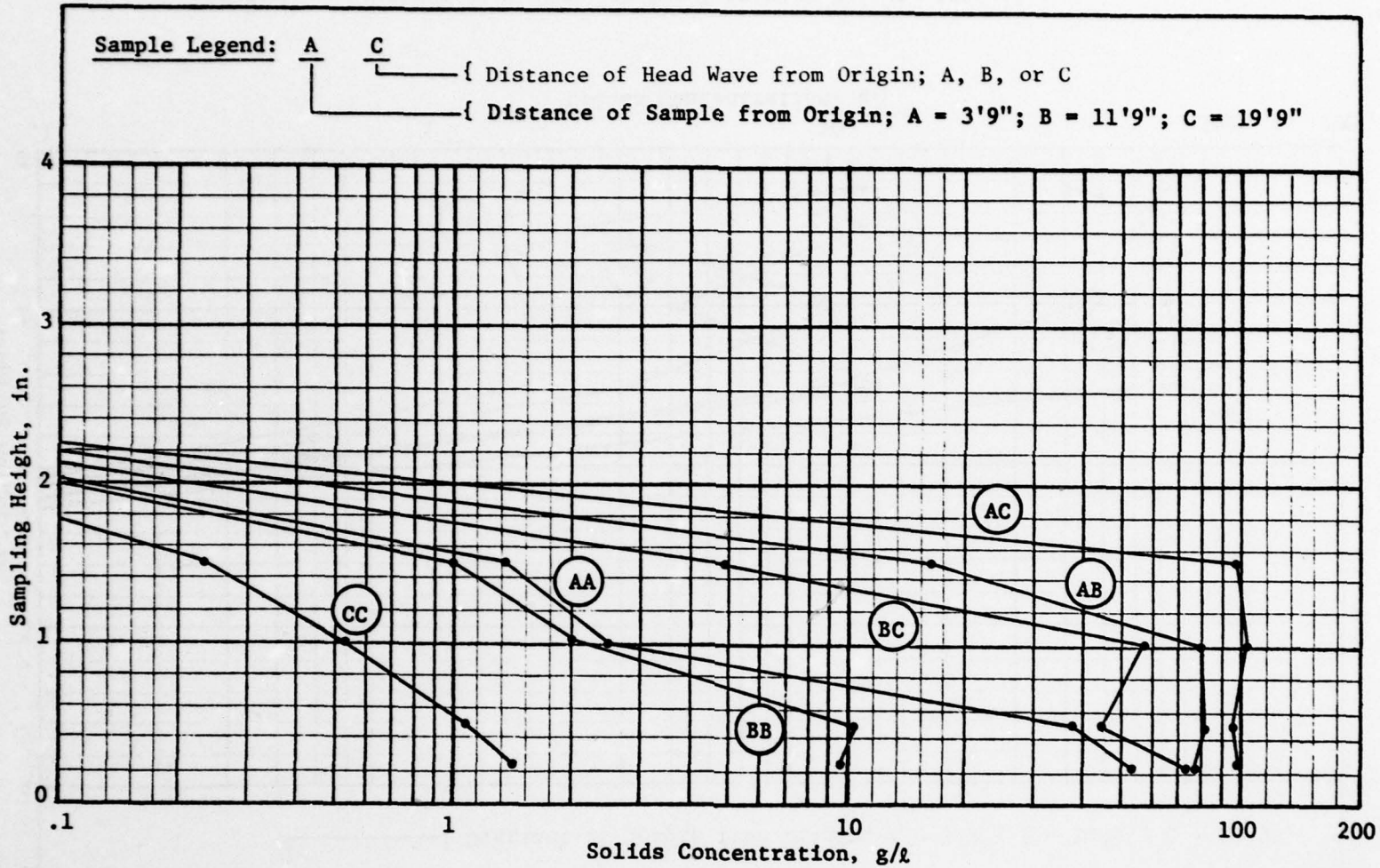

Figure C2. Concentration profiles for 2-in. slot height, test 37

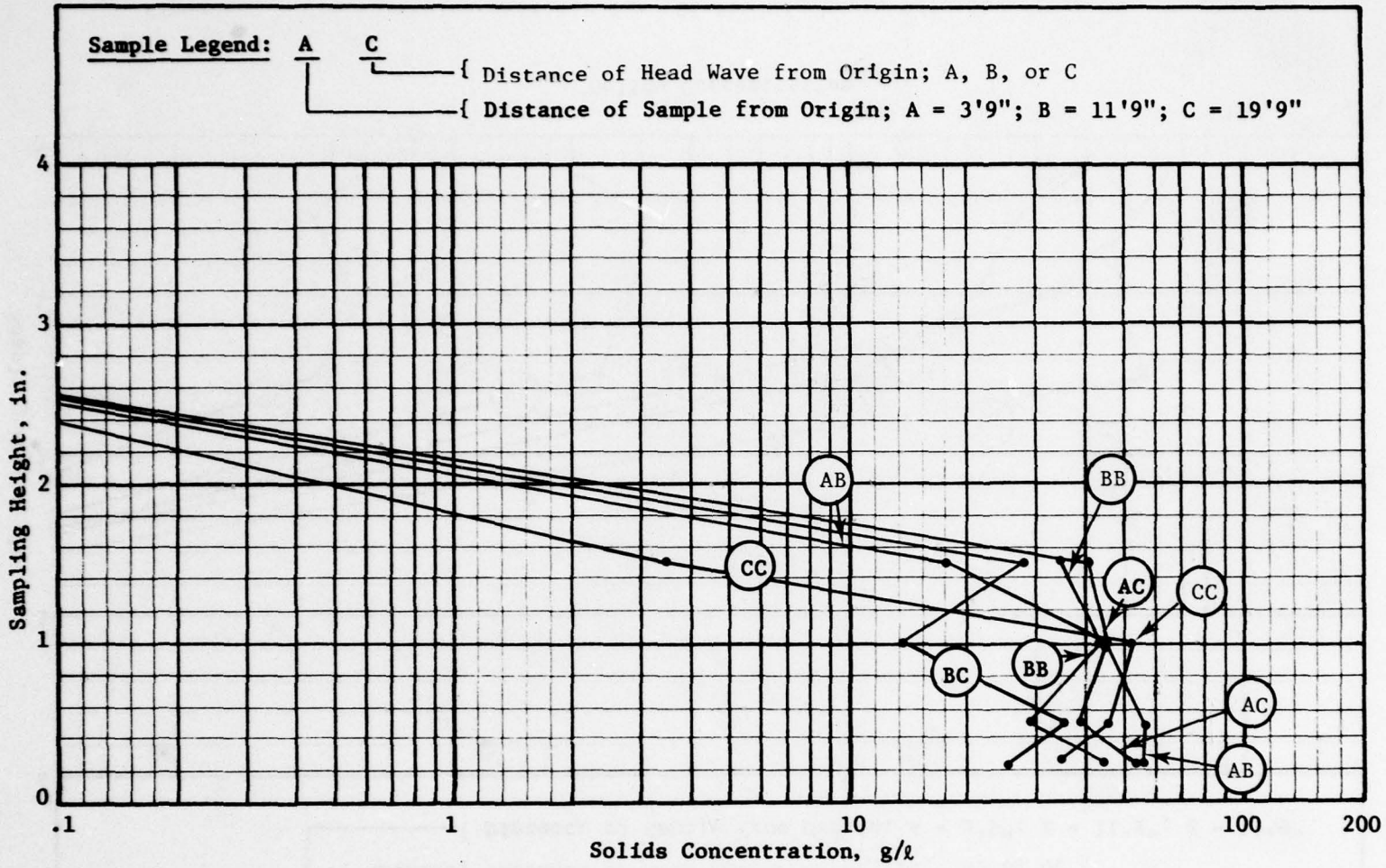

Figure C3. Concentration profiles for 3-in. slot height, test 12

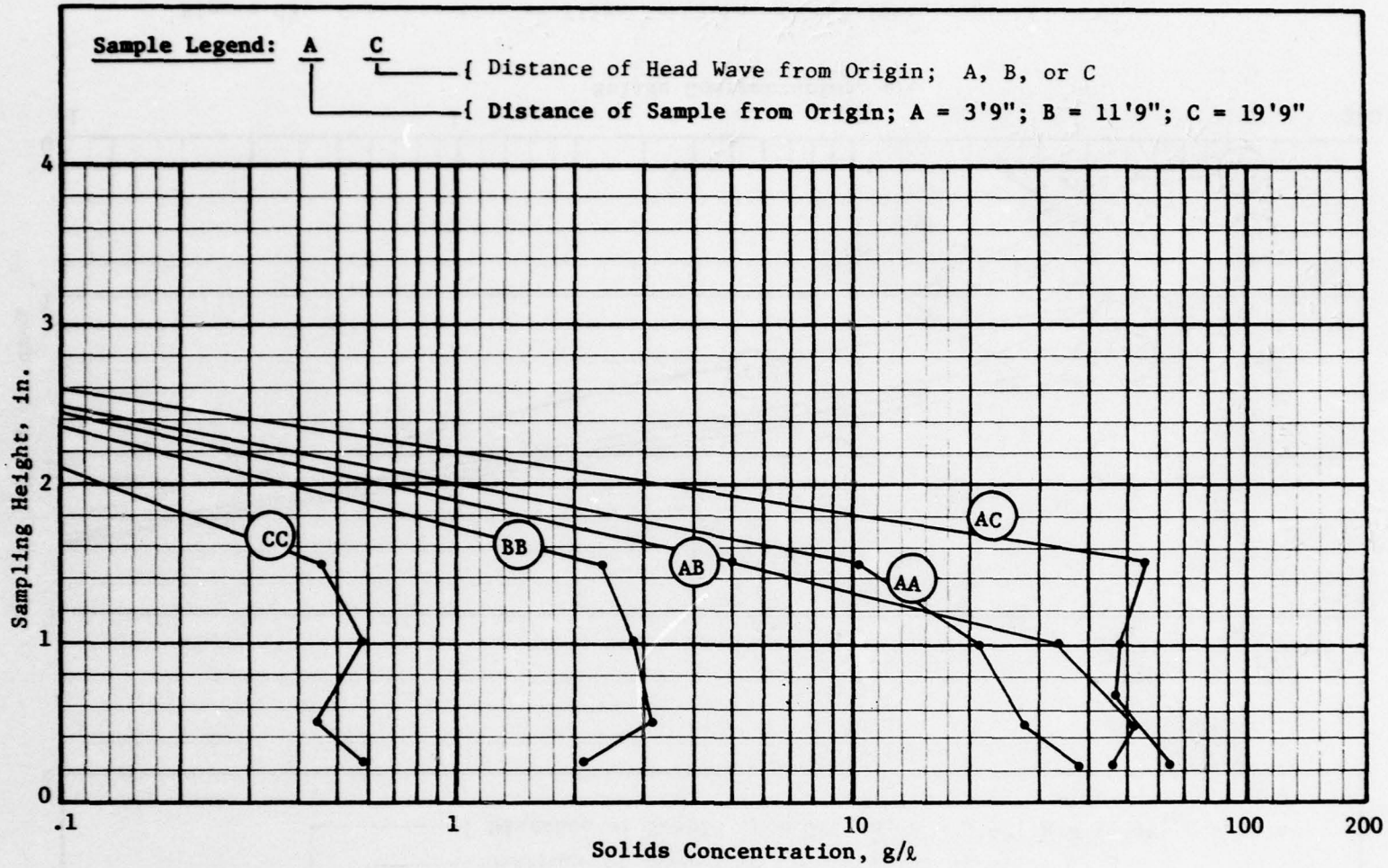

Figure C4. Concentration profiles for .05-fps discharge velocity, test 14

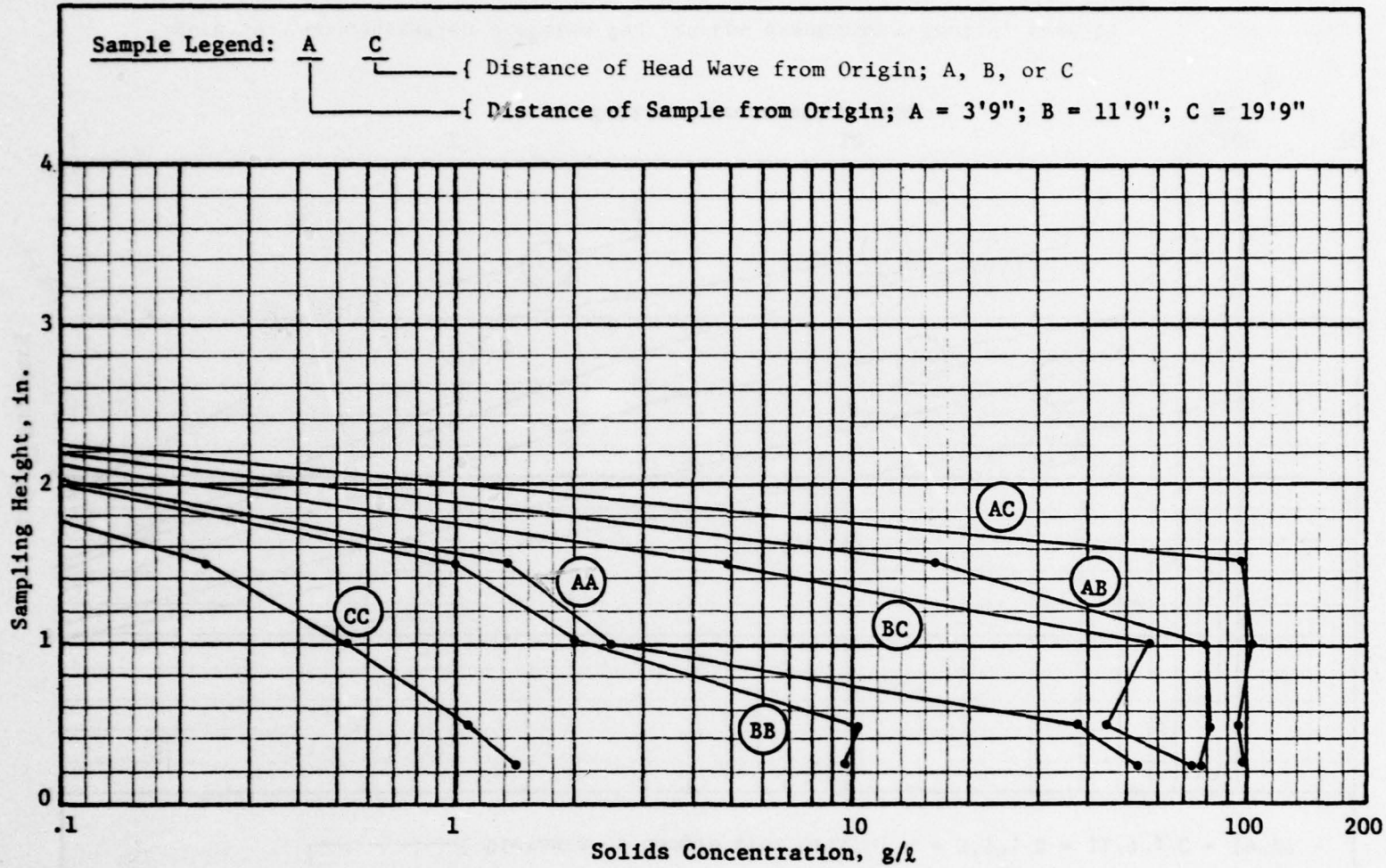

Figure C5. Concentration profiles for .10-fps discharge velocity, test 37

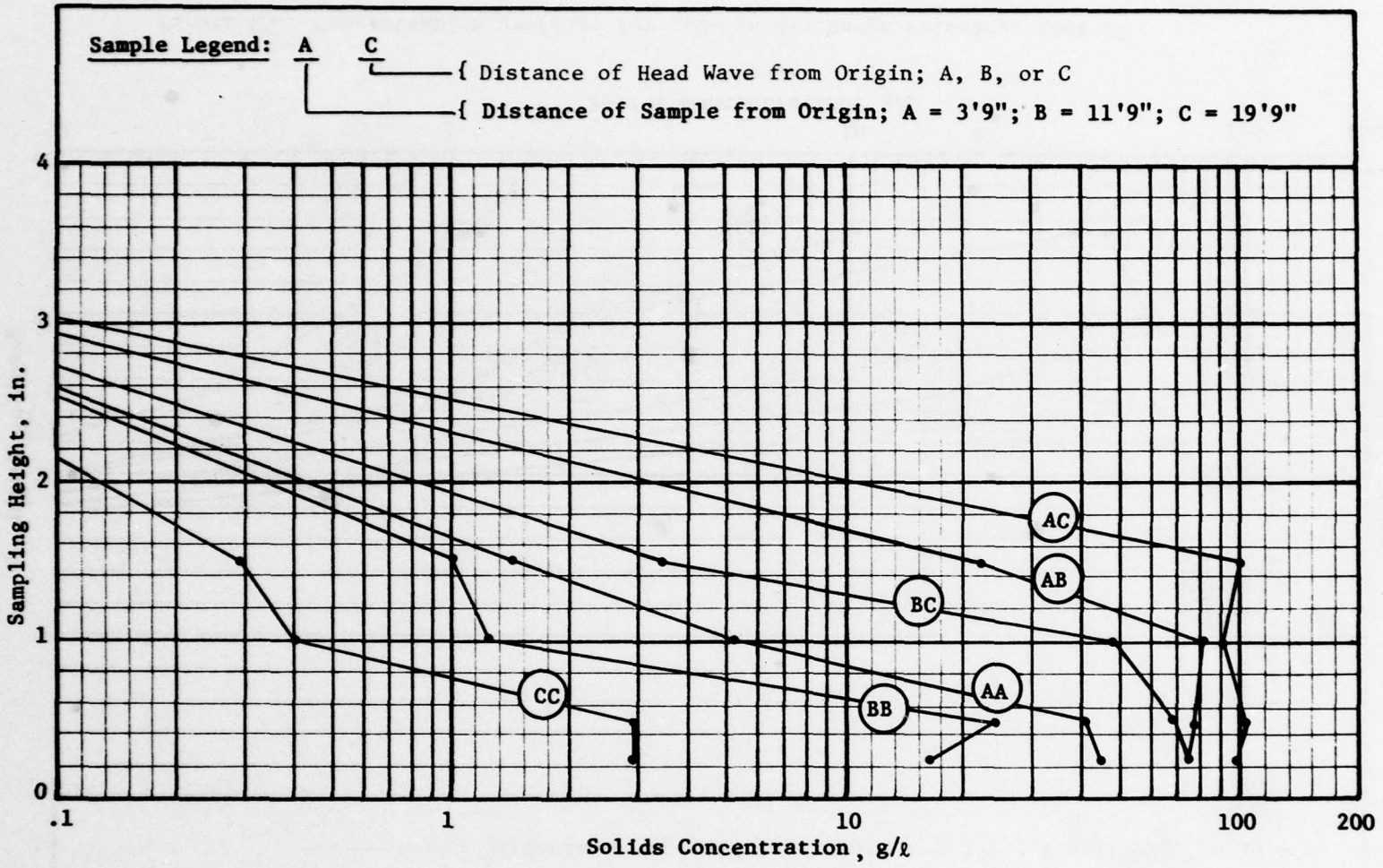

Figure C6. Concentration profiles for .14-fps discharge velocity, test 13

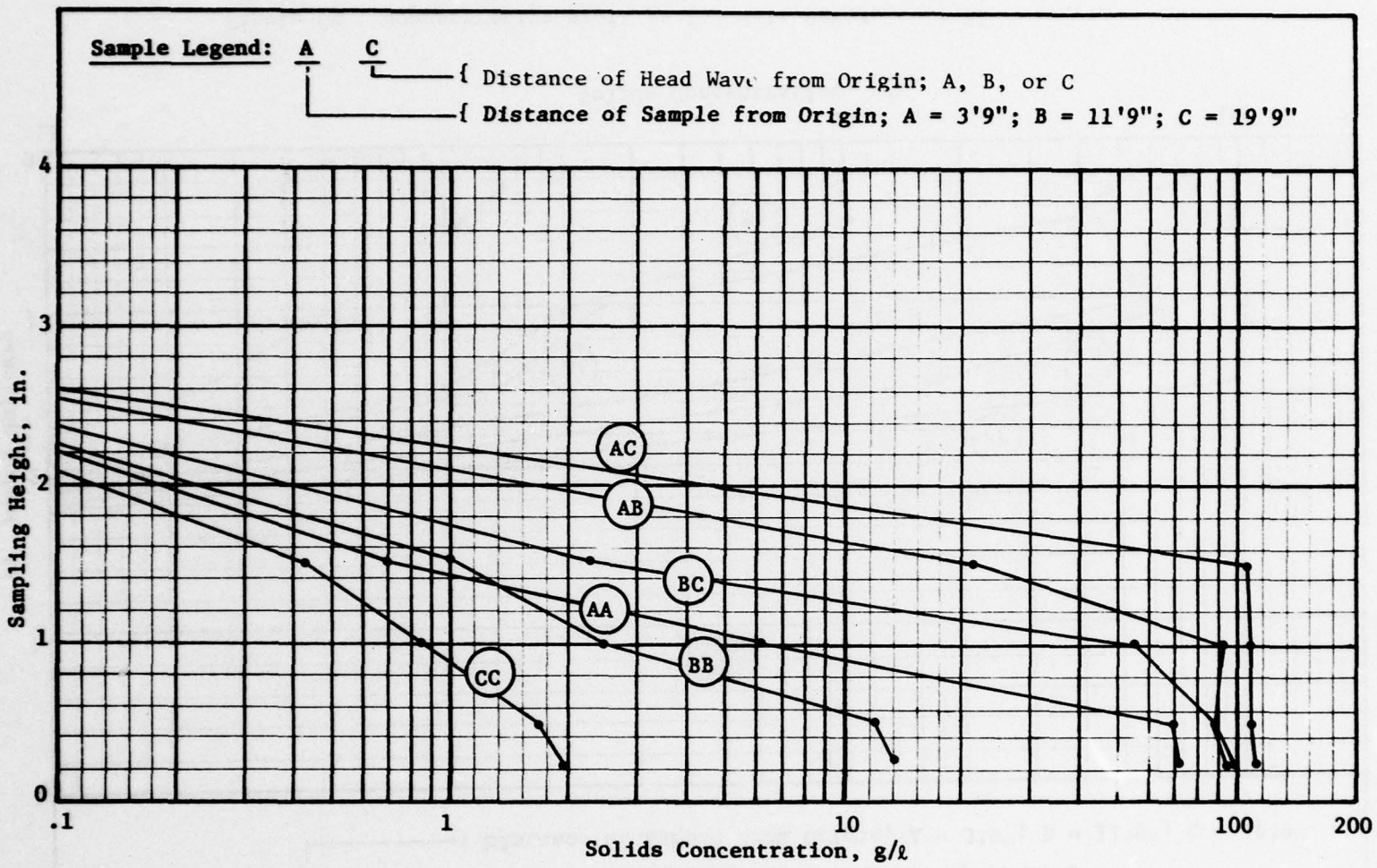

Figure C7. Concentration profiles for fresh water, test 19

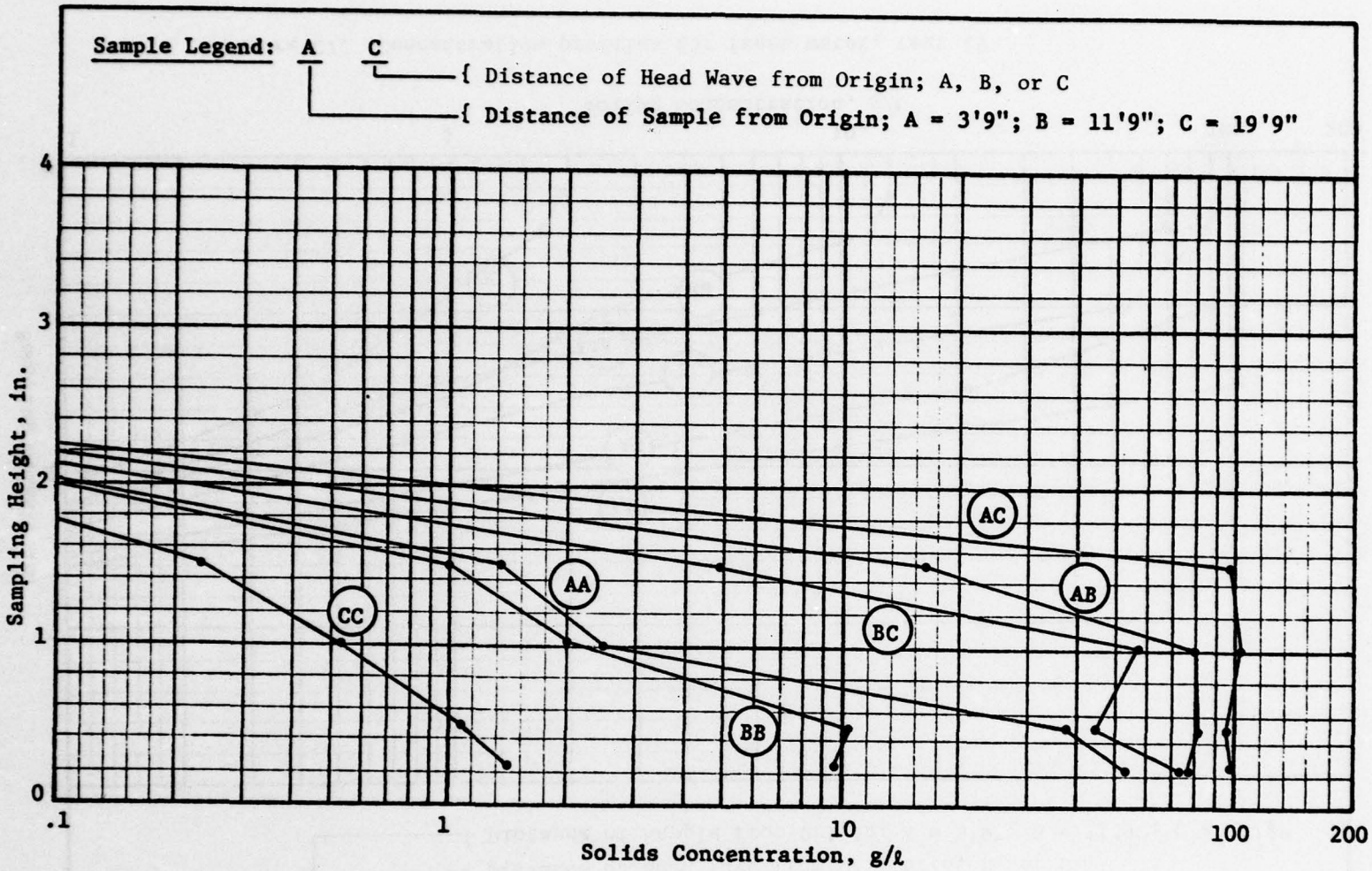

Figure C8. Concentration profiles for salt water, test 37

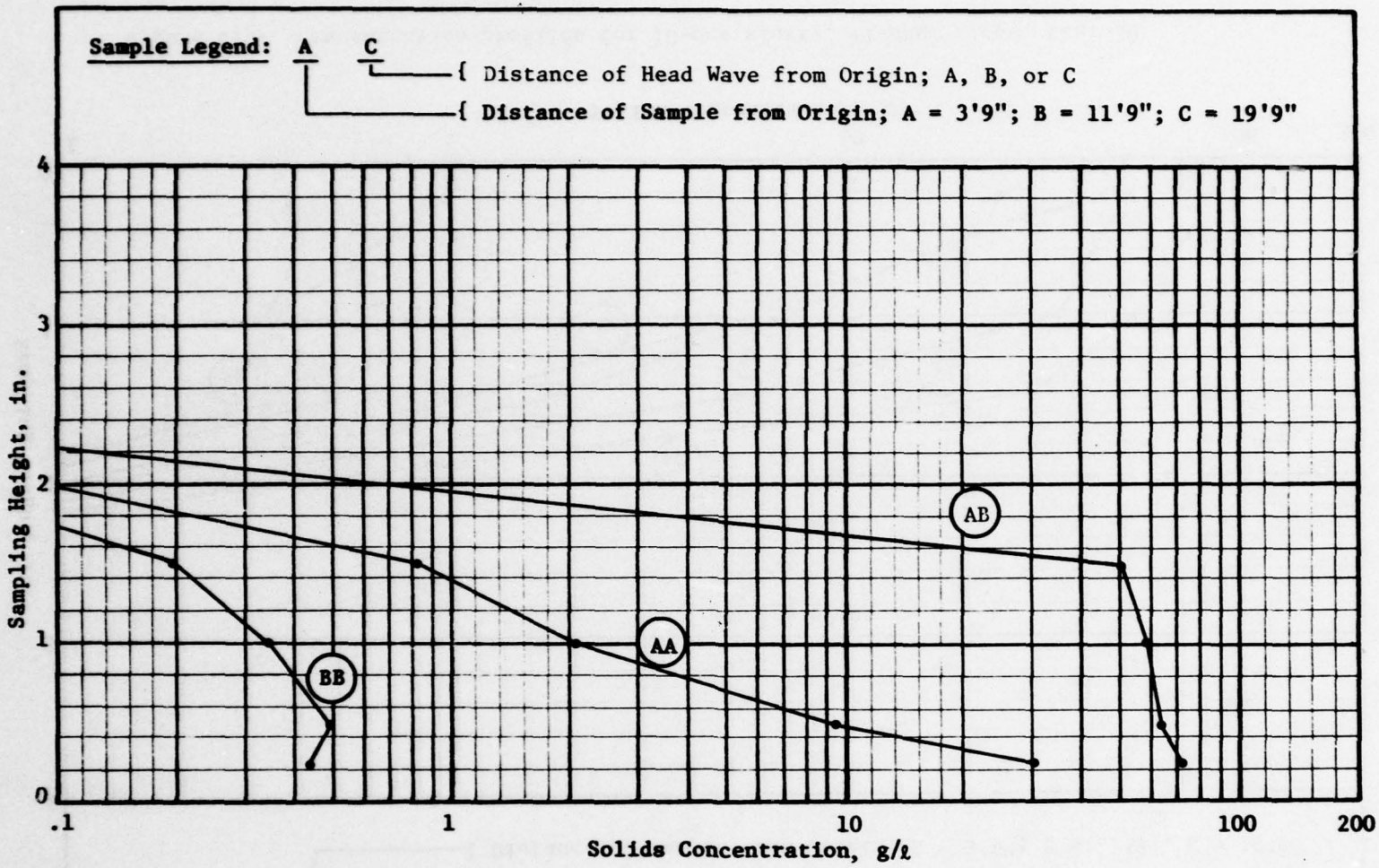

Figure C9. Concentration profiles for 10-pcs slurry, +2-deg slope, test 29

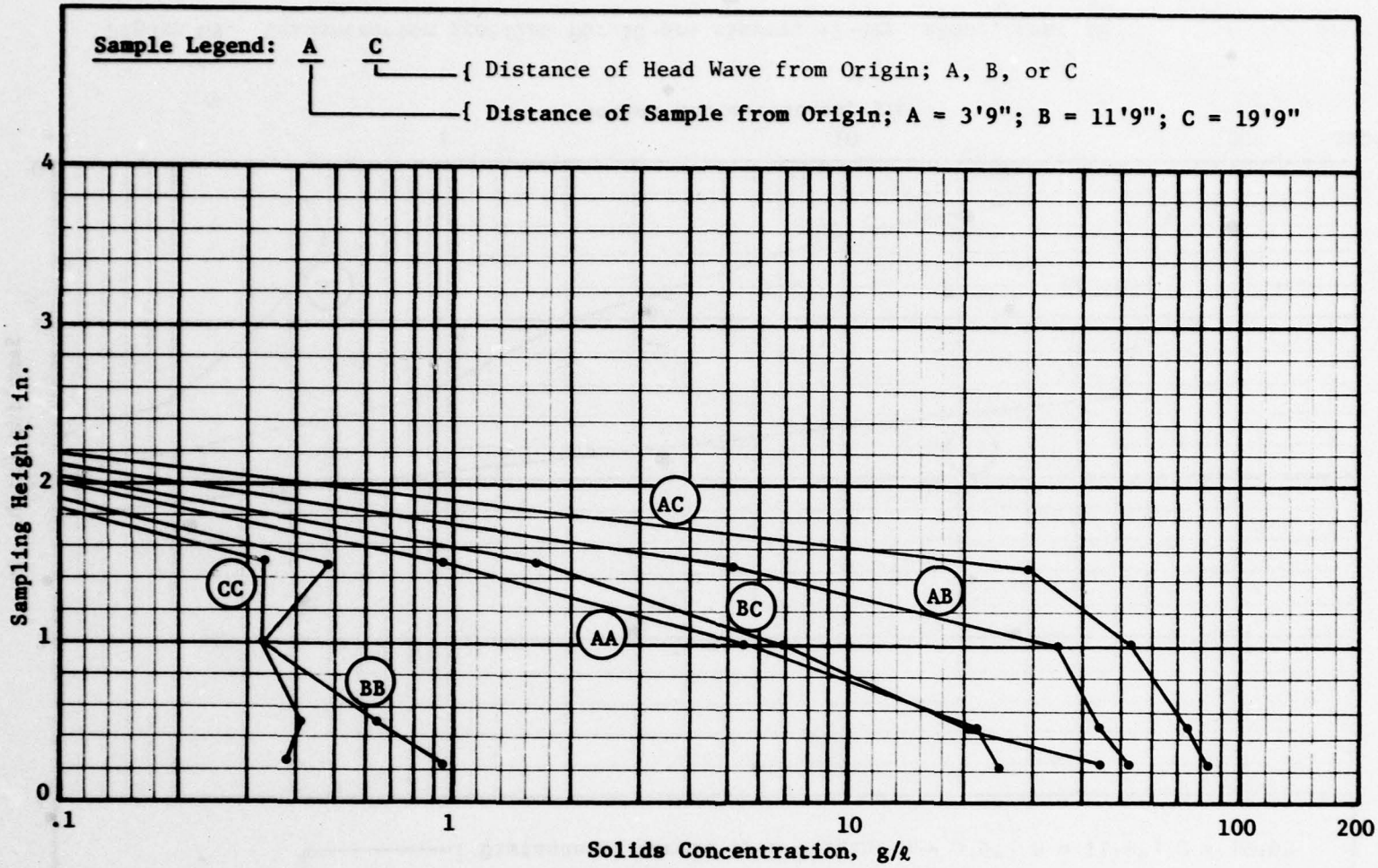

Figure C10. Concentration profiles for 10-pcs slurry, +1-deg slope, test 30

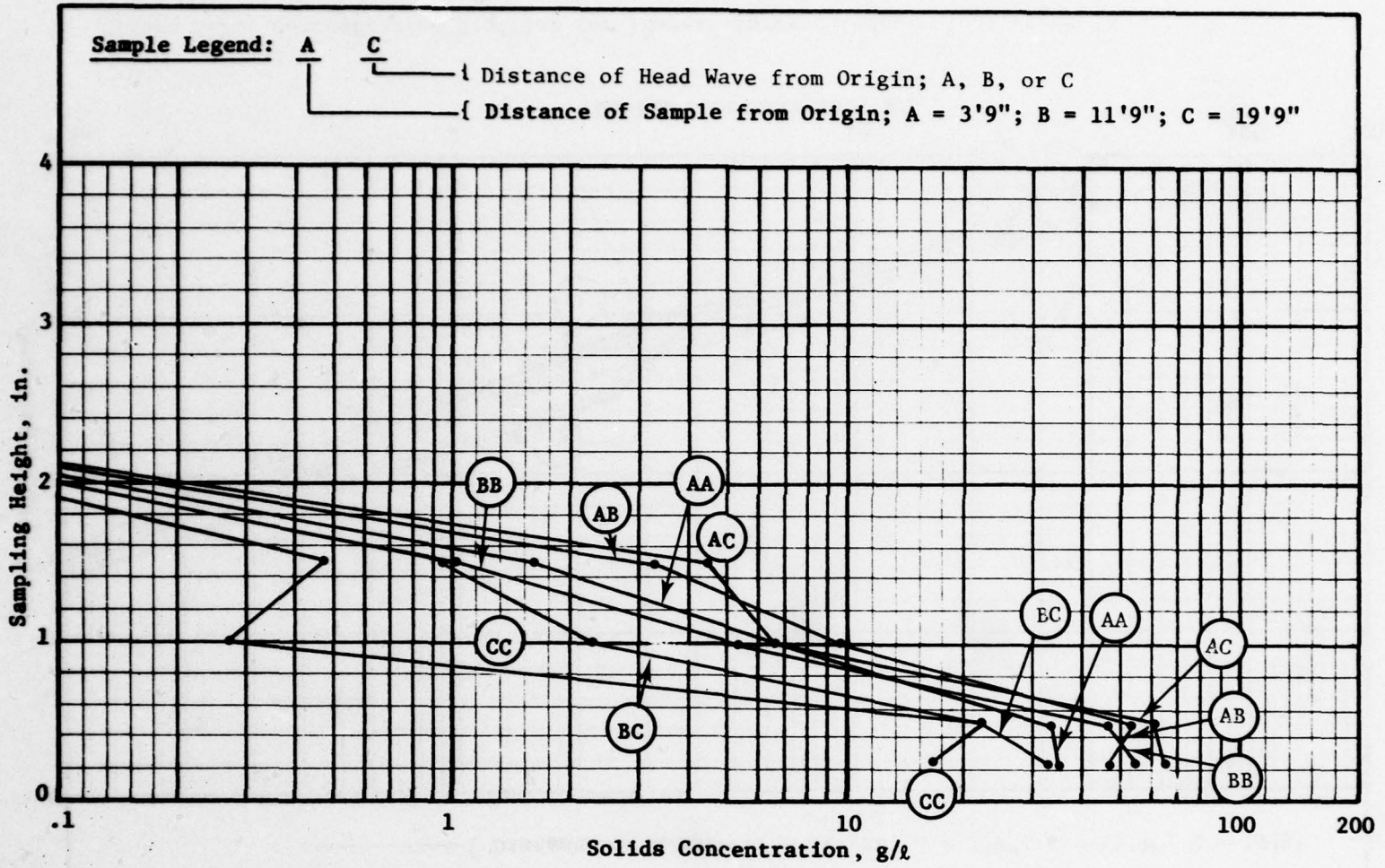

Figure C11. Concentration profiles for 10-pcs slurry, 0-deg slope, test 31

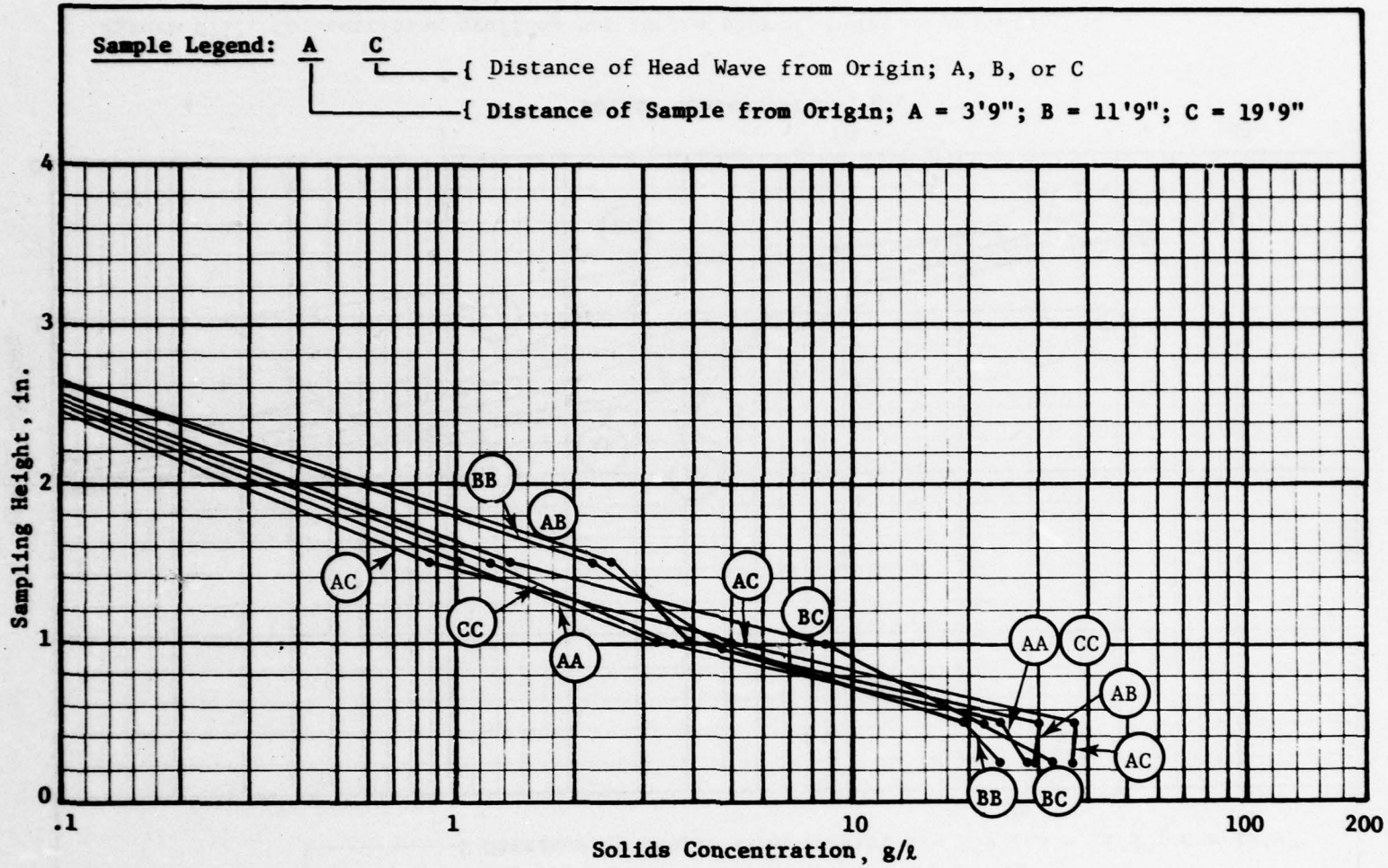

Figure C12. Concentration profiles for 10-pcs slurry, -1-deg slope, test 32

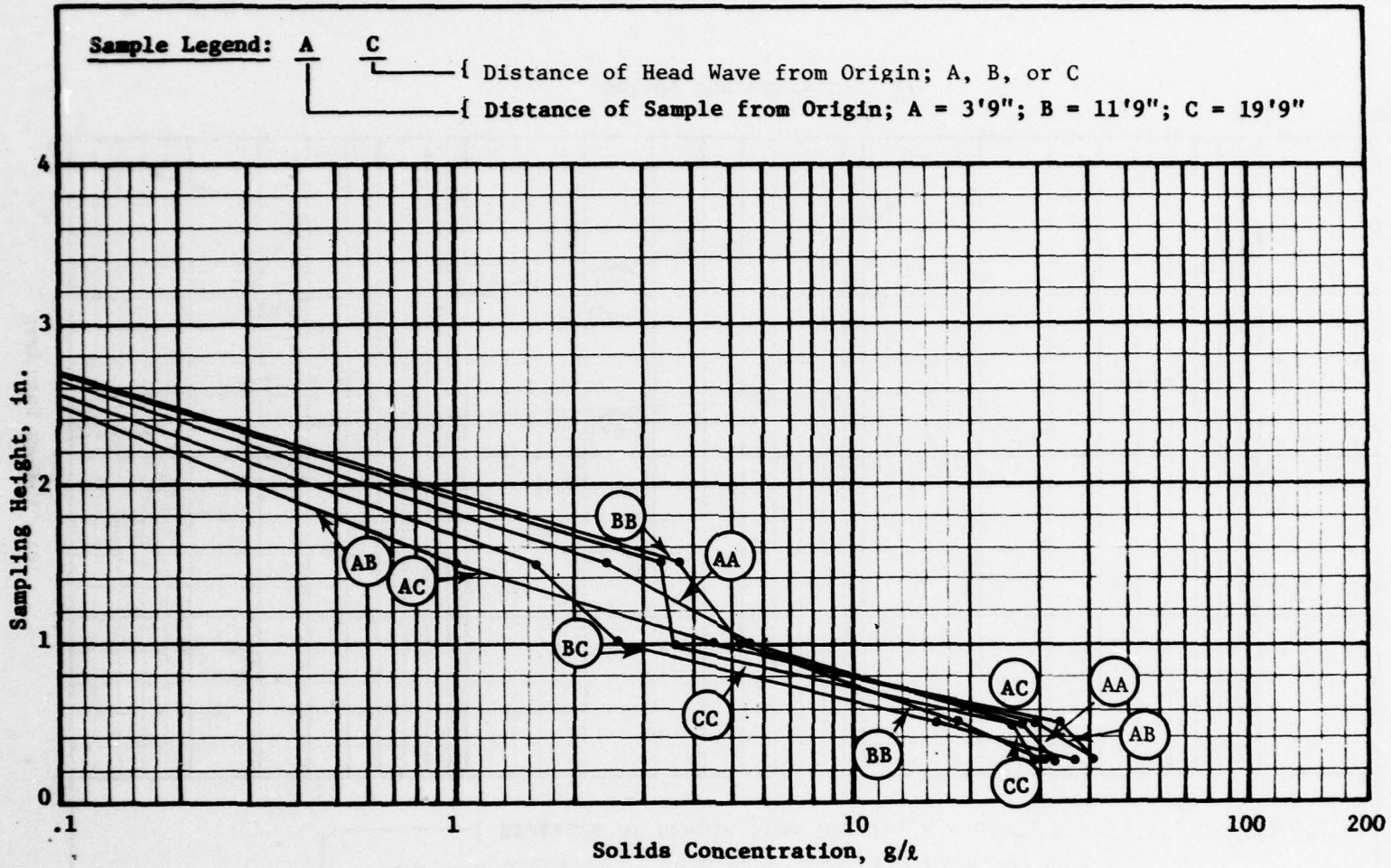

Figure C13. Concentration profiles for 10-pcs slurry, -2-deg slope, test 33

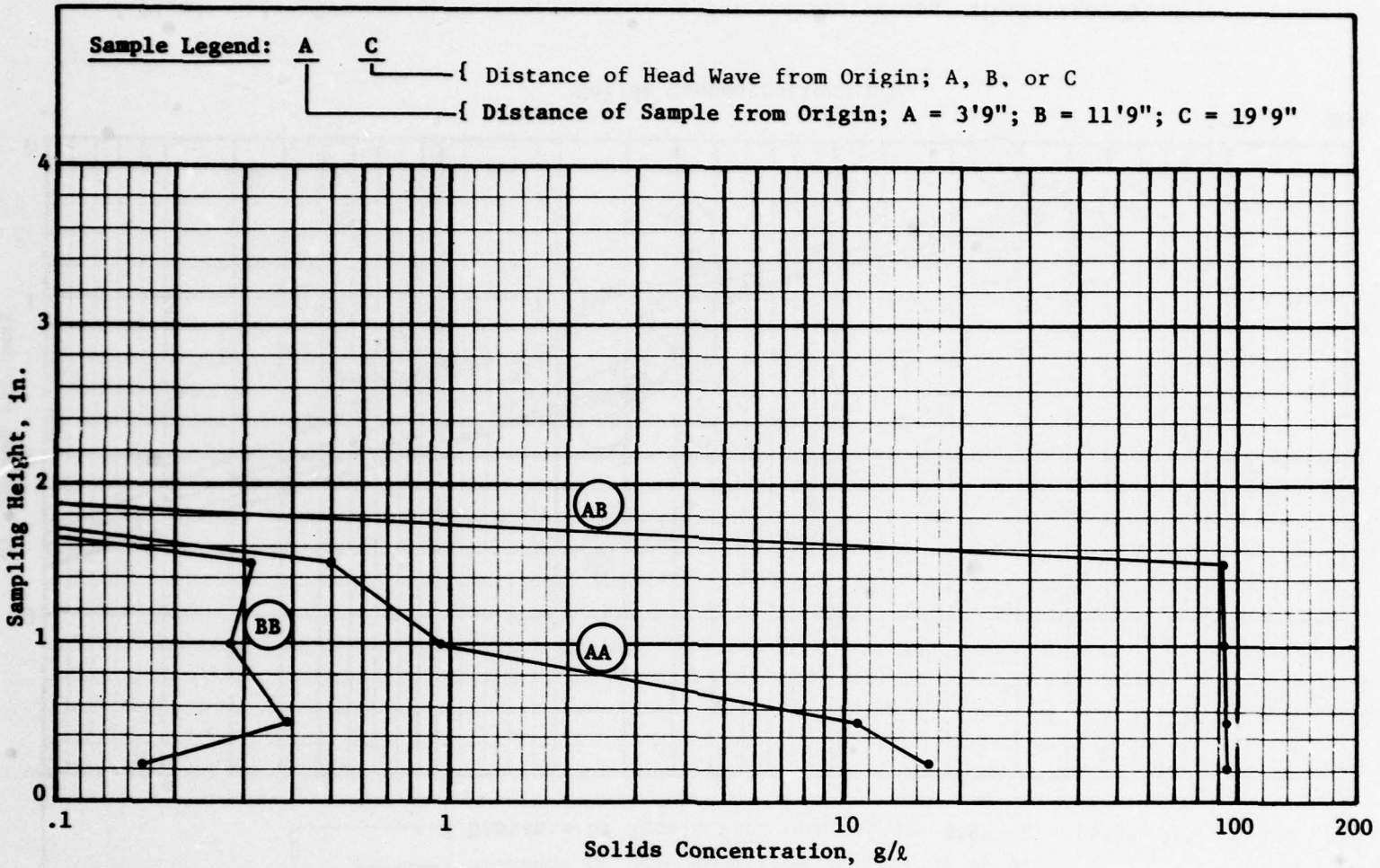

Figure C14. Concentration profiles for 15-pcs slurry, +2-deg slope, test 20

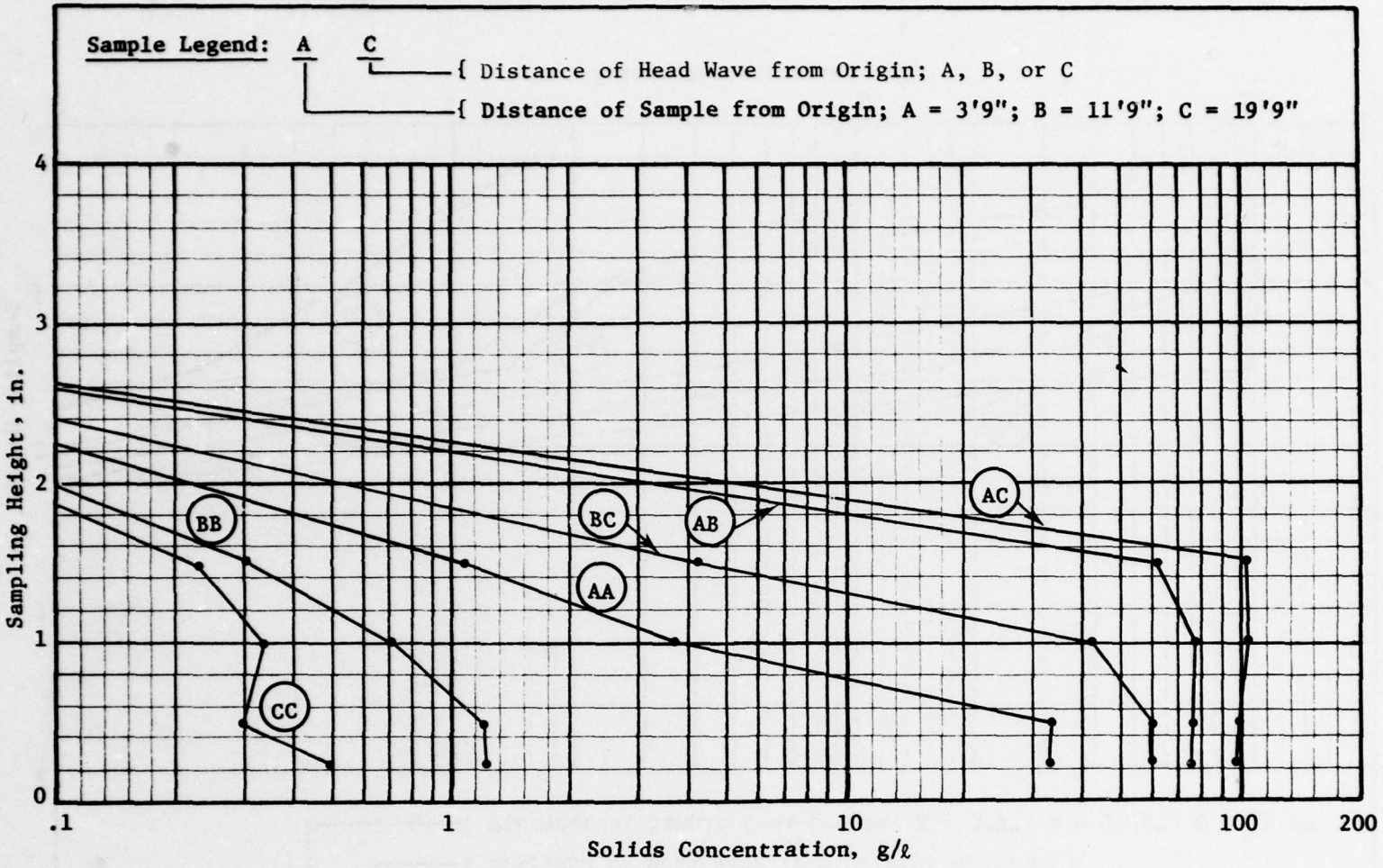

Figure C15. Concentration profiles for 15-pcs slurry, +1-deg slope, test 21

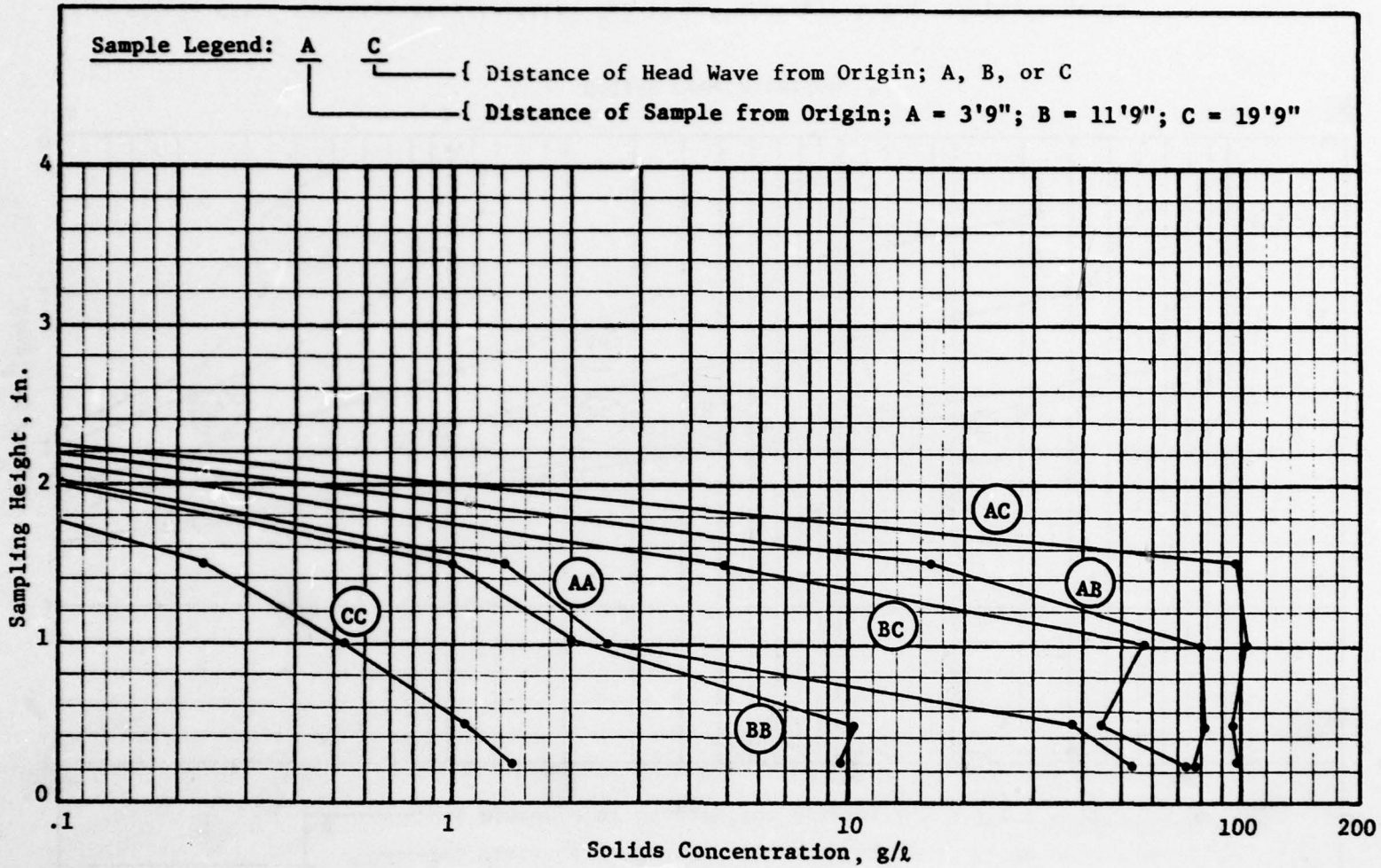

Figure C16. Concentration profiles for 15-pcs slurry, 0-deg slope, test 37

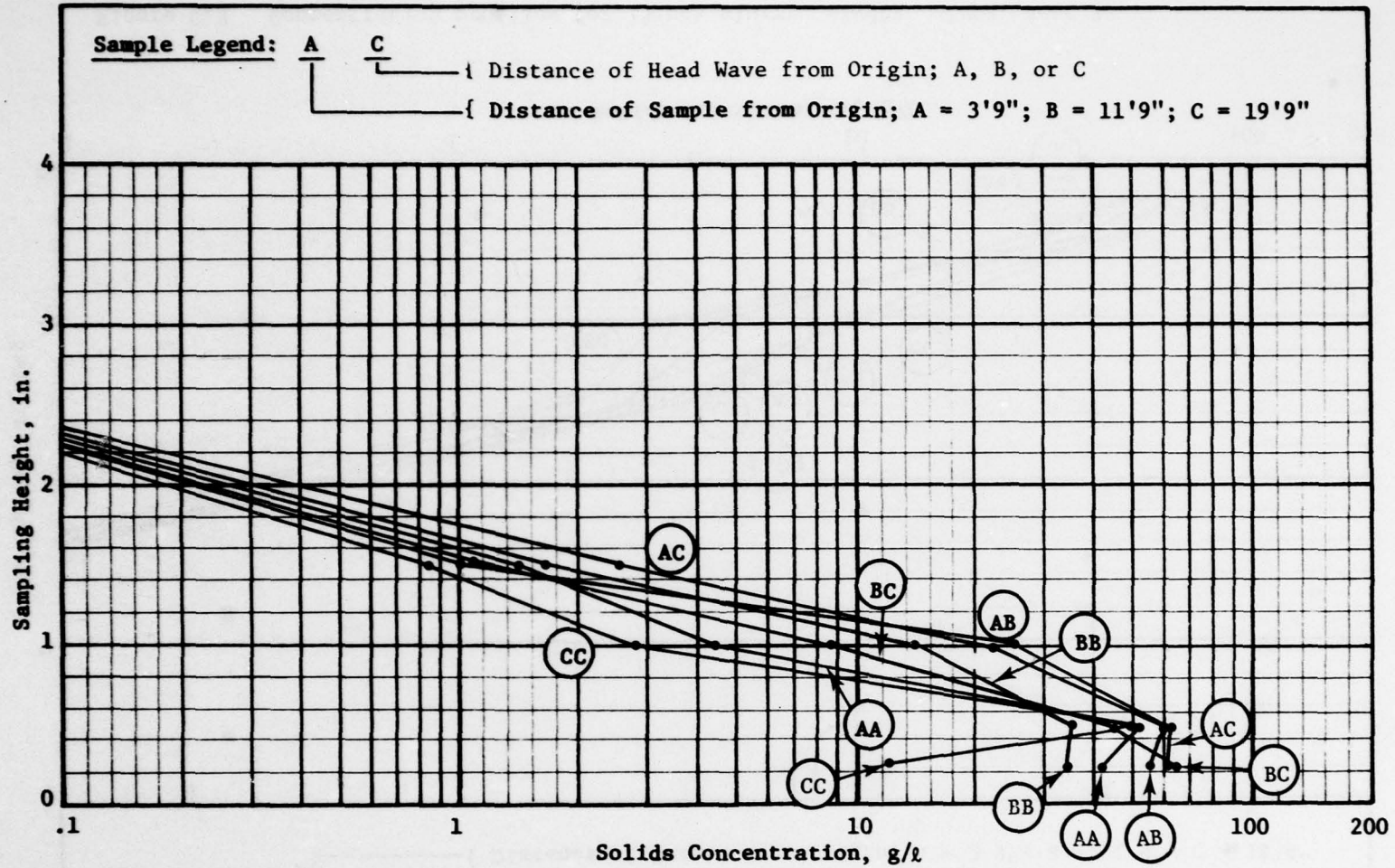

Figure C17. Concentration profiles for 15-pcs slurry, -1-deg slope, test 22

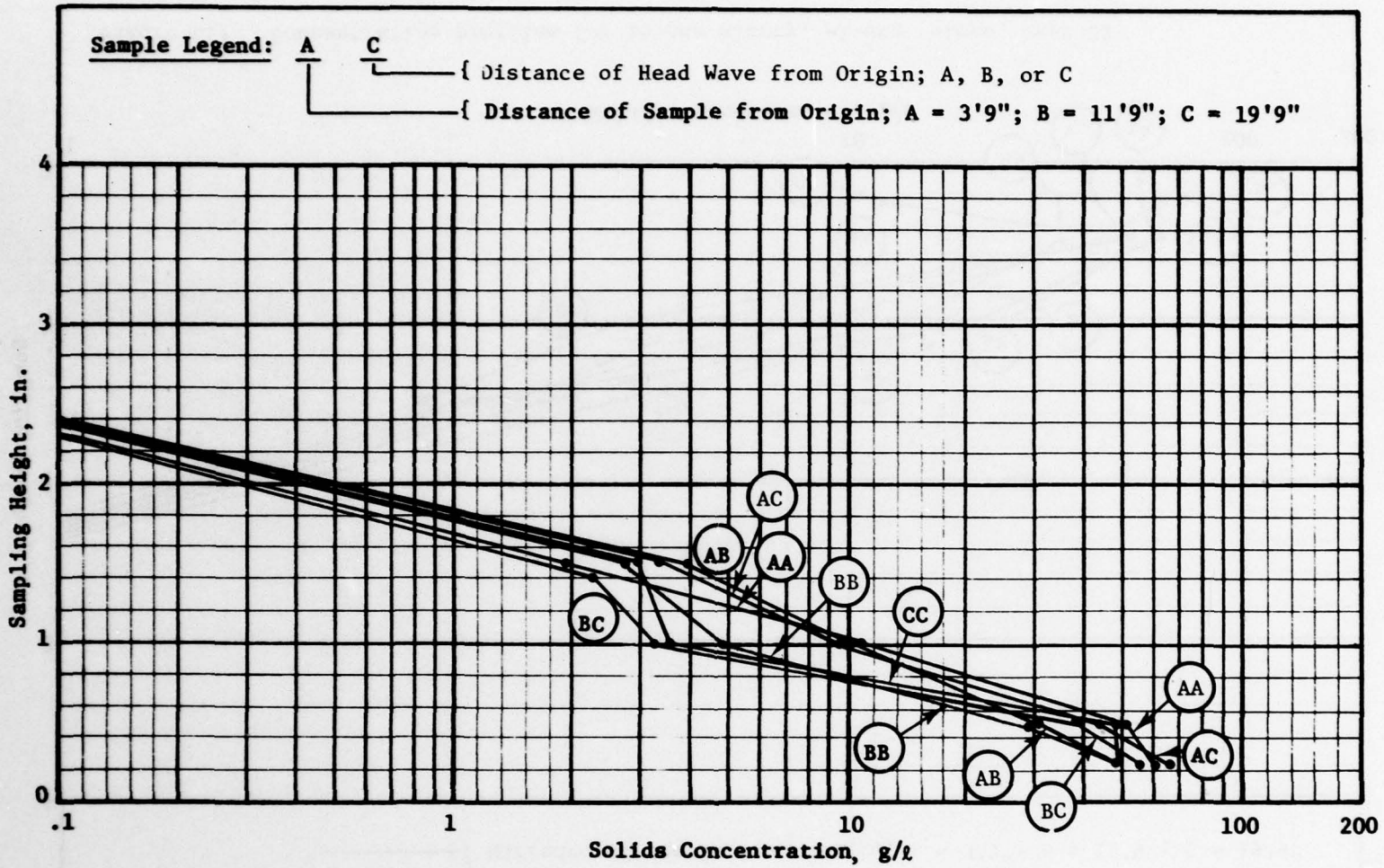

Figure C18. Concentration profiles for 15-pcs slurry, -2-deg slope, test 23

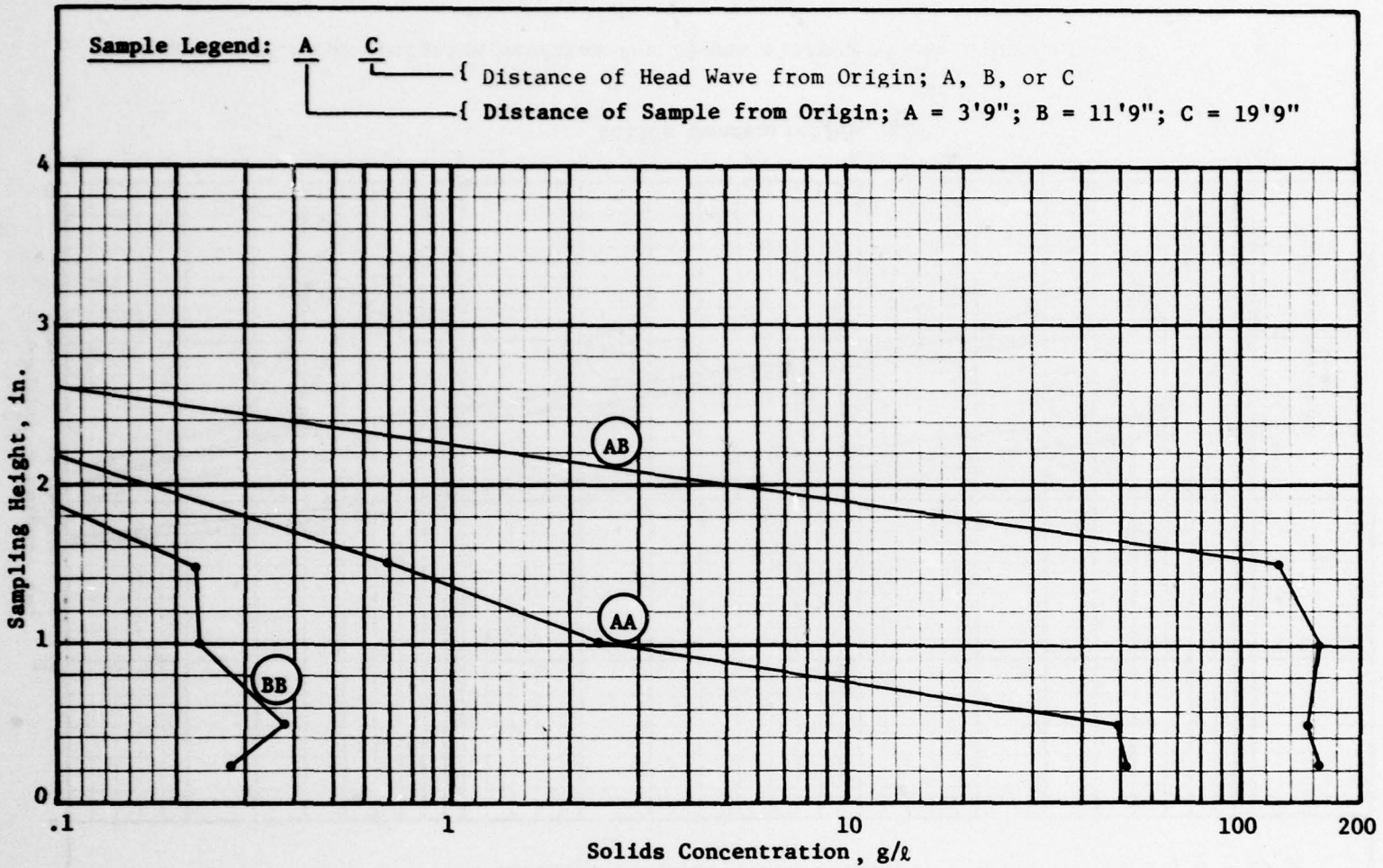

Figure C19. Concentration profiles for 20-pcs slurry, +2-deg slope, test 24

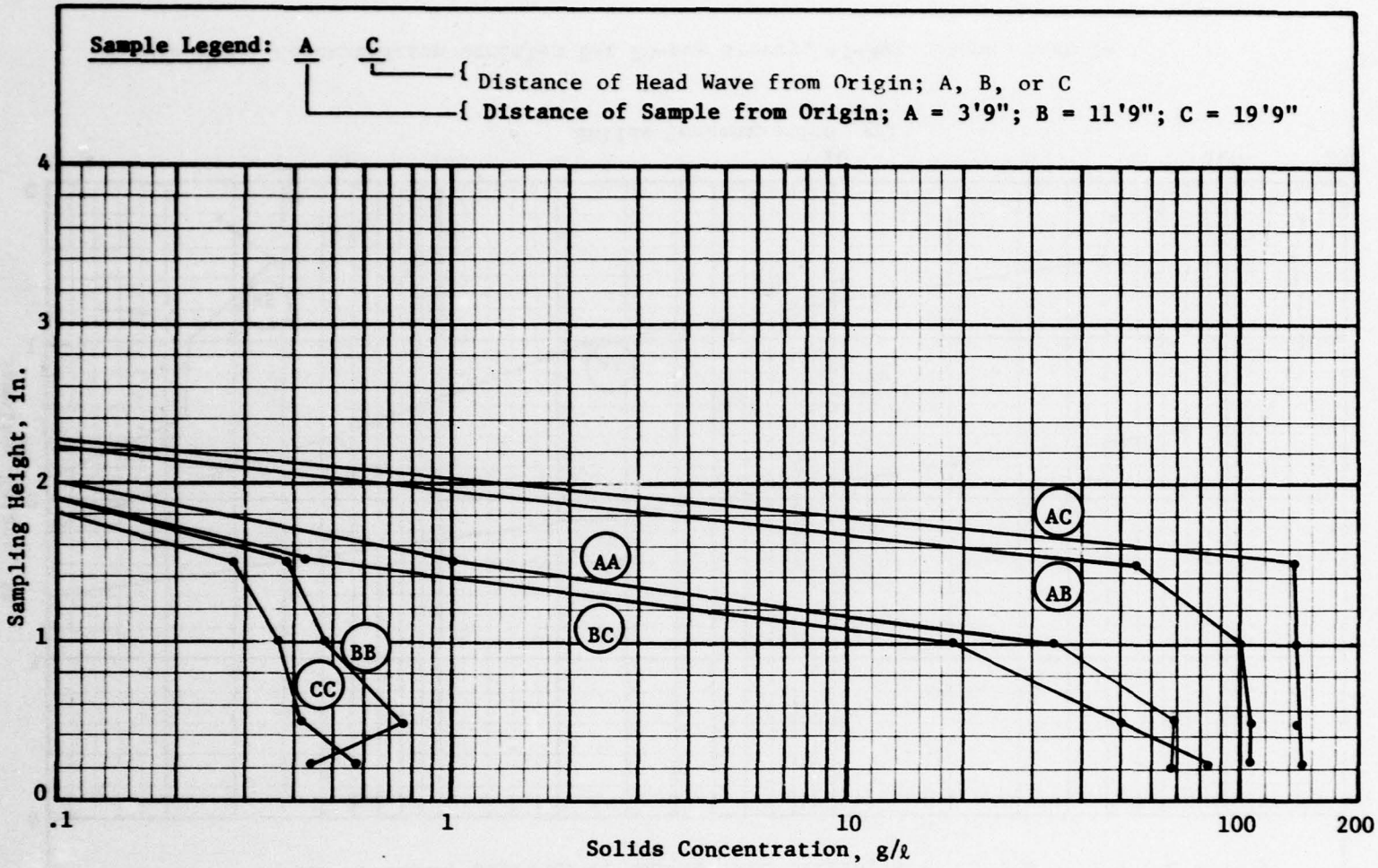

Figure C20. Concentration profiles for 20-pcs slurry, +1-deg slope, test 25

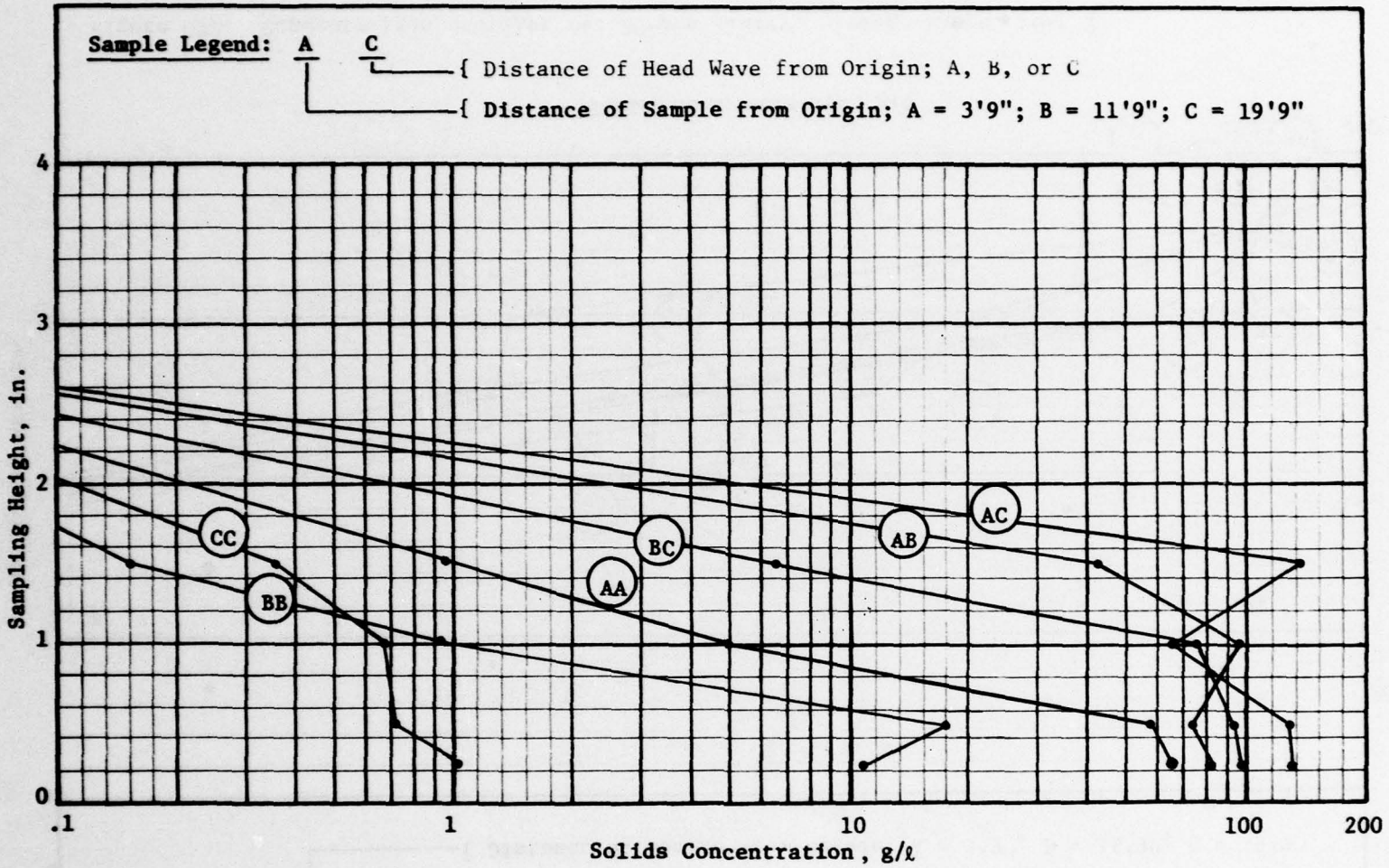

Figure C21. Concentration profiles for 20-pcs slurry, 0-deg slope, test 37

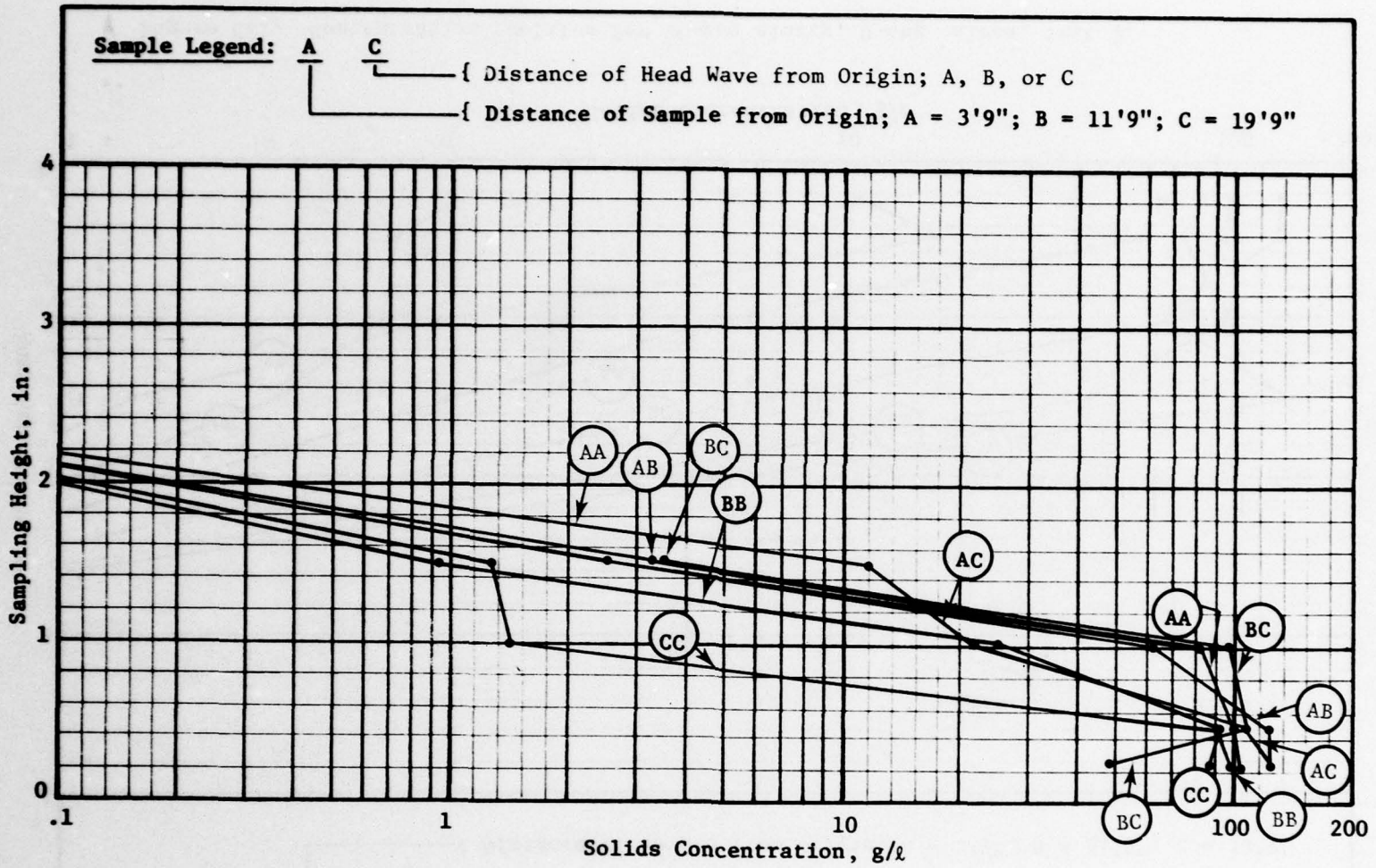

Figure C22. Concentration profiles for 20-pcs slurry, -1-deg slope, test 27

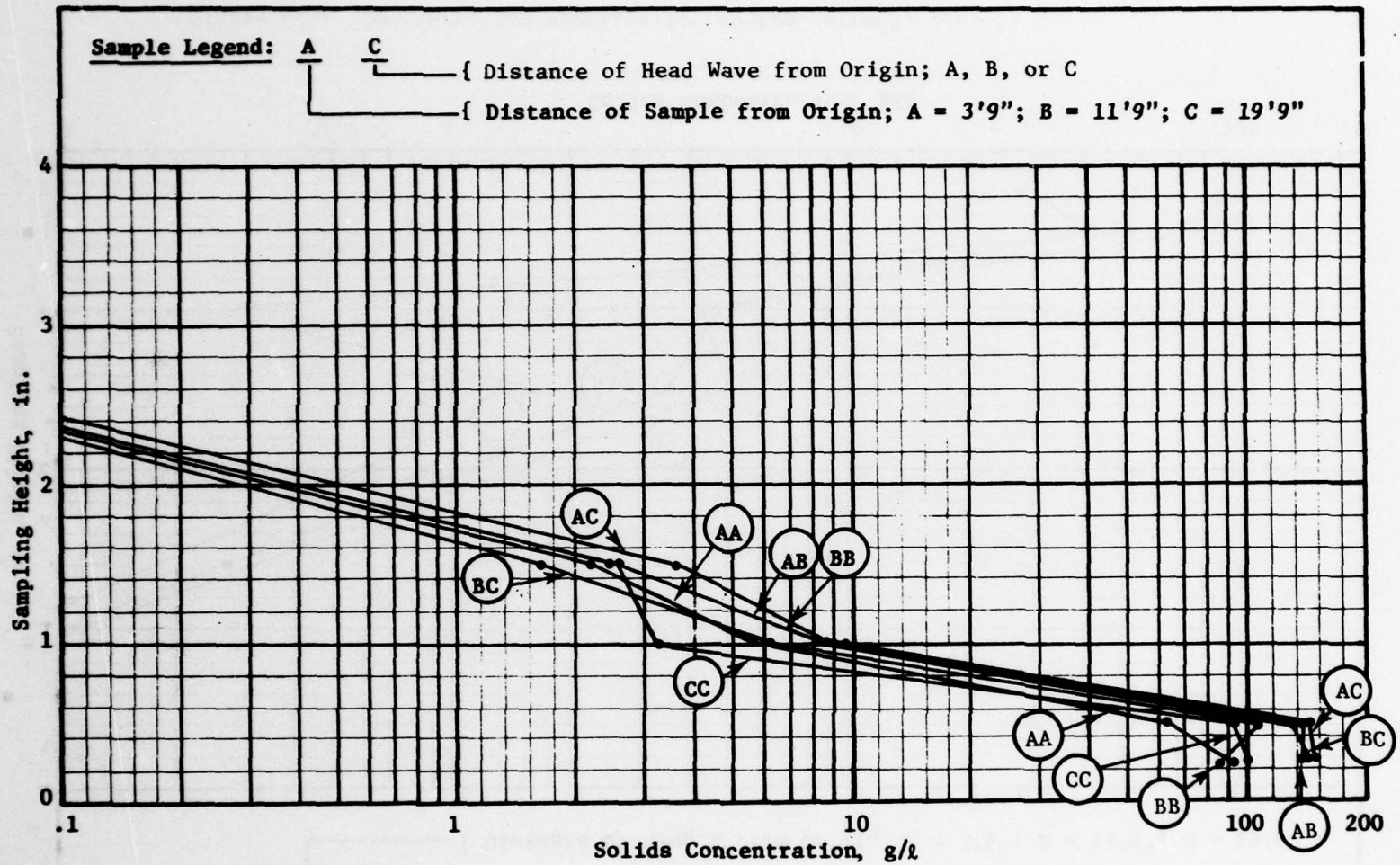

Figure C23. Concentration profiles for 20-pcs slurry, -2-deg slope, test 28

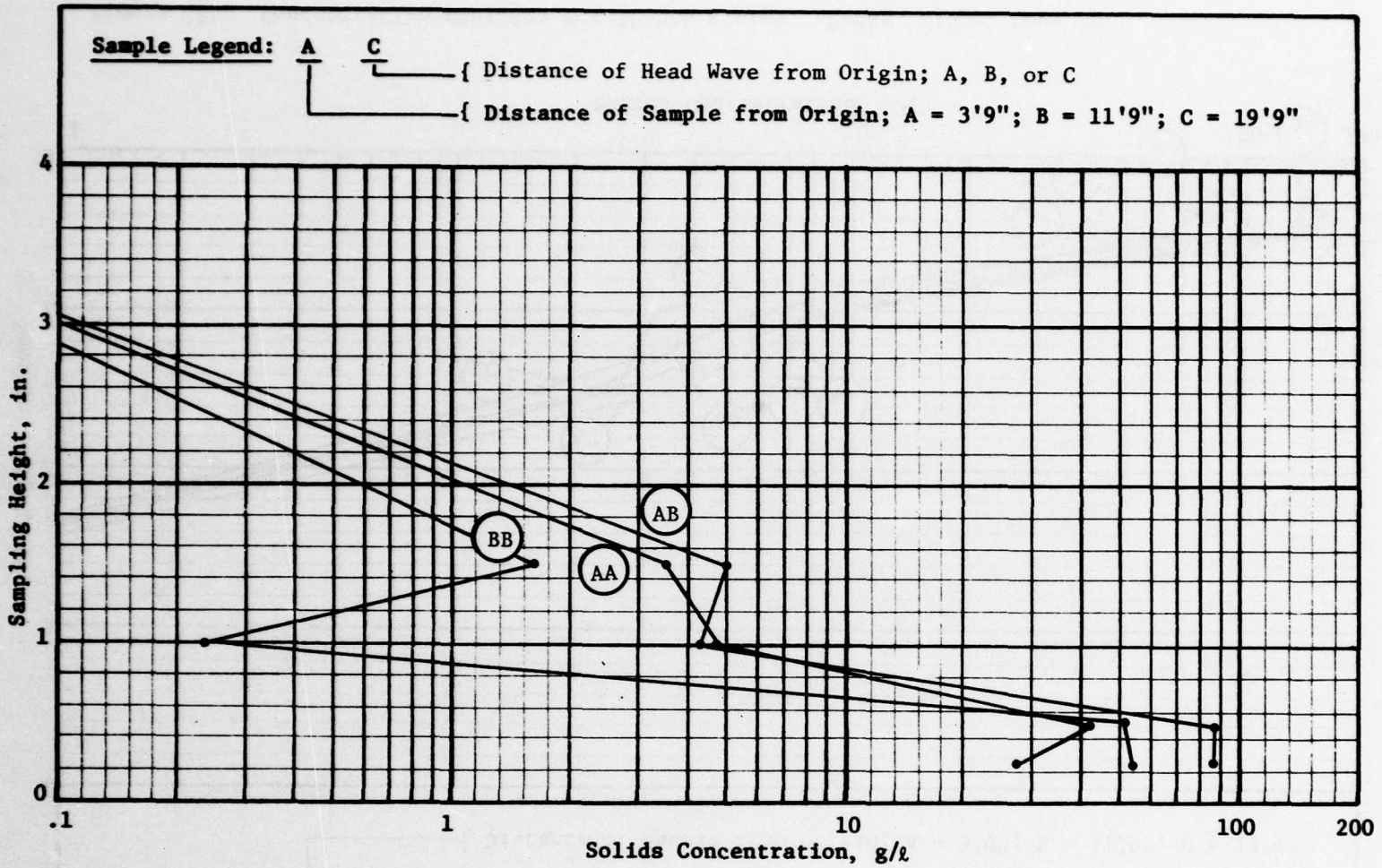

Figure C24. Concentration profiles for -6-fpm current, test 18

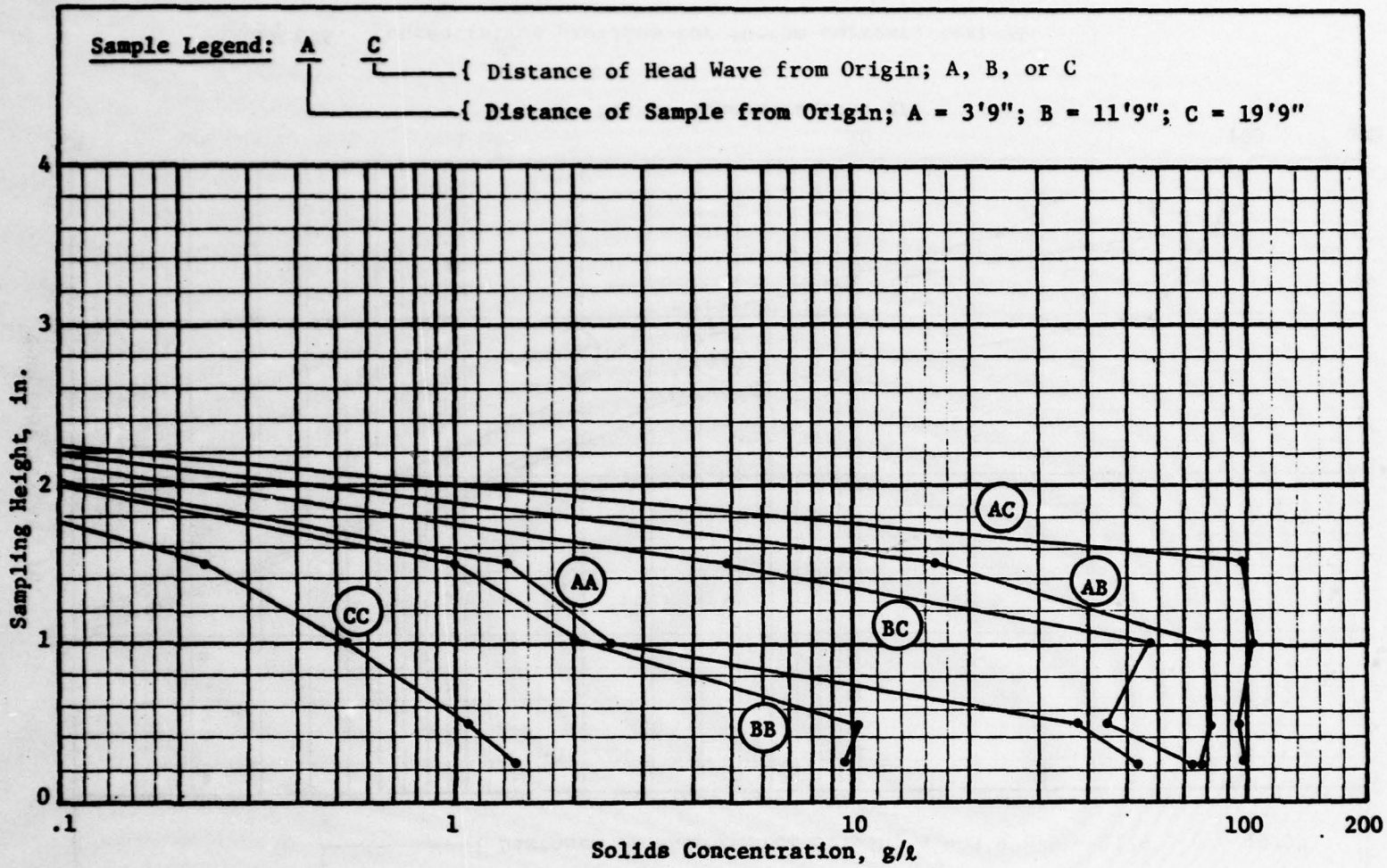

Figure C25. Concentration profiles for zero current, test 37

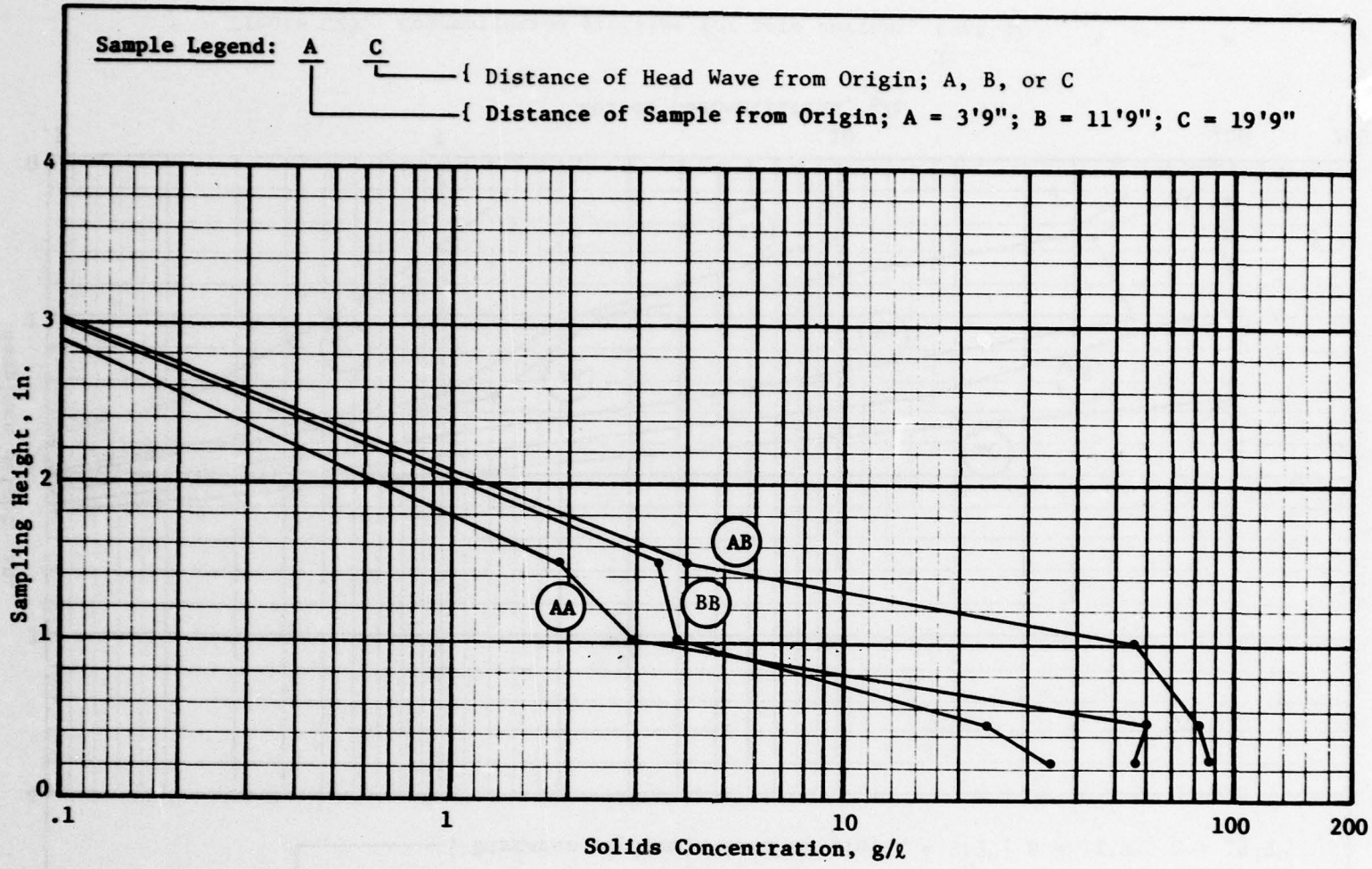

Figure C26. Concentration profiles for +6-fpm current, test 36

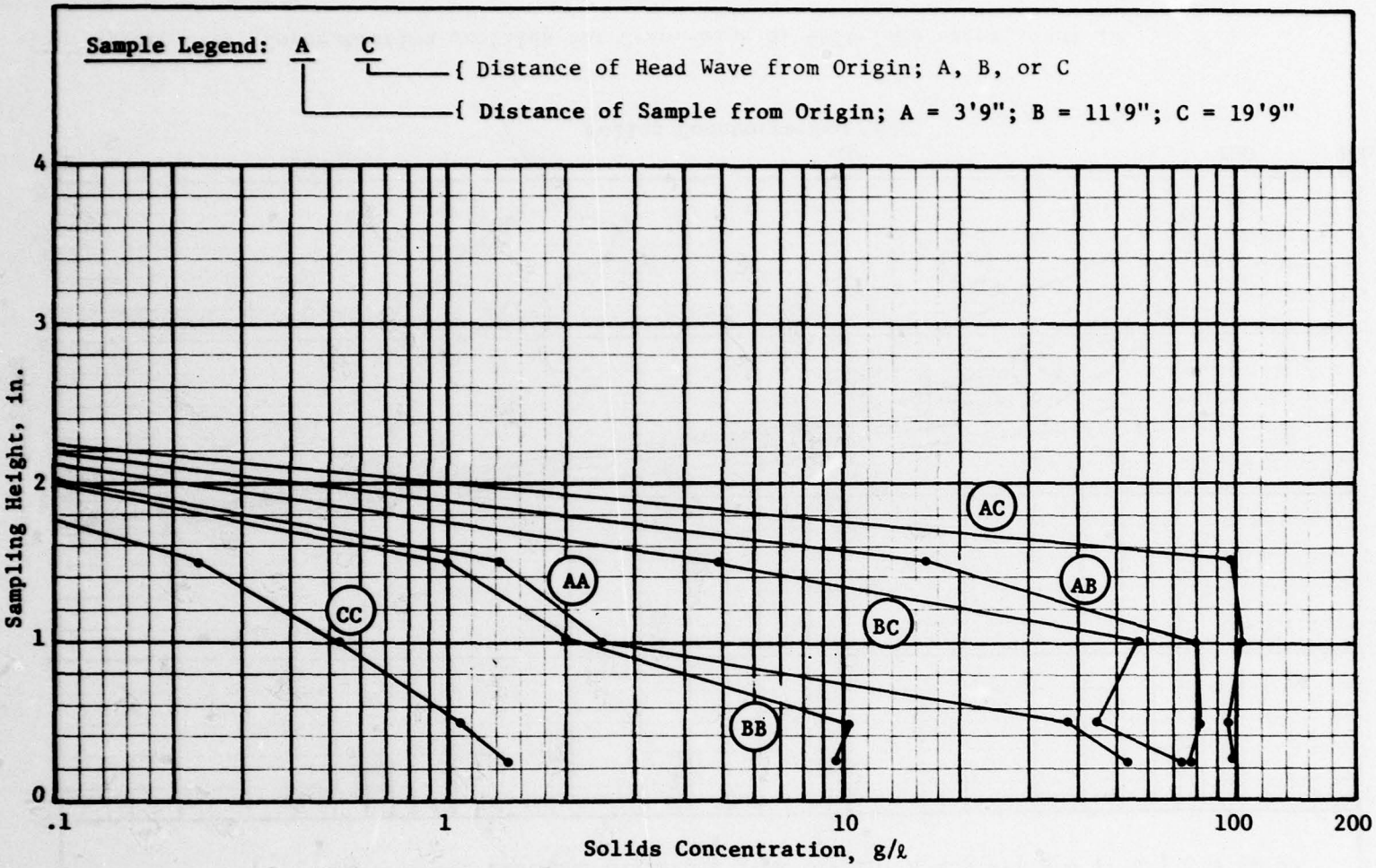

Figure C27. Concentration profiles for no waves, test 37

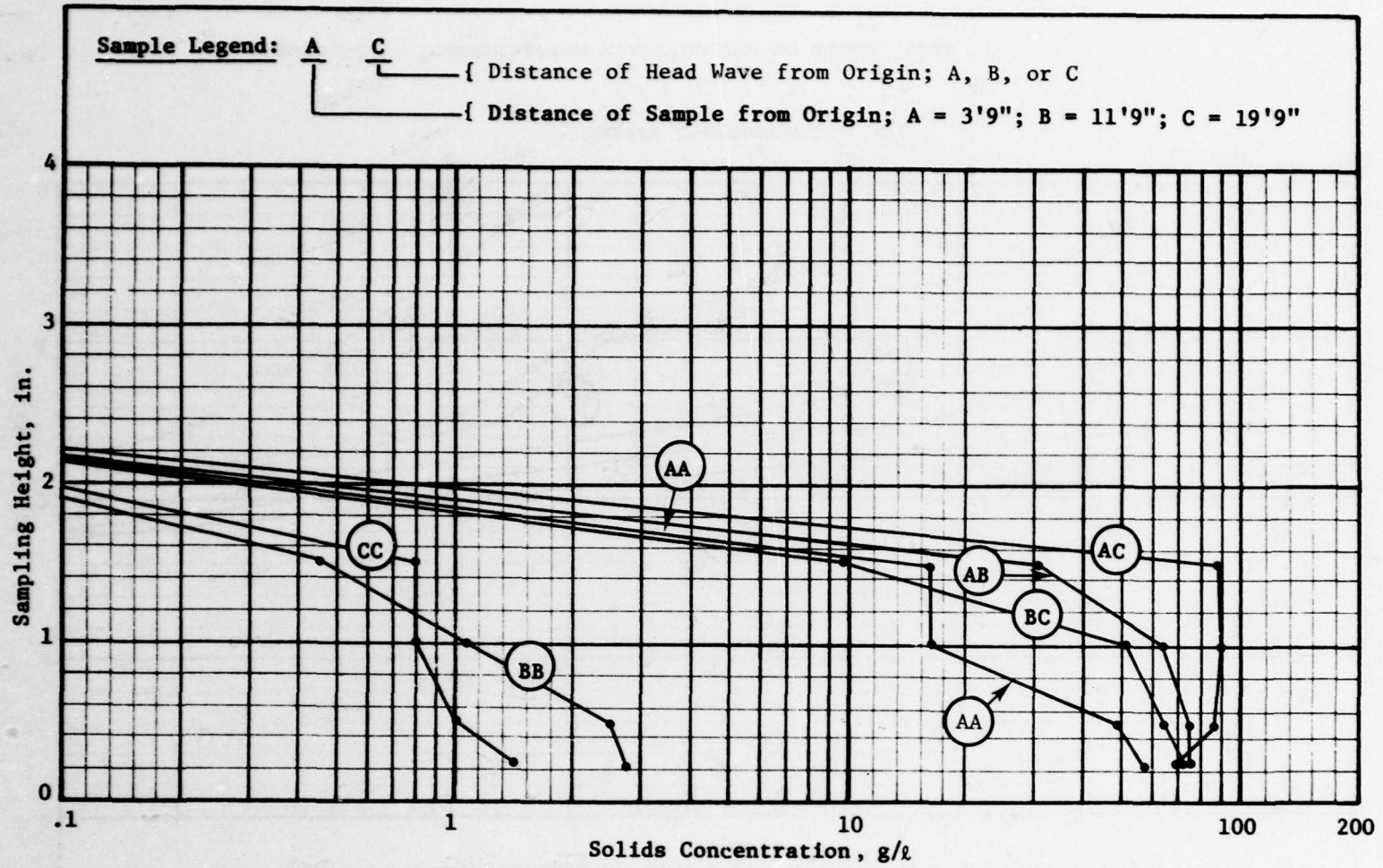

Figure C28. Concentration profiles for 2-in.-high by 4-ft-long waves, test 15

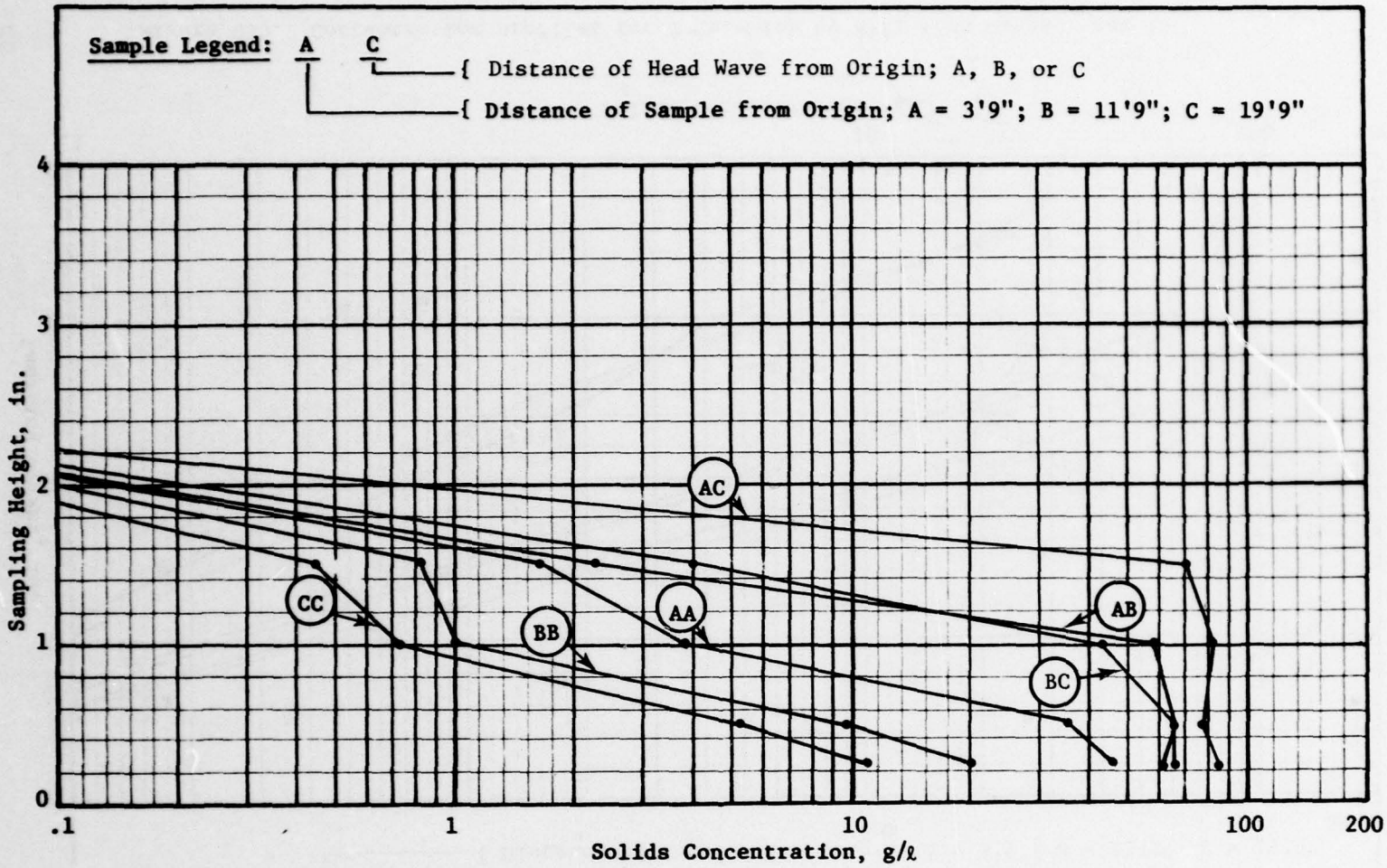

Figure C29. Concentration profiles for 2-in.-high by 5.3-ft-long waves, test 35

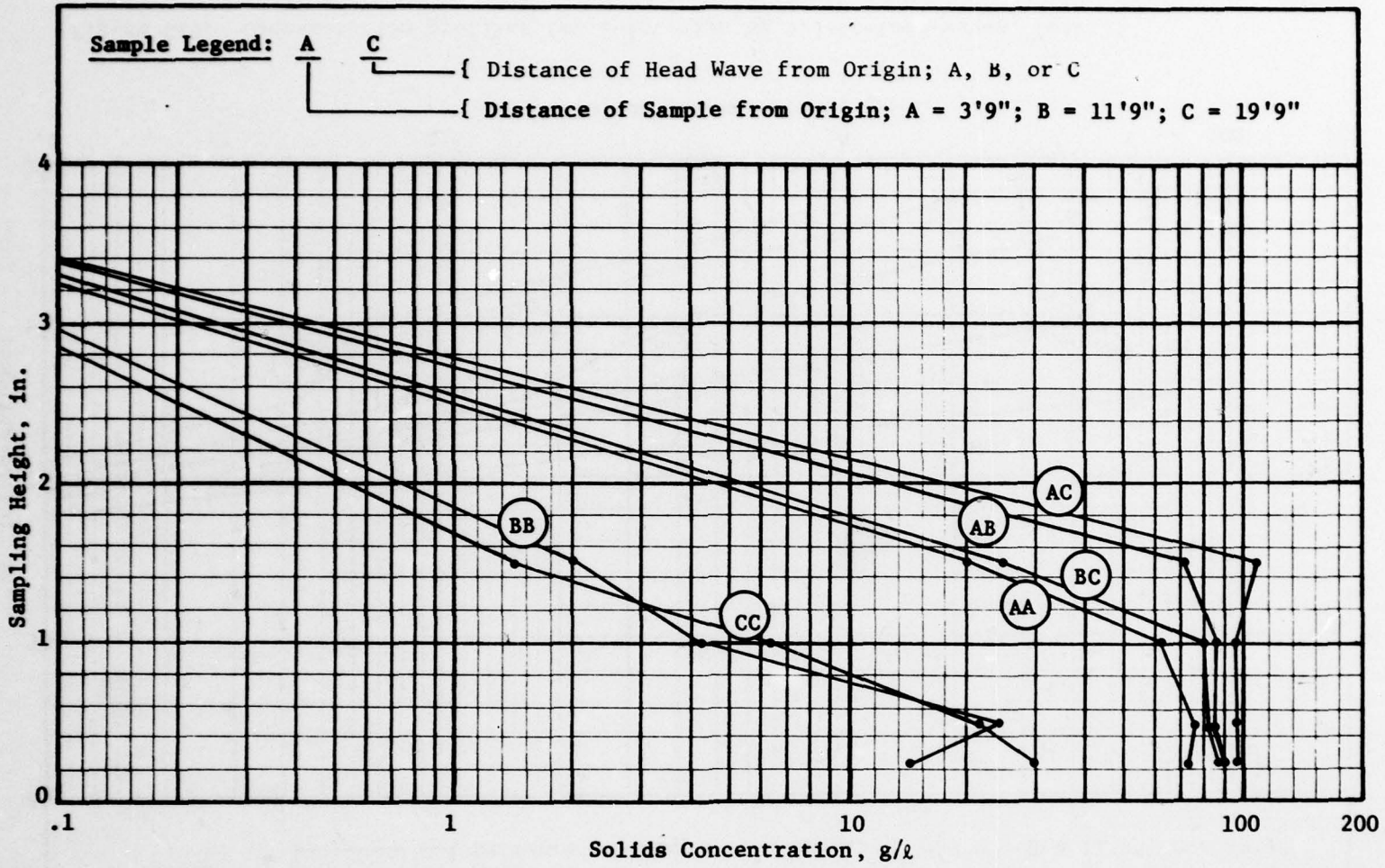

Figure C30. Concentration profiles for 2-in.-high by 8-ft-long waves, test 16

In accordance with letter from DAEN-RDC, DAEN-ASI dated 22 July 1977, Subject: Facsimile Catalog Cards for Laboratory Technical Publications, a facsimile catalog card in Library of Congress MARC format is reproduced below.

Henry, George
Laboratory investigation of the dynamics of mud flows generated by open-water pipeline disposal operations / by George Henry, Robert W. Neal, Stephen H. Greene, JBF Scientific Corporation, Wilmington, Massachusetts. Vicksburg, Miss. : U. S. Waterways Experiment Station ; Springfield, Va. : available from National Technical Information Service, 1978.
112, [46] p. : ill. ; 27 cm. (Technical report - U. S. Army Engineer Waterways Experiment Station ; D-78-46)
Prepared for Office, Chief of Engineers, U. S. Army, Washington, D. C., under Contract No. DACW39-76-C-0173 (DMRP Work Unit No. 6C09)
References: p. 111-112
1. Dredged material. 2. Dredged material disposal. 3. Dredging. 4. Mud. 5. Mud flows. 6. Open water disposal. 7. Pipelines. 8. Slurries. 9. Solids flow. I. Greene, Stephen H., joint author. II. Neal, Robert W., joint author. III. JBF Scientific Corporation. IV. United States. Army. Corps of Engineers. V. Series: United States. Waterways Experiment Station, Vicksburg, Miss. Technical report ; D-78-46.
TA7.W34 no.D-78-46